Bone's functional and geometric properties in dystrophin-deficient mice and the efficacy of low intensity vibration training to improve musculoskeletal function

A THESIS
SUBMITTED TO THE FACULTY OF THE GRADUATE SCHOOL
OF THE UNIVERSITY OF MINNESOTA
BY

Susan Anne Novotny

IN PARTIAL FULFILLMENT OF THE REQUIREMENTS
FOR THE DEGREE OF
Doctor Of Philosophy

March, 2013

Acknowledgements

I would like to extend my gratitude to the many co-investigators that have contributed their time and intellect to my dissertation work. These authors include: Dr. Kristen A. Baltgalvis, Dr. Jarrod A. Call, Brian C. Eby, Michael D. Eckhoff, Angela G. Greising, Dr. Robert E. Guldberg, Angela S. Lin, Dr. Dawn A. Lowe, Tara L. Mader, Dr. David Nuckley, and Dr. Gordon L. Warren III.

I would like to thank Conrad Lindquist and Dr. Hitesh Mehta for their technical design and assistance with the vibration device, the Biomaterials Characterization and Quantitative Histomorphometry Core at the Mayo Clinic in Rochester, MN for their quantification of our dynamic histomorphometry measurements.

My dissertation has been supported by grants from the Muscular Dystrophy Association (Research Grant 114071), the National Institutes of Health (University of Minnesota Muscular Dystrophy Center P30-AR057220, Minnesota Muscle Training grant T32 AR07612, Dr. Dawn Lowe K02-AG036827), the Minnesota Medical Foundation (Dr. Dawn Lowe), the Patrick and Kathy Lewis Fund at the University of Minnesota, the Kinesiology Block Grant program, the Greg Marzolf Jr. Foundation, University of Minnesota Undergraduate Research Opportunity program, and the Lillehei Heart Institute Summer Research Scholars Program.

Bone's functional and geometric properties in dystrophin-deficient mice and the efficacy of low intensity vibration training to improve musculoskeletal function

by Susan Anne Novotny

ABSTRACT

Overall, my dissertation work has shown that bone health is affected in dystrophic mice secondary to the muscle disease (Chapter 3), and both prednisolone and physical inactivity accentuate these declines (Chapter 4). I identified two sets of low intensity, high frequency vibration parameters (45 Hz at 0.6 g and 90 Hz at 0.6 g) that initiated an osteogenic response in *mdx* mice. Further experiments were performed utilizing the 45 Hz and 0.6 g setting, the results of which indicated that vibration was safe for dystrophic muscle (Chapters 5 and 6). However, long-term training adaptations for musculoskeletal function were not realized (Chapter 6). The lack of adaptations following vibration training in *mdx* or wildtype mice does not negate the utility of vibration as a potential therapeutic exercise modality for DMD, but further research, utilizing alternative strategies, is needed to determine the full extent of vibrations capacity to improve musculoskeletal health.

Contents

List of Tables

List of Figures

Chapter 1

Introduction

Duchenne muscular dystrophy (DMD) is a disease characterized by progressive muscle weakness and physical inactivity, which reduces the frequency and magnitude of mechanical loads placed on bone. Consequent to these reductions in mechanical loading is the initiation of bone loss, which structurally weakens the bone and predisposes it to fracture. Fracture incidence is on the rise in DMD patients and ranges between 18-44%, where higher incidence rates parallel increased age, physical limitations and disease states [1, 2, 3]. Despite increased fracture incidence, few studies have characterized skeletal health in DMD patients beyond bone mass [4, 5, 6], and at the time of initiating this dissertation work, clinical interventions focused on identifying bone-sparing modalities of exercise were not published. This is largely attributed to the fact that DMD patients are advised to avoid osteogenic physical activities, due to the potential that these high intensity activities may injure the inherently fragile muscle tissue. Thus, the development of safe, yet effective, therapeutic modalities are warranted to preserve bone health in DMD. The overall purpose of this dissertation was therefore, to determine the safety and efficacy of low intensity, high frequency vibration training to improve musculoskeletal health in a mouse model of DMD. The following three specific aims were developed to address this issue. The first aim was to confirm that bone health was compromised secondary to the muscle disease in mouse models of DMD and to identify the underlying mechanisms. The second aim was to determine the extent to which physical inactivity and prednisolone treatment (i.e., the glucocorticoid which is the gold-standard treatment to preserve muscle strength in DMD) further impact dystrophic bone health. The final aim was to determine the safety and efficacy of low intensity, high frequency vibration training as a potential therapeutic modality to preserve, and potentially improve, dystrophic musculoskeletal health.

Chapter 2 provides contextual background necessary to understand the motivation behind this dissertation work. This chapter reviews the relevant literature with regard to the importance of mechanical loading on bone health, the role of muscle in mechanical loading, the muscle disease DMD, the impact DMD has on bone health, and the use of vibration as a potential therapy to improve musculoskeletal health.

Chapters 3-6 are written in manuscript form and represent the sequential aims of my dissertation. Chapter 3 is a paper characterizing the extent to which tibial bone strength was compromised in two mouse models of DMD (i.e., *mdx* and double-knockout (*dko*)

mice) compared to healthy wildtype mice and what geometric and intrinsic material properties of bone contributed to alterations in strength. Two studies had previously investigated skeletal health in *mdx* mice; however, their findings were conflicting and consequently it remained unknown if these mice had a skeletal phenotype similar to boys with DMD [7, 8]. Therefore, the basis for this study was to characterize the phenotype of young and aged *mdx* and *dko* mice. The results of this study confirmed that dystrophic mice indeed have compromised bone strength, smaller cortical bone geometry, and altered trabecular bone morphometry, making them useful models to identify therapeutic regimens aimed at improving dystrophic skeletal health.

Chapter 4 discusses the findings of a study that examines the extent to which two known catabolic factors of DMD, that is, prednisolone treatment and restrictions on physical activity, translate to further deteriorations in *mdx* bone strength and geometry. Prednisolone is the active form of the drug prednisone, which is the gold standard of treatment in boys with DMD due to is ability to improve skeletal muscle strength and function; however, the drug has known deleterious effects on bone. Prior to this work, the impacts of prednisolone and physical activity on bone in dystrophic mice and DMD patients were unknown. It was presumed that both factors influenced the deleterious alterations to bone health, but it was unknown if their actions were independent or synergistic. This study demonstrated that prednisolone treatment and restricted physical activity independently accentuated reductions in the strength and geometry of *mdx* bone, but had no impact on the material properties of the bone. However, it remains to be determined if this pattern translates to patients within DMD.

Chapter 5 discusses the findings of a study that investigates the utility of low intensity high frequency vibration to stimulate an osteogenic response in *mdx* mice and extensively examines the safety of vibration treatment to the inherently fragile muscle of dystrophic mice. To address the utility of vibration in stimulating an osteogenic response, seven different sets of vibration stimuli were compared, where the parameters of vibration (i.e., acceleration and frequency) were manipulated and mRNA levels of genes associated with bone formation and bone resorption were measured. This study determined that 45 Hz at 0.6 g best initiated an osteogenic response and was therefore considered to be the optimum set of parameters of vibration for *mdx* mice. Safety of vibration treatment was addressed in two subsequent studies. These studies determined

the extent to which vibration at 45 Hz and 0.6 g impacted skeletal muscle contractility and altered the expression of genes associated with inflammation and myogenesis in *mdx* mice as well as two other models of DMD with more severe phenotypes. Combined, these three studies indicate that vibration at 45Hz and 0.6 g is safe for dystrophic muscle and may be a potential therapeutic modality to improve musculoskeletal health in DMD.

The paper in Chapter 6 follows directly from the paper in Chapter 5, to determine the efficacy of longer-term low intensity vibration training to improve musculoskeletal health in wildtype and *mdx* mice. The data presented in this chapter suggest that eight weeks of vibration training at 45 Hz and 0.6 g, 15 min per day, 5 days per weeks, did not significantly impact tibial bone strength, structure, or trabecular architecture. Muscle function was also not improved by vibration, however it is important to note that long-term vibration training was not injurious to inherently fragile dystrophic muscle and therefor is a safe therapeutic modality. The one positive benefit that arose from long-term training was that vibrated mice did have smaller fat pads. This may be potentially desirable in DMD as excessive weight gain results from inactivity and the use of prednisone.

Chapter 7 serves as an overview of the combined findings presented in this dissertation. The chapter concludes by addressing strategic recommendations for further studies investigating the utility of vibration, and future directions of bone research in DMD.

Chapter 2

Literature Review

This chapter is intended to provide a background on bone including basic terminology and anatomy, the functional and geometric alterations of bone that result in altered bone strength. The next section will review the role of skeletal muscle in bones functional and geometric alterations that occur with the progression of Duchenes Muscular Dystrophy in humans as well as in mouse models of the disease. The last section of this chapter focuses on vibration as a potential therapy and its potential to improve bone health in various populations.

2.1 Background Of Bone

The following section aims to define the types of bone that were investigated in my dissertation studies, the methods to quantify bone health, as well as the outcome measures obtained from these methods. Following the introduction of these terms, I will define and discuss whole bone strength and the two primary contributing properties of bone strength (i.e., geometric and intrinsic material) along with a brief description of how these properties are measured. Lastly, I will introduce a the leading theory describing how bone senses and responds to mechanical loading and the resulting affects this has on the geometric and intrinsic material properties of bone and therefore whole bone strength.

2.1.1 Types, Structural Composition and Purpose of Bone

The appendicular skeleton is comprised of two types of bone, cortical (or compact bone) and trabecular (or cancellous and spongy bone). Cortical bone creates the thick walls of long bones such as the tibia or femur, while trabecular bone is found at the ends of long bones as well as along the inside wall of cortical bone, which surrounds the marrow space (Figure 2.1, and 2.2A). The spatial arrangement and structure of bone varies by skeletal region, and is customized to the spectrum and magnitude of mechanical loads placed on the bone. Details on how bone perceives and responds to these loads will be described later in this chapter.

In general, the thick walls of cortical bone in long bones are arranged in densely packed concentric circular structures, referred to as osteons. Osteons that are old, or contain a fracture, are removed and replaced over time via a process called remodeling

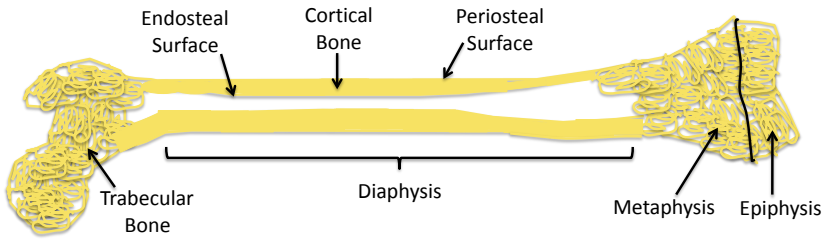

Figure 2.1: Longitudinal cross-section of the femur that denotes the location of cortical bone in both the diaphysis and epiphysis regions of the femur as well as the location of trabecular bone in the distal and proximal ends of the femur (as presented in [9]).

(briefly discussed later in this chapter). Thus the concentric layers of an osteon represent individual layers of new bone, formed from the outside in, by the cells called osteoblasts. Besides having strength and stiffness provided with concentric circular architecture, each layer of new bone has differential alignment, which further increases the strength of the bone and its resistance to loading. Consequently, this arrangement of osteons allows cortical bone to be both rigid and flexible at the same time. This property of cortical bone allows it to provide structural support while being able to deform with loading.

Trabecular bone on the other hand, is designed as a lattice of plates and struts that allows for greater flexibility compared to cortical bone (Figure 2.1A and 2.2B). This flexibility is advantageous, because it allows the ends of whole bones to simultaneously withstand multidirectional loading and absorb the energy associated with these loads. In addition, the arrangement of the horizontal plates and vertical struts can be adapted to accommodate the dynamic stresses and strains experienced by the bone.

Trabecular bone is often deemed to be more metabolically active and sensitive to alterations in mechanical loading than cortical bone; however, this is primarily attributed to 1) the larger surface area of trabecular bone (eight times larger than cortical bone) and 2) its proximity to bone precursor cells in the marrow and relatively better nutrient availability compared to cortical bone.

Prior to providing a background of bone, the following section will review the bone terms utilized throughout this entire dissertation. In cortical bone (Figure 2.2A), there are two primary surfaces upon which bone can be added or removed. The first is the periosteal surface, which is the outermost layer of cortical bone, and the second is the endosteal surface, which is the innermost layer of cortical bone. The distance between

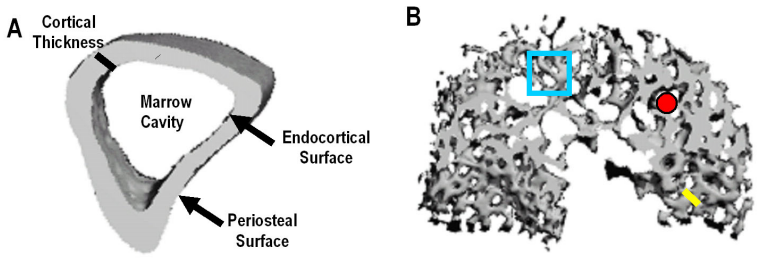

Figure 2.2: Panels A and B are exemplar micro Computed Tomography (μCT) images obtained from the tibial bone of a wildtype mouse at the A) mid-diaphysis (cortical bone) and B) proximal metaphysis (trabecular bone). A) For cortical bone geometry, the two surfaces of bone identified along with cortical thickness. B) Trabecular architecture is defined by trabecular thickness (i.e., the yellow line), bone volume fraction (i.e., bone volume per tissue volume, BV/TV), trabecular number (i.e., number of trabecular within a given region; blue square), and trabecular spacing (i.e., the largest sphere that fits within the space between trabeculae; red circle). All terms have been defined and quantified according to international nomenclature and standards [10].

these two surfaces represents the cortical thickness. Additional geometric properties can be derived from μCT, and include the cross-sectional area of cortical bone as well as the periosteal diameter. Trabecular bone (Figure 2.2B), is characterized by quantifying (1) trabecular thickness (2) trabecular bone volume fraction (BV/TV), (3) trabecular number, and (4) trabecular spacing.

2.1.2 Functional Capacity and Geometric Properties of Tibial Bone

After defining the types of bone and the key terms utilized throughout the dissertation, it is necessary to introduce whole bone strength and the two primary properties that contribute to strength (i.e., bone geometry and intrinsic material properties). These properties can change independently or simultaneously to alter bone strength; therefore, it is important to quantify both to delineate their respective contributions to alterations in bone strength. Detailed explanations of these terms and how they are measured follows below.

Functional Capacity of Tibial Bones

To assess the mechanical functional capacity of bone, meaning its ability to withstand loads, mechanical tests such as three-point bending are commonly utilized. For this functional test, tibial bone limb length is measured, and from this, the mid-diaphysis (i.e., limb length divided by two) is identified and marked. The tibial bone is then placed within the three-point bending apparatus on the two lower support beams with the lateral edge of the tibia facing downward (Figure 2.3A). The bone is centered such that the upper support beam (i.e., the upper crosshead containing the force transducer) is directly above the mid-diaphysis of the bone. The crosshead is slowly lowered onto the bone until the applied load is $\sim$0.02 N.

When testing is initiated, the crosshead displaces downward at a quasi-static rate, while the applied force on the bone and the total distance the crosshead has displaced is recorded. The bone is continually loaded at a constantly slow rate, causing the bone to bend, until the bone ultimately fails, or breaks. Throughout the entire testing procedure, the force applied to the bone and the total distance the crosshead displaced is recorded, and a force-displacement curve is then produced using custom designed software (Figure 2.3B [11, 12]).

Ultimate load and stiffness are the primary outcome measures of three-point bending. The ultimate load represents the greatest load the bone can withstand before it begins to undergo micro-fractures (i.e., the peak of the force-displacement curve), at which point the force begins to decline (Figure 2.3B). The stiffness of the tibial bone represents the bones capacity to resist length change, or in this circumstance, bending. Stiffness is measured as the steepest slope of the force-displacement curve (Figure 2.3B). Secondary measures of three point-bending include deflection to ultimate load and failure load, as well as energy to ultimate load and failure load. Deflection is defined as the total distance of crosshead displaced at the time ultimate load and failure load are reached. This is quantified by measuring the distance along the x-axis of the force-displacement curve to ultimate load and failure load. The energy measures (i.e., energy to ultimate load and energy to failure load) are determined by calculating the integral of the force-displacement curve, or the area under the curve, up to ultimate load and failure load. Combined, these seven measures reflect upon the structural integrity and strength of the bone as well as the energy required to break the bone [14]. Detailed

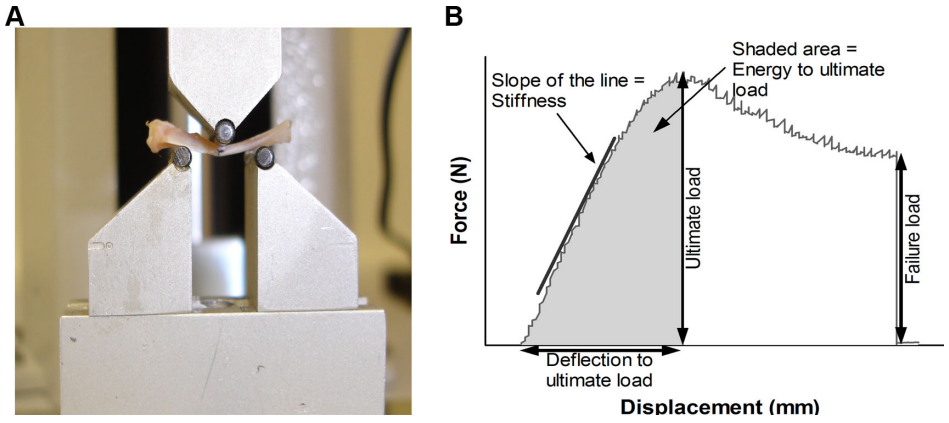

Figure 2.3: (A) Pictorial representation of a mouse tibial bone undergoing three-point bending testing. B) Representative force-displacement tracing obtained during testing of a mouse tibial bone (as presented in [13]). The primary outcome measures derived from the force-displacement curve include ultimate load, stiffness, and energy and deflection to ultimate load. The point at which the whole bone fails (i.e., failure load), is also indicated. Reprinted from [13], Copyright 2011, with permission from Elsevier and *Neuromuscular Disorders*.

figures of these secondary measures can be found in Figure 2.1A of Chapter 3.

Further calculations can then be performed to quantify the intrinsic material properties of the bone, which include ultimate stress and modulus of elasticity. Ultimate stress and modulus of elasticity are calculated on a mouse-by-mouse basis using classical beam theory. Ultimate stress is calculated using the following equation: ultimate stress = (UL*d*L)/(8*CSMI), where UL, d, L and CSMI are ultimate load, medial-lateral periosteal diameter, bottom support span length, and cross-sectional moment of inertia, respectively. Modulus of elasticity is then calculated using: modulus of elasticity = ($k*L^3$)/(48*CSMI), where k equals stiffness [11, 12].

The main advantage of three-point bending is that it provides a full characterization of a bones quality, or more specifically, its functional capacity and intrinsic material properties. When combined, these measurements provide a unique finger print of bone health, and allow the investigators to interpret changes in force-displacement curves that occur with disease, or following treatment. For example, three different types of bone disease are compared to normal bone in Figure 2.4 [15]. The pathophysiology of these three diseases are known, and therefore utilizing these finger prints for comparison

may aid in identifying factors causing ideopathic bone phenotypes.

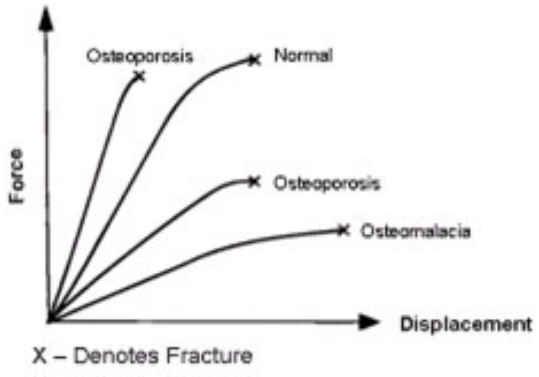

Figure 2.4: Unique force-displacement curves result from pathophysiologies of bone. Thus three-point bending is a useful tool to identify how disease has impacted the mechanical competence of bone compared to other diseases of known pathology, which can aid in the identification of appropriate treatment regimens. (Reprinted with permission from [15], Copyright 1999 American Chemical Society).

The only disadvantage to this technique is that the bone is broken in the measurement process, and as such, it can only be applied *ex vivo*. The advantage is that it yields information that cannot be directly measured via any other technique and it reflects upon the mechanical function of the bone following disease or intervention treatment. Thus, the characterization of mechanical function can aid in developing appropriate therapeutic regimens. Alternative, non-destructive, surrogates for measuring bone strength have emerged in recent years with the advancement of imaging techniques and these new surrogates have been shown to be better correlated to bone strength and fracture incidence than bone mineral density. These methods include characterizing bone geometry and outcome measures are described in the following sections.

Current Imaging Techniques and the Utility of Measuring Geometric Properties of Bone

The two most commonly used bone-imaging techniques in the literature include Dual-Energy X-ray (DXA) absorptiometry and computed tomography. These techniques provide complimentary information pertaining to skeletal health; however the outcome

measures associated with computed tomography are becoming increasingly better indicators of skeletal health than DXA. Simply stated, DXA provides information about how much bone is present in various regions of the skeleton, and computed tomography provides information for where this mass is structurally distributed in space. Therefore computed tomography provides and indication of the geometry, or the structural shape, of the bone which is one of the two primary factors contributing to bone strength. The following section is aimed to describe these two imaging techniques and how they are utilized to assess of bone health and provide an indication of bone geometry and strength.

Dual-Energy X-ray Absorptiometry

Initially measurements of bones geometric properties were estimated by measuring periosteal diameter and cortical thickness with calipers on radiographs [16]. Based on these measures, cortical area and thereby strength of the bone could be calculated, providing a rough estimate of alterations in bone geometry over time. Several years later, dual-energy x-ray absorptiometry (DXA) became widely available to quantify bone mass and areal bone mineral density (Figure 2.5). The primary advantage of DXA is that bone mass and areal bone mineral density (i.e., density of bone mass within a given area, rather than a traditional volumetric measure) are both strongly correlated with fracture risk [17]. Consequently, bone mass, and areal bone mineral density are commonly used surrogates for whole bone strength.

A shortcoming of the DXA technique is that the geometry of the bone, where the bone mass is distributed in space, is not measured. To aid in this explanation, compare the three theoretical bones in Figure 2.6. As measured by DXA, each of the theoretical bones are equal in terms of their bone mass, however due to differences in how the bone mass is distributed in space, the cylinders do not have equivalent strength. As a result, better imaging techniques have been devised to overcome this problem, and are discussed below.

Computed Tomography

Figure 2.5: DXA quantifies the amount of bone mass (i.e., regions of white) within a given skeletal region. The density of bone is represented by the intensity of white within a single pixel. For example, notice the difference in pixel intensity between the skull and spine. Fat mass and lean can also be quantified using this technique. (Image courtesy of Petit, M.A., 2009).

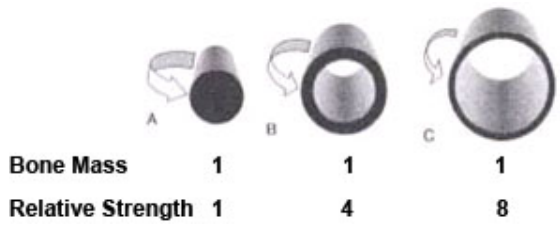

Figure 2.6: Three bones with equivalent bone mass are depicted, however the spatial distribution of this mass differs between bones A, B and C. Distribution of bone mass further away from the bones neutral axis (i.e., the center of the bone) translates to improvements in bone strength. For example, the relative bending strengths are 4 to 8 times larger in bones B and C, respectively, compared to bone A. (Image courtesy of Petit, M.A., 2009).

Currently four types computed tomography imaging techniques are utilized to characterize the geometry, or the shape, of bone. These techniques include peripheral quantitative computed tomography (pQCT), micro-computed tomography (μCT), ultra computed tomography (ultraCT), and nano-computed tomography (nCT). The primary differences between these techniques are the size of the object that can be imaged (e.g., a human tibia versus a mouse tibia) and the resolution of the image (i.e., size of the 3-dimensional element which measures bone. A small voxel size translates to a more detailed image of the bone and vice versa). The two options for human usage (whole bone) are pQCT and ultraCT, whereas μCT and nCT are primarily used for bone biopsies in humans, or on whole bones from smaller animals such as rodents.

The bore size (i.e. the circular opening in the CT, where limbs are placed to be imaged, see Figure 2.7A) limits the size of the bone that can fit into the machine. For example, in the pQCT shown in Figure 2.7, the distal femur, or the entire tibia or radius of humans can fit within the bore. For μCT and nCT, the maximum specimen size is considerably smaller. The maximum specimen size that fits within the bore of our μCT is 36.9 mm x 80 mm. The advantage of the smaller bore size is that the resolution of the image improves as voxel (i.e., data element that quantifies bone within a 3-dimensional grid) size decreases. For instance, to characterizing trabecular architecture in young mice with an average trabecular thickness of 41 μm [13], the 12 μm voxels size of μCT would have at least three voxels describing the thickness of the trabeculae, whereas, a single voxel by pQCT (i.e., 70 μm) would span the entire thickness and therefore provide less information about how the bone is distributed in space. With pQCT, trabecular bone volume is measurable; however the voxel size is too large to characterize trabecular thickness, number or spacing. In rodents, μCT has the capacity to sufficiently measure both trabecular architecture and cortical bone geometry.

Each of the computed tomography techniques images the bone in sequential three-dimensional slices of bone (Figure 2.7B), with the height of the slice representing the resolution (or voxel size). These sequential images are then stacked on top of each other and then reconstructed using computerized software (Figure 2.7C). The outcome measures of pQCT include: bone volumetric density (vBMD), cortical bone geometry, and calculated surrogates for of bone strength. The pQCT derived surrogates for bone

strength were not utilized for the present dissertation, and therefore will not be discussed. The outcomes of μCT include: vBMD, cortical bone geometry, and trabecular architecture (as defined in Figure 2.2 of the current chapter). The commercial availability of ultraCT and nCT systems has improved in recent years; however, techniques have not been utilized to date within muscular dystrophy nor vibration and consequently the use of these two techniques will not be further discussed.

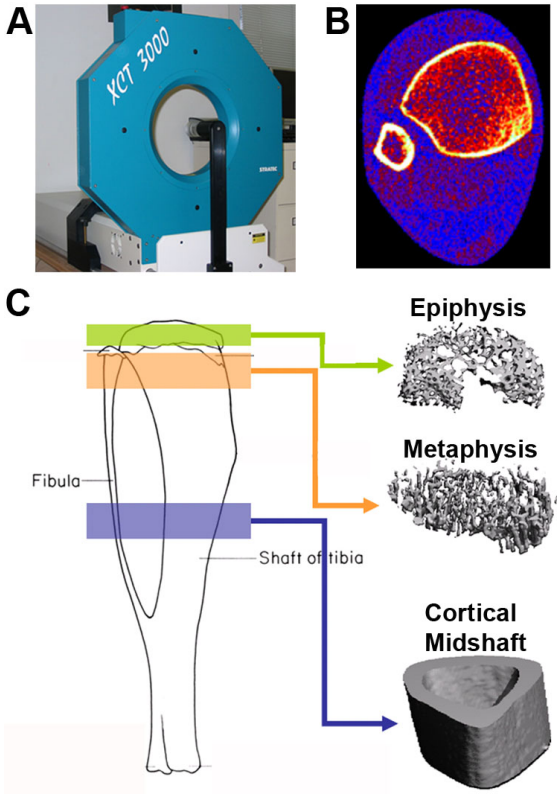

Figure 2.7: (A) Image of a pQCT, showing the size of the bore (i.e., central aspect of the machine where the bone is placed to be imaged). Exemplar images of tibial bones from B) human imaged by pQCT and C) mouse imaged by microCT *ex vivo*. Panel C also defines the three skeletal regions of mouse tibial bone measured throughout this dissertation, as well as exemplar three-dimensional reconstructions of those skeletal regions of bone.

Cross-sectional moment of inertia

The primary outcome of interest from μCT is the minimum principle cross-sectional moment of inertia ($CSMI_{min}$, referred to as CSMI for the remainder of this thesis) because it is a surrogate for whole bone strength [14]. This measure best corresponds to the moment of inertia about the bone bending axis during three-point bending testing. This variable is derived using engineering principles which quantifies each individual voxels moment of intertia relative to the bones neutral axis. The inertia values for all voxels within a slice of bone are then summed within a CT slice and then average across the entire region of interest to provide a precise estimate of bone strength [14]. After applying this calculation to the three bones illustrated in Figure 2.6, it becomes immediately apparent that bone C has a eight-fold increase in resistance to bending compared to bone A, thereby highlighting the importance of altered bone geometry on bone strength.

2.2 Regulation of Bone Geometry and Architecture In Response to Mechanical Loading

After establishing that bone strength is measured directly by mechanical testing and indirectly through imaging techniques, the mechanisms by which bone alters its mass, shape and strength can now be introduced and later applied to disease states. Bone is a dynamic structural material, in that it constantly makes adjustments to preserve its mechanical competence based on the prevailing loads it endures. In addition, bone is considered a minimal-mass structure [18], meaning that bone aims to be as strong and efficient as possible at the lowest metabolic costs associated with maintaining bone mass. Thus, as previously alluded to, expanding periosteal bone diameter is one means of improving bone strength without increasing bone mass, and therefore, metabolic demand.

Mechanical loading is theorized to be the primary factor that stimulates bone to self-regulate its functional, geometric, and intrinsic material properties. Prior to discussing these processes, it is necessary to define: how mechanical loading is sensed by the bone tissue, the cells within bone tissue that sense the mechanical load, and how the bone

responds to loading including the theory that governs this response.

2.2.1 Definition of Strain

The quantifiable unit of mechanical loading in bone is the strain applied to the bone. Prior to defining strain, it is necessary to define stress. Stress in any material is defined as the load per unit area. Once stress is placed on the bone, the bone deforms and the resulting change in length caused by the load, relative to the original length, represents the applied strain and is reported in units of microstrain (or may be denoted as $\mu\epsilon$).

The mechanism(s) by which strain is sensed by the bone cells remains elusive. However, osteocytes have been theorized to be the primary sensors of mechanical loading (Figure 2.8). Osteocytes are presumed to be the mechanosensors of mechanical loading for the following reasons: (1) osteocytes are the most abundant cell type within bone, (2) osteocytes are strategically placed within the bone matrix and have vast 3-dimentional communication networks with neighboring osteocytes (via gap junctions), and (3) osteocytes can live up to 15-20 years without replication [19, 10].Thus osteocytes are the best candidates for sensing mechanical loading-induced strain as well as initiating bone remodeling upon their death.

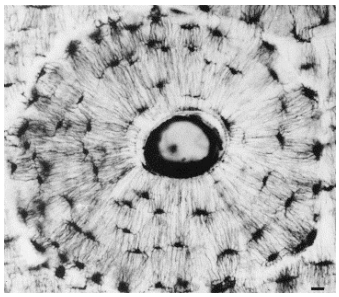

Figure 2.8: Osteocytes and their canaliculi (i.e. cell processes) are shown in black, where the cortical bone is white. (Reprinted from [20] with permission from Elsevier).

The importance of osteocytes in the sensation and response of bone to mechanical loading has only begun to emerge in the past decade. For example, reductions in osteocyte number and sensitivity are thought to be contributing factors to the decline in bones response to mechanical loading with age. Specifically, the viability of osteocytes

declines by 15% with age in adulthood [19]. In addition, others have noted lower osteocyte density in deep bone (>45μm from the surface) compared to more superficial bone [21], which is hypothesized to impact how bone perceives and responds to mechanical loads. Combined, age-associated bone loss may be partially attributed to a decreased number of viable osteocytes as well as an altered strain sensing capacity, which may translate to a blunted response to mechanical loading, resulting in a reduction in bone mass.

2.2.2 Mechanostat Theory of Bone Self-Regulation

After establishing that bone has the capacity to perceive mechanical loading via osteocytes, the response of osteocytes, pertaining to the regulation of bone mass and structure, to loading environments can now be discussed. The proposed theory of adaptation is referred to as the Mechanostat theory, developed by Harold Frost [22]. The basis of the Mechanostat theory is that a particular bones typical loading environment will dictate the bones mass and where this mass is structurally placed.

The Mechanostat theory suggests that bones response to mechanical loading is similar to that of a thermostat. To set the stage, consider that the thermostat in a home is set to 72 ^{o}C. When the temperature is below 72 ^{o}C, error signals, or negative feedback loops, will be transmitted from thermostat to turn the furnace on until the temperature in the room reaches the desired threshold. The same applies if the temperature were to exceed 72 ^{o}C, which could initiate an error signal to turn the furnace off. In bone, strain levels are the stimulus for negative feedback loops (Figure 2.9). Specifically, when strains perceived by osteocytes are higher than normal, osteocytes will initiate cellular responses to increase bone formation in effort to lower the strain magnitude associated with a given mechanical load. This pathway will continually be activated until enough bone is formed to sufficiently reduce the stress applied to the bone, and therefore bring the associated strain of a given mechanical load, back within the typical range of strain levels. The opposite also occurs when strains are lower than normal. Specifically, following reductions in typical strain levels, bone will undergo resorption (i.e., the removal of bone mass) causing stress levels, and therefore strain to increase.

Another way the Mechanostat theory has been presented it shown in Figure 2.10. In this diagram, normal loading patterns, or typical strain levels, are shown in the central

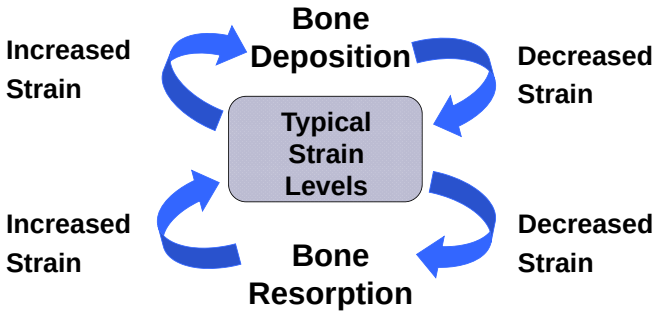

Figure 2.9: The Mechanostat theory suggests how bone responds to alterations in typical levels of mechanical loading. For example, bone deposition results on the periosteal surface when strain magnitudes exceed typical levels. This increase in bone area acts to decrease the stress and strain associated with a given load and therefore, the bone returns to the initial typical strain level. The opposite occurs during periods of unloading, where the reduction in typical strain levels causes bone to be removed. As a result, strains that were previously considered typical will now be perceived by the bone as elevated strain, and will result in bone deposition. (Modified with permission and Copyright 1984 from Springer Science and Business Media and the *Calcified Tissue International* [23]).

rectangle. When strains are lower than normal, the bone is considered to enter a stage of disuse (e.g., inactivity, bed rest or disease), and bone loss will occur through a process called bone remodeling (described later in this chapter). As a result, bone strength will decrease relative the amount of inactivity (shown as the black line in Figure 2.10). In response to overload, bone modeling is initiated (described later in this chapter), which typically places bone on the periosteal surface to increase the diameter and strength. Further detailed explanations and evidence for overload and disuse follow in the next two sections.

2.2.3 Bone Modeling versus Remodeling

Beyond osteocytes, there are two other primary types of cells in bone: osteoclasts and osteoblasts. Osteoclasts resorb, or remove, bone that is old, damaged, or no longer needed. Osteoblasts synthesize new bone and regulate the deposition of mineral within bone. These cell types are then involved in two processes called bone modeling and bone remodeling. Bone modeling occurs in response to two primary stimuli: longitudinal limb

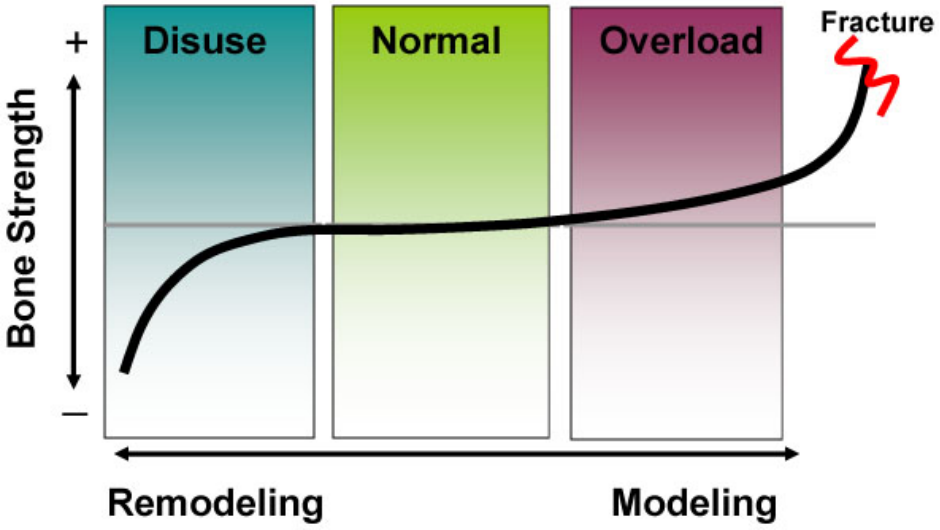

Figure 2.10: When mechanical loading results in strains that exceed typical levels, the bone enters a stage of overload, causing the bone to deposit bone on the periosteal surface (i.e., modeling). The increase in bone mass further from the neutral axis also increase bone strength. The opposite occurs during periods of unloading, where the reduction of strain levels from normal causes bone to enter a stage of disuse, where bone is removed, and bone strength is detrimentally compromised. (Reprinted and Modified from [24]), Copyright 2002, with permission from Elsevier).

growth during childhood, and overload in adults.

During childhood bone modeling, osteoclasts and osteoblasts are simultaneously removing and forming bone; however, these cells are working on two different surfaces of the bone. This approach results in bone growth in length and width, by simply removing bone from one region of bone and placing it in another. Specifically, osteoclasts remove bone from the inner surface of the marrow cavity as well as the epiphysis (Figure 2.11A). This bone material is then utilized by osteoblasts to place bone on the periosteal surface and on the ends of the bone to increase the width and the length (Figure 2.11A), resulting in increased bone strength. Beyond longitudinal growth, bone modeling occurs on the periosteal and endocortical surfaces, but at much slower rates (Figure 2.11B). While this is advantageous in childhood, the bone eventually reaches a point of diminishing returns, and continued modeling may actually predispose the bone to fracture late in life.

Bone remodeling on the other hand, removes and replaces bone that is old or damaged with new bone. Specifically, osteoclasts and osteoblasts work in tandem to each other on the exact same region of bone (Figure 2.12). Through this process, the entire skeleton is completely replaced approximately every 10 years. Thus, skeletal issues with age are not due to the bone being old, but rather inefficient bone remodeling (e.g., bone resorption may exceeds bone formation leading to net bone loss) or alterations in the material properties of bone (i.e., minor substitutions in the chemical structure of bone material, which change the structural integrity of bone material). The other case in which bone remodeling is commonly initiated is disuse. In disuse-mediated remodeling, the bone that is resorbed is no longer needed due to the decreased stress/strain associated with disuse, and is removed to lower the metabolic cost of maintaining this bone tissue. Bone formation may follow to a minimal extent.

2.2.4 Overload: Mechanical Loading is Higher than Normal

Overload, or overuse, is a term typically utilized to describe periods in which the bone experiences strains that are higher in magnitude than normal. Animal models (e.g., rat and turkey) have been employed to characterize the response of bone to overloading[28, 29]. An example of functional and geometric benefits of overloading bone is demonstrated in Figure 2.13A, in which external loading was applied to the right ulna of rats [28].

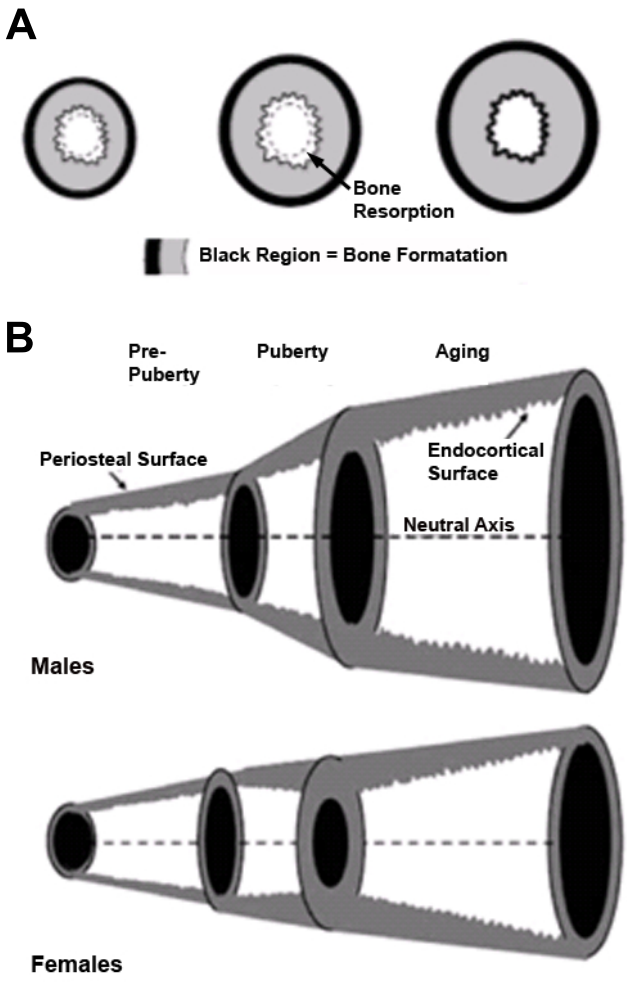

Figure 2.11: A) Growth-induced alterations in cortical bone structure (i.e., increase in age from left to right) are attributed to the expansion of the periosteal surface due bone formation as well as expansion of the marrow cavity associated with endocortical resroption. (Reproduction with permission and Copyright 2002 from John Wiley and Sons and the Journal of Bone and Mineral Research [25]). B) Age and sex differences in periosteal bone formation and endocortical resorption in long bones across the lifespan. (Reproduction with permission and Copyright 2008 from Springer Science and Business Media and the *Journal of Bone and Mineral Metabolism* [26]).

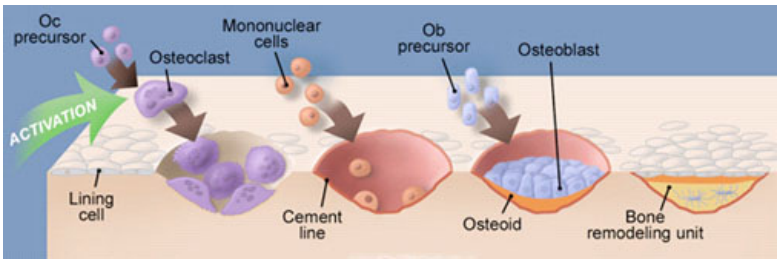

Figure 2.12: Bone remodeling is initiated by the removal of bone tissue by osteoclasts. At this same region of bone, the resorption pit created by osteoclasts is slowly filled in one layer at a time by osteoblasts (i.e., labeled osteoid). (Image courtesy of IBMS BoneKEy, [27]).

Histological findings indicate that bone apposition, or formation, was apparent in the loaded limb compared to the non-loaded limb (i.e., region of bone between the red and green labels in the right panel of Figure 2.13B). Consistent with other animal models, bone accumulation was not random, but was strategically placed in regions where strain levels were highest. The net result of overload is increased CSMI and bone strength of the loaded limb, making the bone structurally and functionally adapted to the new loading environment compared to the non-loaded limb.

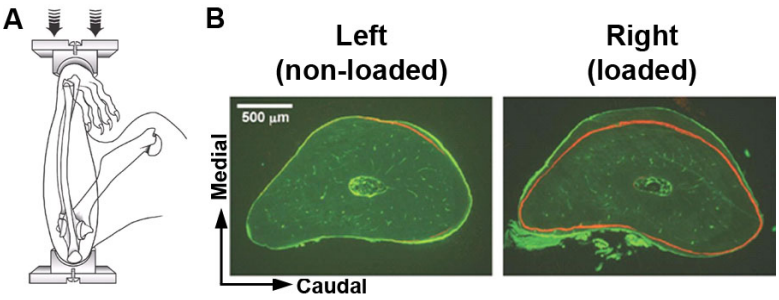

Figure 2.13: (A) The rat ulnar mechanical loading model developed by Turner and Robling applies a strain directly the bone. This technique is typically performed on a single forearm, such that the contralateral limb serves as a control. B) In response to this form of loading, bone formation strategically occurs in regions of the ulna that experienced overload. Bone formation is indicated by dynamic histomorphometry, which fluorescently labels the surfaces of bone at baseline (i.e., red line) and one day prior to sacrifice (i.e., green line). The region of bone formed between the red and green labels represents bone formation. (Reproduced with permission and Copyright 2002 of the *Journal of Bone and Mineral Research* [30]).

2.2.5 Disuse: mechanical Loading is Lower than Normal

On the other hand, during periods of disuse such as immobilization (e.g., casting), bed rest, space flight, disease, or hindlimb unloading, the bone endures strains that are lower than normal. As a result, the bone is essentially over-adapted to the new loading environment (there is more tissue than what is needed to support the reduced function of the bone), which places an unnecessarily high metabolic demand on the tissue [31]. This triggers a cascade of events that will remove unnecessary bone mass, typically from the endocortical surface or within the cortical wall. Radiographic comparisons of young dogs casted for 40 weeks compared to controls demonstrates this dramatic loss of bone that results from periods of disuse (Figure 2.14)[32].

Figure 2.14: Radiographic images depicting the bone loss that resulted from 40 weeks of casting (bone on the right compared to the healthy bone on the left) in young dogs. (Reproduced with permission and Copyright of the British Editorial Society of Bone and Joint Surgery [32]).

As bone enters a stage of disuse, both trabecular and cortical bone will be lost; however, the rates and timing of bone loss are different for each type of bone. Specifically, trabecular bone loss begins in the acute stages of immobilization, when bone formation rates decrease [33, 34, 35, 36, 37] and trabecular resorption rates increase [35, 36, 37]. The combined result is a decline in trabecular number, connectivity, and bone area [35]. Disuse-mediated bone loss has also been shown to reduce the mechanical competence of trabecular bone by 26-72% compared to controls [38]. Bone loss from hindlimb unloading in rodents and casting in dogs has been reported to cease between

10-18 weeks, indicating that enough bone loss has occurred to re-establish a balance between bone mass and the stresses and strains, as previously described by Mechanostat theory (Figures 2.9 and 2.10) [39, 35].

Compared to trabecular bone, periosteal cortical bone adapts to disuse via a two-step process with formation nearly ceasing within two weeks of disuse followed by a significant increase in endocortical resorption (see example in Figure 2.15) [35, 32]. As a result, the periosteal diameter remains constant, while the marrow cavity expands to reduce cortical thickness. Bone resorption in cortical bone has been suggested to stabilize around 18 weeks in hindlimb unloading models [35], however up to 60 weeks is required in casting models [39].

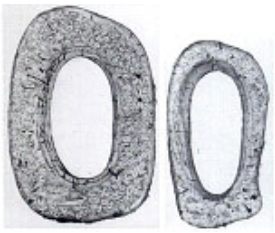

Figure 2.15: Images represent transverse histological sections of cortical bone from dogs that have either undergone hindlimb unloading (bone on the right) or typical loading patterns (bone on the left). Hindlimb unloading deleteriously altered bone geometry, as indicated by the lack of periosteal expansion and increased marrow cavity. This results in a thinner and smaller bone. (Reproduced with permission and Copyright of the British Editorial Society of Bone and Joint Surgery [32]).

Typically, the net bone loss during periods of disuse is reversible upon re-ambulation [40, 41]. Applying the Mechanostat theory to this situation, would suggest that re-ambulation initiates a state of overload, driving bone formation to reduce the newly-increased strains applied to the bone during walking. However in cases such as spinal cord injury or progressive muscle diseases like Duchene muscular dystrophy, ambulation may not be regained and thus, alternative means of preserving bone mass are warranted.

2.3 Background of Skeletal Muscle and Muscle Diseases Related to Bone

2.3.1 Skeletal Muscle Function

A skeletal muscle is composed of a series of nested bundles. These bundles sequentially decline in size with fascicles being the largest, followed by muscle fibers and myofibrils being the smallest. The contractile elements within each myofibril (i.e., myosin and actin) are arranged into structures called sarcomeres, which align in series and in parallel (Figure 2.16). The activation of cross bridging between actin and myosin, results in the production of force. The contractile action of the muscle also results in the synchronous folding of the sarcolemma, or the sheath surrounding the myofibril. Through this action, a fraction of muscle force is transmitted longitudinally within the muscle to the tendon, while the majority of the force is transmitted laterally to the sarcolemma.

The key structural elements that transfer force laterally from myofibrils to the sarcolemma are found in the dystroglycan complex and are referred to as costameres (Figure 2.17). The function of costameres is to: 1) physically attach peripheral sarcomeres to the sarcolemma and coordinate synchronous folding of the sarcolemma, and 2) connect neighboring sarcomeres to one another facilitating maintenance of coordinated sarcomere length during activation [43]. Thus, the contractile elements within sarcomeres produce force that is transferred laterally by structural elements to the sarcolemma and tendon resulting in the transmission of stresses and strains to the bone.

2.3.2 Skeletal Muscle Disease

In the previous section, the function of the dystroglycan complex and the costamere were introduced and their role in stabilizing muscle fibers and transmitting force was emphasized. This is important because various mutations are known to occur in certain proteins in the dystroglycan complex, resulting in the development of muscular dystrophies. Depending on the location of the mutation, there is either a lack of force production or an absence of force transmission [43].

The most common muscular dystrophy is Duchene Muscular Dystrophy (DMD),

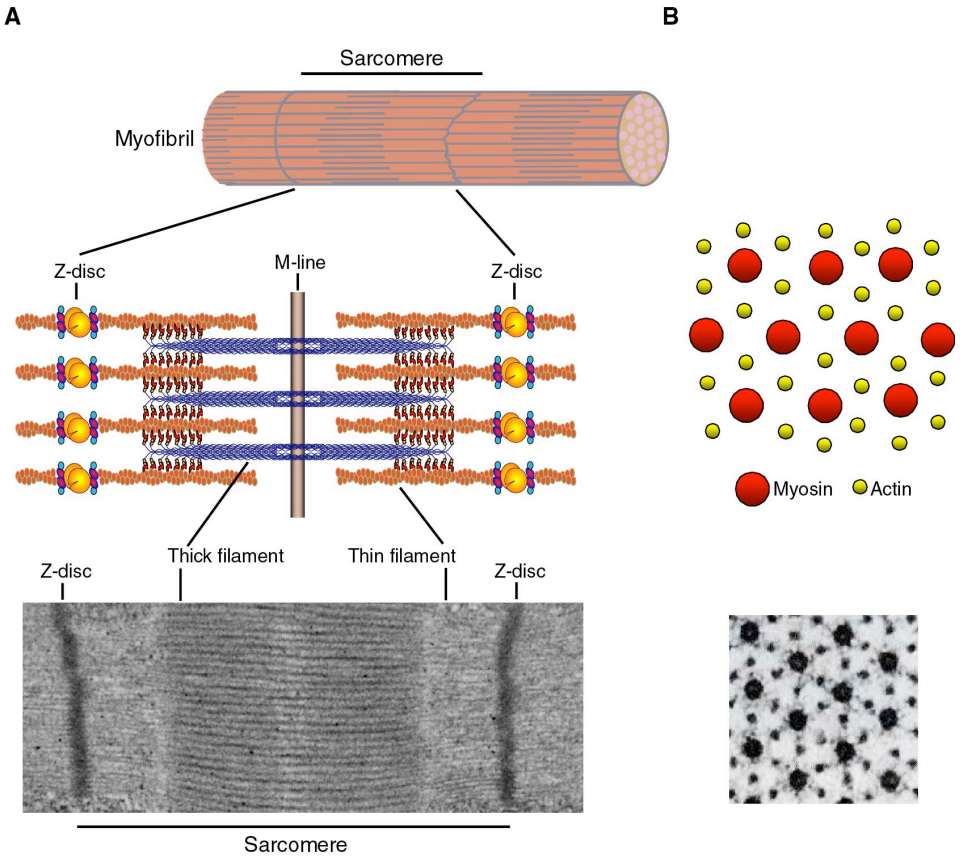

Figure 2.16: Cross bridging of the myosin and actin proteins in the sarcomere results in force production, which is then transferred laterally to the sarcolemma. (Reproduction with permission and Copyright 2012 of Wiley Periodicals, Inc. [42]).

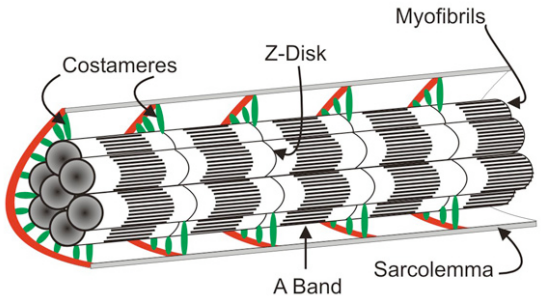

Figure 2.17: Costameres (denoted by green lines) serve as tethers between the z-disk of the myofibril and the sarcolemma, and thus are circumferentially arranged. These protein complexes act to transfer the force produced by the contractile proteins within the sarcomeres laterally to the sarcolemma. (Reproduced with permission from the *Journal of Biological Chemistry* [43]).

which impacts 1 in 3500 male births [44]. DMD is caused by a mutation in the dystrophin gene (located on the X chromosome), which encodes for the production of the dystrophin protein. The presence of a mutation does not prohibit the production of the protein dystrophin; however, the structure and function of the protein are affected. The dystrophin protein is responsible for 1) organizing costameres and maintaining sarcolemma integrity [45, 46] and 2) limiting the movement of molecules into and out of cells [47, 48]. Thus the lack of dystrophin causes sarcolemma instability which leads to a host of downstream events including reduced force production [49].

While the complete pathophysiology of DMD remains elusive, DMD is characterized by contraction-induced muscle injury resulting in a loss of force production [45, 50, 51]. As the disease progresses, damaged contractile elements are replaced by connective tissue and fat [45, 50, 51] giving the muscle a pseudo-hypertrophied appearance beginning around the age of 4 years. The lower extremities tend to be affected by disease first and proximal muscles are more affected than distal muscles [51]. Contractures of the elbows, knees and hips also develop [51], resulting in the loss of independent ambulation and making boys wheelchair bound by the early teenage years [[52, 44, 53]. As a consequence of disease progression, boys with DMD become progressively inactive and unable to independently perform activities of daily living.

2.3.3 Effects of Duchene Muscular Dystrophy on bone

As dystrophic muscle becomes weaker, fewer and less forceful contractions are applied to the bone. This in theory causes the bone to enter a stage of disuse resulting in bone loss. The majority of studies to date investigating skeletal health in boys with DMD have focused solely on areal bone mineral density (aBMD) determined by DXA as an indicator of bone health [54, 2, 1, 55, 56] as the use of pQCT to characterize bone geometry have only been reported in abstract form [5, 6]. These data consistently show that aBMD is reduced in various skeletal regions of boys with DMD compared to age matched peers (exemplar data are shown in Figure 2.18).

The importance of muscle-induced mechanical loading in maintaining skeletal health is also highlighted in Panel B of Figure 2.18. Specifically, following the loss of independent ambulation at ∼10 years of age (range: 7.4 to 11.6y), hip aBMD in boys with DMD (i.e., filled squares) begins to drastically deviate from their peers (i.e., open circles) [55]. Similar findings have been reported for the hip, where the bone mineral density values for boys with DMD fell nearly 4 standard deviations below the mean of their peers after becoming wheelchair bound [2]. Combined, these data highlight the secondary losses in bone mass that result from the loss of muscle strength and the inability to perform simple activities such as walking or standing.

The main functional consequence of bone loss is that the weaker bone is predisposed to fracture. Therefore, it follows that, boys with DMD have an elevated risk for fracture (18-44%) compared to matched controls, which is more pronounced as the disease progresses [2, 1, 3]. These fractures predominately occur in the lower limb after falling from standing or sitting height, classifying them as fragility fractures [3, 57].

In an effort to impede the progression of muscle deterioration, the glucocorticoid prednisone is the treatment of choice. Prednisone has been shown to thwart muscle deterioration, improve physical endurance, decrease falls, improve stair climbing, and prolong independent ambulation in patients with DMD [58, 59, 60]. Simultaneous to these benefits to muscle tissue, glucocorticoids induce osteoporosis and increase fracture risk by increasing osteocyte and osteoblast apoptosis as well as extending the lifespan of osteoclasts [61, 62, 63]. Specific to DMD, the use of glucocorticoids has been shown to accentuate reductions in bone mass and density [1, 55, 64], increase the incidence of long

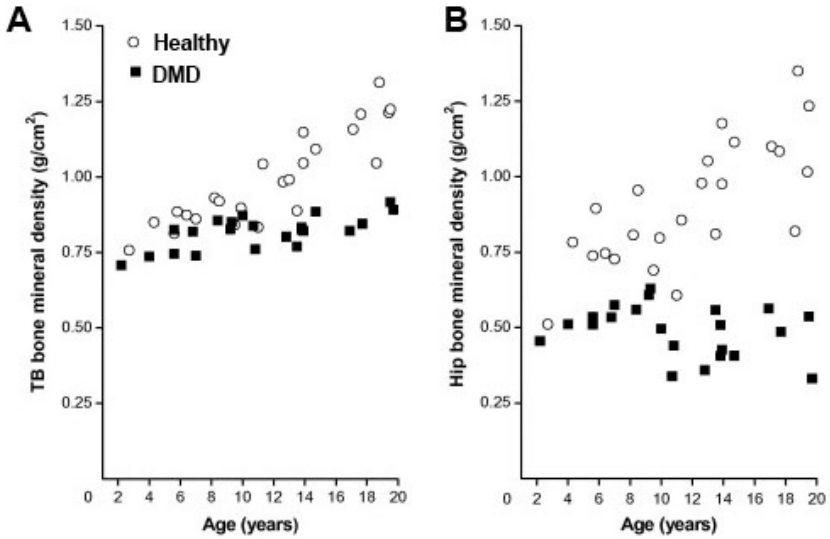

Figure 2.18: Each data point represents a childs bone mineral density for (A) the total body and (B) the hip. Boys with DMD are shown as filled squares and their age-matched peers as open circles. The differences in bone mineral density between groups increased with age, however the largest deviations occurred in the hip around the time that ambulation was lost (i.e., 10 years of age). (Reprinted from [55], Copyright 2007, with permission from Elsevier).

bone fractures by nearly three-fold [64], and provoke the emergence of vertebral compression fractures which do not occur in DMD patients not treated with glucocorticoids [64, 65]. These results suggest that altered osteoblast and osteoclast viability disrupts the homeostasis of bone remodeling and therefore may translate to compromised bone structure and strength. Considering that bone is inherently compromised in strength and has altered geometry in individuals with DMD [13, 5, 6, 7, 8, 66, 4], the addition of glucocorticoids and reduced physical activity may cause further decrements to the structural and material integrity of bone. The combined contributions of these insults have not been thoroughly investigated prior to our work (See Chapter 4 for details).

2.3.4 Dystrophic Mouse Models

Two established mouse models of DMD (i.e., *mdx* and *dko* mice) are often utilized to characterize the disease as well as identify potential therapies. The *mdx* mouse model has a single point mutation in the dystrophin gene and has been shown to develop many of the hallmark characteristics of DMD including progressive muscle weakness [67]. The severity of the diseases, and therefore the phenotype, of *mdx* is mild compared to boys with DMD. The mild phenotype is attributed to the upregulation an analogous protein of dystrophin, called utrophin. Utrophin in *mdx* mice functions similar to dystrophin and as such is able to rescue the phenotype. This utrophin-induced reversal of the disease typically begins around 10 weeks of age. As a result, the *mdx* model may not be suitable for investigating long-term deteriorating bone health in DMD.

The *dko* model on the other hand is a more severe model of DMD and its phenotype better mimics DMD than does the *mdx* mouse model. *Dko* mice are deficient in both dystrophin and utrophin, and therefore lack the ability to rescue the muscle disease and reverse the phenotype, making the model more similar to the disease progression observed in humans. In these mice, muscle weakness begins early in life and progresses quickly leading to joint contractures and premature death at $\sim$10 weeks of age [68].

At the time of my dissertation proposal, only two studies had utilized *mdx* mice to investigate bone health [7, 8] and none had utilized the *dko* mouse model. Anderson reported that tibial bones were weaker in 4- and 18-week old *mdx* mice, compared to age-matched, wildtype mice [7]. The reduction in bone health was indicated by smaller ultimate loads, smaller cross-sectional areas, and thinner cortical walls. In contrast,

Montgomery et al. found that 16-week old *mdx* mice had stronger, wider and denser femurs compared to those from wildtype mice [8], but these genotypic differences were abolished after adjusting for the greater body mass of the *mdx* mice. Thus, it remained elusive whether or not *mdx* bones were functionally compromised as a secondary consequence of the muscle disease.

The results of Montgomery et al. and Anderson et al. provided a foundation of bone geometry and functional properties in *mdx* mice; however, better characterization of bone was warranted especially in the window of time where functional declines in muscle are taking place (i.e., less than 12 weeks of age). To address this, my preliminary work compared (1) tibial bone geometry and (2) trabecular bone architecture of both *mdx* and *dko* mice at 7-weeks of age relative to wildtype mice. My data indicate that *mdx* mice have reduced: bone strength, cortical geometry and trabecular architecture compared to wildtype mice (described in Chapter 3). This study also characterized the *dko* mouse model of DMD and established that *dko* mice are more severely affected than *mdx* mice

In a subsequent study, discussed in Chapter 4, I showed that reduced physical activity and prednisolone treatment (i.e., the active form of the drug prednisone) independently accentuate reductions in bone strength and geometry in *mdx* mice, but do not influence the intrinsic material properties of the bone tissue. The effects of physical inactivity had greater impacts than prednisolone, highlighting the importance of maintaining physical activity levels in patients with DMD. Because DMD is accelerated by exercise-induced injury, alternative mechanisms for improving bone strength are warranted that do not necessarily require high-force muscular contractions. The development of low magnitude high frequency vibration could become an attractive therapy for those with DMD as it directly applies mechanical loads to the bone, equivalent in strain magnitude as those produced by postural-muscle activation patterns, while circumventing the need for the muscle to actually contract.

2.4 Low Intensity, High Frequency Mechanical Vibration

Low intensity vibration as a therapeutic modality has been receiving increasing attention as a non-invasive tool to improve musculoskeletal health, despite a lack of clear mechanistic pathways. Chronic exposure to short bouts of low-acceleration, high-frequency vibration have been shown to improve muscle power and strength [69], thwart bone loss [70, 71, 72], provoke an anabolic bone response [73], and enhance bone strength as well as reduce fracture risk [74]. The follow section will provide a brief background of the most commonly theorized mechanisms of action and why vibration is an attractive modality for DMD.

Bones response to mechanical loading is governed by the Mechanostat theory (discussed in Figures 2.9 and 2.10). It is important to realize however, that bone responds to a continuum of strains (i.e., 10 to >2000 microstrains), and does not preferentially respond to high intensity strains. This response to mechanical loading is governed by an inverse power law (Figure 2.19), which indicates that a few high-intensity loads are just as effective to maintain bone strength as thousands of low-intensity loads (i.e., pink line in Figure 2.19) [75]. Thus, to maintain skeletal health 1-3 high-intensity loads, such as running or jumping, may be just as effective as the activation of postural muscles (i.e., 10 microstrains) ∼800,000 times per day.

Low intensity, high frequency vibration operates on the low intensity microstrain end of the inverse-power law continuum, and has been suggested to act as a surrogate for muscle contractions [76]. Activation patterns of postural muscles during vibration are similar to those produced during standing [77]. Thus, vibration is an attractive therapeutic modality to maintain, and potentially improve, bone health in disease populations where muscle strength and function, and thus bone are impacted. For DMD patients, who are advised to avoid high intensity loads due their propensity to cause muscle damage, the low intensity nature of vibration makes it an attractive therapeutic modality to preserve bone health, especially as disease progression causes muscle weakness and physical inactivity increase.

Despite reports of beneficial effects of vibration (see Appendix 1 for results in rodents), the overall efficacy of low intensity vibration has been challenged due to inconsistent findings across studies and the lack of clinically-meaningful results across various

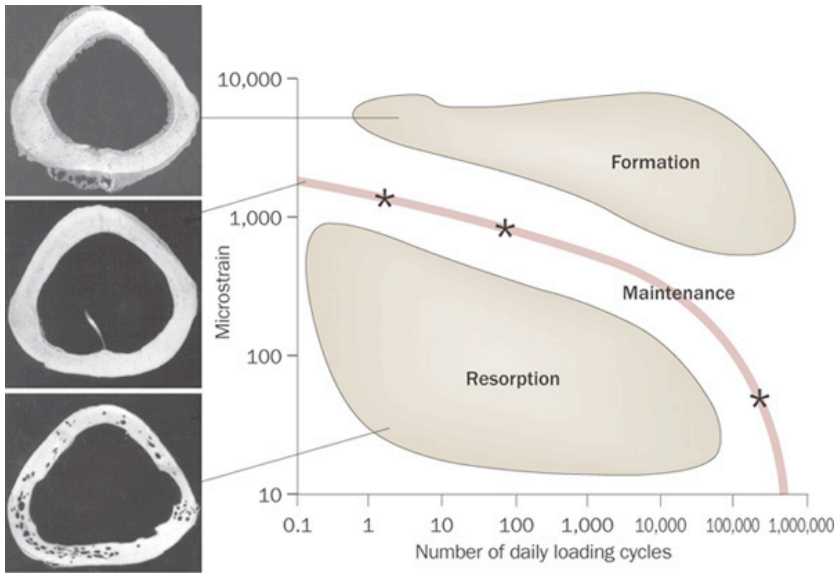

Figure 2.19: Bones response to mechanical loading has been shown to follow an inverse power law between the cycle number and strain magnitude. Maintenance of bone mass exists on a continuum (denoted by the pink line), and therefore a number of distinct loading strategies can be utilized to prevent bone resorption. Thus four cycles at 2,000 microstrain may be just as effective as hundreds of thousands of cycles of signals of well below 10 microstrain. In addition, falling below or above the preferred strain continuum would result in bone resorption or formation, respectively. (Reprinted by permission from Macmillan Publishers Ltd: *Nature Reviews Rheumatology* [75], copyright 2010).

populations [78]. This lack of efficacy may be the result of applying sub-optimal vibration parameters, such as frequency and acceleration, to the model of interest. Judex et al, for example, found that the osteogenic response to a single set of vibration parameters in differed greatly among three commonly used genotypes of healthy mice [79]. Similar findings have been noted in humans. Specifically, the musculoskeletal response to vibration exposure appears to be more robust in compromised skeletons such as those of disabled children, postmenopausal women or women with low bone mass, compared to healthy skeletons [80, 81, 82]. It is reasonable to assume that the musculoskeletal systems response to vibration may not be equivalent across disease models, sexes, age ranges or other modifiable factors. This highlights the importance of individualizing parameters of the mechanical signal delivered by vibration equipment to the model or disease of interest in order to evoke the greatest response. The issue is addressed in further detail in Chapter 5. Upon determining osteogenic parameters of vibration for dystrophic mice, the efficacy of 8 weeks of vibration training to alter bone strength, geometry and material properties in mice is addressed in Chapter 6.

2.5 Summary

Mechanical loading plays a substantial role in determining bone strength, geometry, and material properties. Declines in bone health are known to occur following reductions in mechanical loading (i.e., casting, bed rest, and hindlimb unloading) and are thought to be predominately attributed to alterations in muscle-induced loads applied to bone. Thus, in muscle diseases such as DMD, disuse-mediated bone loss is hypothesized to be initiated in response to progressive muscle weakness and physical inactivity. The loss of bone mass likely deleteriously impacts bone strength and would contribute to the increased rate of fragility fractures that are known to occur in this population.

Low intensity, high frequency vibration is hypothesized to act as a surrogate for muscle-induced loading of bone, making it an attractive therapeutic modality to preserve, and perhaps improve, bone health in DMD. Chronic exposure to short bouts of vibration has been shown to improve muscle power and strength [69], thwart bone loss [70, 71, 72], provoke an anabolic bone response [74], and enhance bone strength as well as reduce fracture risk [74]; however, it remains to be determined how efficacious

vibration training would be for musculoskeletal health in DMD

Chapter 3

Bone is functionally impaired in dystrophic mice but less so than skeletal muscle

Susan A. Novotny[1], Gordon L. Warren[2], Angela S. Lin[3], Robert E. Guldberg[3], Kristen A. Baltgalvis[4], and Dawn A. Lowe[5]

[1]Department of Kinesiology, University of Minnesota, Minneapolis, Minnesota

[2]Division of Physical Therapy, Georgia State University, Atlanta, Georgia

[3]Institute for Bioengineering and Bioscience, Georgia Institute of Technology, Atlanta Georgia

[4]Department of Biochemistry, Molecular Biology, and Biophysics, University of Minnesota, Minneapolis, Minnesota

[5] Program in Physical Therapy and Rehabilitation Sciences, University of Minnesota, 420 Delaware Street SE, Minneapolis, Minnesota 55455, USA

3.1 Abstract

The primary purpose of this study was to determine if tibial bone strength is compromised in dystrophic mice and if so, what geometric and material properties contribute. Results of three-point bending tests showed that tibia of *mdx* and *dko* (dystrophin- and utrophin-deficient) mice had up to 50% lower strength and stiffness compared to wild-type mice. Micro-computed tomography indicated that dystrophic tibia had reductions of 6-57% in cortical cross-sectional moment of inertia and cross-sectional area. Metaphyseal trabecular bone morphometry was also altered up to 78% in dystrophic mice. Bone-to-muscle functional ratios (i.e., three-point bending measures:muscle strength) indicated that bone strength was relatively high in 7-week-old dystrophic mice compared to muscle strength, but ratios were similar to wild-type mice by 24-months of age. Thus, as in boys with Duchenne muscular dystrophy, young dystrophic mice have compromised bone strength; these models may be useful for designing therapeutic regimens aimed at improving the skeleton.

3.2 Introduction

Bone fractures are on the rise in the nearly 8,000 boys in the United States affected by Duchenne muscular dystrophy (DMD), with little progress being made toward remediation [2, 1, 3, 83]. DMD is characterized by progressive muscular weakness attributed to contraction-induced muscle injury followed by inefficient repair [84]. Thus as the disease progresses, boys become less physically active and unable to perform activities of daily living [53, 52, 44], both of which reduce the frequency and magnitude of mechanical loads placed on bone. As a result, bones should enter a stage of disuse, resulting in bone loss and structurally weakened bones that are more prone to fracture. Indeed, fracture incidence in boys with DMD is reported to be between 18-44%, where higher incidence rates parallel increases in age, physical limitation and disease state [2, 1, 3]. Fractures typically occur in the lower extremities after falling from standing or sitting height [3, 57], indicating that bone strength is compromised. This loss of bone strength may be due to altered bone geometry and/or other extrinsic or intrinsic material properties (e.g., density or composition of the bone). Dual energy X-ray absorptiometry (DXA) has been utilized to monitor the loss of areal bone density in various skeletal regions with age in DMD [2, 55], but the relative contribution of bone loss and that of compromised bone geometry and material properties to bone strength have not been evaluated in DMD. Delineating the roles of these factors will provide a better indication of whole bone function and fracture risk in the context of muscular dystrophy.

Mouse models of DMD are available and these could aid in the assessment of the diseases effect on bone strength and its underlying mechanical determinants including geometric and intrinsic material properties. There have only been two studies on bone in a DMD mouse model and both utilized the *mdx* mouse [7, 8], the most commonly used animal model of DMD. Similar to boys with DMD, *mdx* mice have dysfunctional dystrophin protein, and as a result develop characteristic muscle weakness early in life, i.e., between 15-20 days of age [85]. Anderson et al. reported that the tibia is weaker in 4- and 18-week-old *mdx* mice, compared to that of age-matched, wild-type mice [7]. The bone weakness was indicated by lower ultimate load, smaller cross-sectional area, and thinner cortices. In contrast, Montgomery et al. found that 16-week old *mdx* mice had stronger, wider and denser femurs compared to those from wild-type mice [84]. In this

latter study, after adjusting for the greater body weight of *mdx* mice, no differences in bone characteristics were detected between *mdx* and wild-type mice. Thus, it remains to be determined whether or not *mdx* bones are functionally compromised as a secondary consequence of the muscle disease.

DXA, X-ray, and histomorphometry are traditional methods used to analyze bone and were used in the two aforementioned studies. A newer and more sensitive technique is micro-computed tomography (μCT), which simultaneously quantifies bone volumetric density and geometry at a higher resolution providing more sensitive assessment of bone. Furthermore, μCT is a non-destructive imaging technique that allows for subsequent evaluations of the bones composition and functional properties to be performed on the same specimen. Collectively, these approaches can be utilized to investigate bone strength and elucidate the mechanisms underlying a loss in bone strength that occur as a result of muscular dystrophy. This information may provide insight for designing strategies that could be used to offset the deleterious effects of the disease on bone.

Therefore, the primary objective of our study was to determine if *mdx* mice indeed have compromised bone compared to wild-type mice, and if so, what geometric and material properties contribute. Specifically, three-point bending tests, μCT imaging and measurements of bone composition were utilized to assess bone strength, geometry and intrinsic material properties of the tibia, respectively. We also used these strategies to assess bone in a second model of DMD, *dko* mice. *Dko* mice lack functional dystrophin and utrophin proteins resulting in a more severe phenotype of the disease relative to *mdx* mice [86]; this phenotype is more similar to that seen in boys with DMD.

Another objective of the study was to directly evaluate the functional relationships between muscle and bone in this mouse model of muscle disease. Previous studies have suggested that skeletal muscle not only provides an anabolic stimulus to bone but is also required to maintain the structural competence of bone [87]. Thus, according to the mechanostat theory [22], the loss of muscle function with DMD disease progression should translate to proportional declines in tibial bone size and strength. To address this theory, we calculated bone-to-muscle ratios of functional capacity using our measurements of ultimate load and stiffness for the tibial bone and force generating capacities for the extensor digitorum longus (EDL) muscle. We hypothesized that dystrophic mice would exhibit similar bone-to-muscle ratios as those of wild-type mice, indicating that

their tibial bone function is diminished to a similar extent as the contractile function of the adjacent EDL muscle.

3.3 Methods

3.3.1 Animals and Experimental Design

Four wk-old wild-type (C57BL/10) and *mdx* mice (n=8 and 7, respectively) in addition to 8-mo-old wild-type and *mdx* retired breeders (n=9 each) were obtained from Jackson Laboratories (Bar Harbor, ME). Four wk-old *dko* mice (n=7) were obtained from our colony [88]. All wild-type and *mdx* mice were male; *dko* mice were male and female (n=4 and 3, respectively). Female *dko* mice were included due to the limited availability of male *dko* mice. Mice were housed in groups of four on a 12:12-h light-dark cycle at 20-23 ^{o}C under pathogen-free conditions. All mice were provided food and water ad libitum. All procedures were approved by the Institutional Animal Care and Use Committee at the University of Minnesota.

At the age of 7 wk or 24 mo, mice were weighed, anesthetized with sodium pentobarbital (100 mg/kg i.p.), and EDL muscles were dissected for contractile analyses. Mice were then sacrificed with an overdose of sodium pentobarbital (200 mg/kg) and tibial bones were excised. These bones were stored in phosphate-buffered saline at -20 ^{o}C until the time of analysis. The 7 wk age was chosen because it was thought to best reflect a time point with functional declines in both muscle and bone. Additional rationale for selecting the 7 wk time point was that it approximates the average lifespan of *dko* mice in our colony. Despite a report that the average lifespan of male *mdx* mice is 21.5 mo [84], all of our *mdx* retired breeders lived to 24 mo and remained apparently healthy. Therefore the 24-mo-old *mdx* mice in this study were mice that had lived with a chronic muscle disease.

3.3.2 Contractility of EDL Muscle

EDL muscle contractile function was measured as previously described [89, 90]. Briefly, the muscle was placed in a 0.38-ml bath assembly filled with KrebsRinger bicarbonate buffer that was maintained at 25 ^{o}C; the proximal tendon was connected with 6-0 suture

to the arm of a dual-mode muscle lever system (300B-LR; Aurora Scientific Inc., Aurora, ON, Canada). Optimal muscle length (L_o) was set and then maximal isometric tetanic force was determined by stimulating muscles with 0.5-ms pulses at 180 Hz and 150 V for 400 ms (Grass S48 stimulator connected to a SIU5D stimulus isolation unit; Grass Telefactor, Warwick, RI). The maximal isometric tetanic force was then normalized to the EDL muscles physiological cross-sectional area (i.e. muscle mass divided by the product of muscle density (1.06 g/ml) and fiber length ($0.44.L_o$)) [91]. Peak eccentric force was determined by passively shortening the muscle from Lo to 0.95 L_o, and then simultaneously stimulating the muscle for 133 ms as the muscle lengthened to 1.05 L_o at 0.75 L_o/s.

3.3.3 μCT of Tibial Mid-Diaphysis and Metaphysis

A μCT system (Scanco Medical μCT 40, Brttisellen, Switzerland) was used to quantify cortical bone geometry and volumetric bone mineral density (vBMD) of the tibia at the mid-diaphysis; trabecular morphometry in the tibial metaphysis was also assessed. The scanner was set to a voltage of 55 kVp and a current of 145 μA, and bones were scanned using an isotropic 12 μm voxel size with a 250 ms integration time. At the mid-diaphysis, 66 sequential two-dimensional grayscale slices (12 μm thickness) were obtained, as previously described [12]. After image segmentation for bone using a global threshold, an algorithm was used to compute the following morphometric outcome measures: cortical cross-sectional area, cortical thickness, periosteal diameter, cross-sectional moment of inertia (CSMI) and vBMD. These measures were assessed for each of the 66 slices, and then the average of the 66 slices was reported. The minimum principal CSMI (CSMImin) was utilized in the present study as it best corresponds to the CSMI about the bone bending axis during the three-point bending test (described below).

Trabecular bone in the proximal tibia metaphyseal region was imaged in 50 sequential slices, beginning 5 slices distal to the last image containing the growth plate. The mean bone volume fraction (BV/TV), trabecular number, trabecular thickness, and trabecular spacing were quantified to characterize bone morphometry. Upon completion of imaging, bones were refrozen in PBS and stored at -80C until the time they underwent mechanical testing.

3.3.4 Three-Point Bending Tests of Tibial Mid-Diaphysis

The procedures used to assess the functional capacities of the mouse tibia have been described in detail previously [12, 11]. Briefly, tibial length was measured with digital calipers and the mid-diaphysis of the tibia was identified. Tibial bone functional properties were then determined by performing three-point bending at mid-diaphysis on a Mecmesin MultiTest 1-D test machine using a Mecmesin AFG-25 load cell (Mecmesin, West Sussex, UK). The tibia was placed onto a set of supports separated by 1 cm such that the lateral side of the bone was placed downward. Bones were placed in this position to provide the most stable loading position possible during the testing procedure. Quasi-static loading was applied to the central aspect of the bone on the medial surface using a displacement rate of 2 mm/min. The load applied to the bone was measured by a load cell with 5 mN resolution. The load and displacement outputs were sampled at 14 Hz by a computer and software (TestPoint version 7; Measurement Computing Corp., Norton, MA).

The load-displacement curve for each bone (e.g., Figure 3.1A) was analyzed using a custom-written TestPoint program [12]. The functional measures of tibial bone were quantified by ultimate load, stiffness, and deflection and energy absorbed to ultimate load. Ultimate load was determined by the program as the highest load obtained prior to failure (Figure 3.1A). Once the point corresponding to ultimate load was determined on the load-displacement curve, deflection and energy to ultimate load were determined. For stiffness, the program searched for the highest slope along the linear portion of the curve prior to ultimate load; the program required that the data segment contain at least 50 data points and that the correlation between load and displacement exceed 0.99.

In addition to bone geometric properties, other extrinsic material properties for each tibia were determined by quantifying dry and wet tibial masses. Intrinsic material properties for each tibia were also determined using vBMD (via μCT at the tibial midshaft and metaphysis), hydroxyproline concentration, ultimate stress and modulus of elasticity. Wet and dry tibial masses were measured immediately prior to measurement of the amino acid hydroxyproline, an amino acid unique to collagen. Hydroxyproline content was assayed following the procedures of Woessner [92]. As previously described [12], ultimate stress and modulus of elasticity were calculated for each tibial bone using

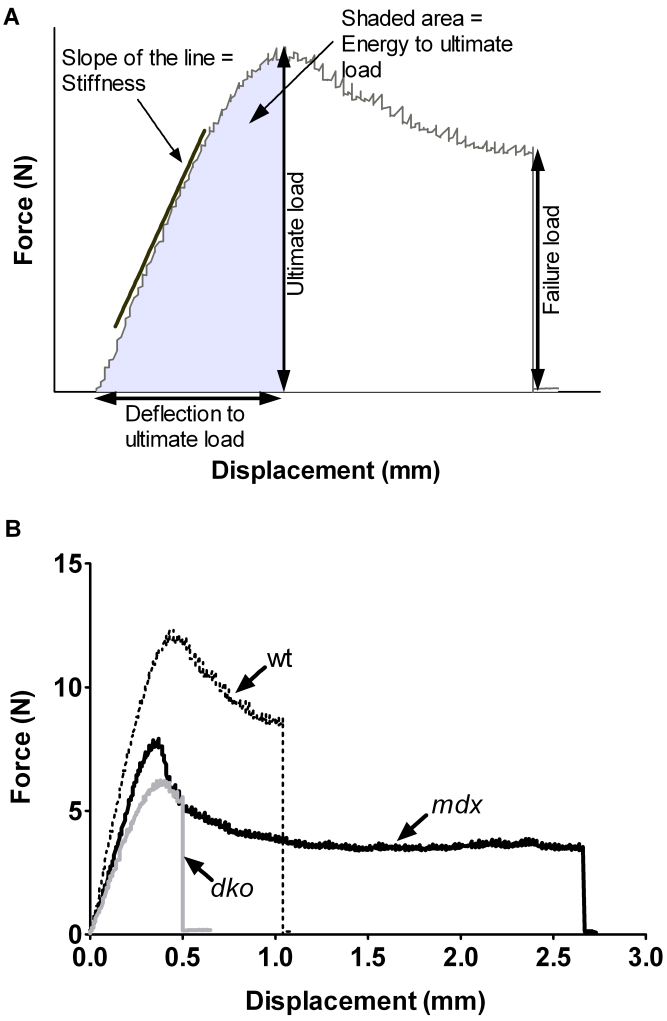

Figure 3.1: (A) Representative load-displacement tracing obtained during a three-point bending mechanical test on a mouse tibial bone. The components of the curve that were analyzed for determining ultimate load, stiffness, energy to ultimate load, deflection to ultimate load and failure load are illustrated. (B) Representative load-displacement tracings obtained during three-point bending mechanical testing on tibial bones from wild-type (wt), *mdx*, and *dko* mice.

classical beam theory. Ultimate stress was calculated using the following equation: ultimate stress = (UL·d·L)/(8·CSMI), where UL, d and L are ultimate load, medial-lateral periosteal diameter, and bottom support span length, respectively. Modulus of elasticity was then calculated using: modulus of elasticity = $(k \cdot L^3)/(48 \cdot CSMI)$, where k equals stiffness.

3.3.5 Bone and Muscle Relationships

To determine whether the tibia was more or less affected by the dystrophic condition relative to the EDL muscles contractile strength, bone-muscle functional relationships were examined. Tibial bones measures of functional capacity (ultimate load and stiffness) were divided by the EDL muscles contractile capacity (maximum isometric and eccentric contraction forces) as previously described [12]. These bone-to-muscle ratios were done on a mouse-by-mouse basis, meaning that if a mouse did not have measurements for both its tibial bone and EDL muscle, the ratio was not calculated. Ratios that are higher than those for the corresponding age-matched control mice indicate that functional properties of dystrophic bone are relatively greater than those of muscle, while ratios that are lower than those for the control mice indicate the reverse.

3.3.6 Statistical Analyses

To analyze the effects of genotype (wild-type vs. *mdx*) and age (7 wk vs. 24 mo), two-way ANOVAs were utilized. When interactions were significant ($p<0.05$), Holm-Sidak post hoc tests were performed to determine which combinations of conditions were different from each other. To assess possible effects of body mass on tibial geometric parameters at the midshaft (i.e., cortical cross sectional area, cortical wall thickness, and periosteal diameter) as well as tibial bone wet and dry mass, two-way ANCOVAs were run using body mass as the covariate.

To examine the effect of disease severity (i.e., the more severe dystrophin and utrophin deficient *dko* mouse model relative to both dystrophin deficient *mdx* mice and wild-type mice), 7 week-old *dko* mice were compared to wild-type and *mdx* mice of the same age. Before this analysis was done, independent t-tests were performed and percent differences were calculated to confirm that gender differences were not present

between male and female *dko* mice. A one-way ANOVA was then done with genotype as the fixed factor. If an effect of genotype was present, Holm-Sidak post-hoc measures were used to determine differences among the genotypes. When assumptions of normality or equal variance were violated, Kruskal-Wallis One Way Analysis of Variance on Ranks was performed along with Dunns post-hoc tests. All statistical analyses were carried out using SigmaStat version 3.5 (Systat Software Inc; Point Richmond, CA) with the exception of the two-way ANCOVAs which were conducted using SPSS version 12 (SPSS Inc., Chicago, IL)

3.4 Results

3.4.1 Effect of genotype on EDL muscle function

To demonstrate the severity of muscle functional impairments in the mouse models of DMD, in vitro measures of EDL muscle contractile forces of dystrophic mice were compared to those of wild-type mice. *Mdx* mice generated less maximal isometric tetanic forces at both 7 weeks and 24 months of age (41% and 21%, respectively) compared to their wild-type counterparts (Table 5.1). Peak eccentric force was also reduced in *mdx* mice (Table 5.1). In an effort to determine the source of these decrements in EDL muscle function in *mdx* mice, both the size of the EDL muscle (i.e., mass) as well as a surrogate for muscle quality (i.e., peak isometric force normalized to muscle cross-sectional area) were analyzed. *Mdx* and wild-type EDL muscle masses were equivalent at 7 weeks of age while *mdx* muscles were >50% larger at 24 months (Table 5.1). Peak isometric tetanic force normalized to muscle cross-sectional area was 20-40% less in *mdx* than wild-type mice (Table 5.1). Thus, despite *mdx* mice having equal or greater muscle masses, contractile function was compromised.

Table 3.1: Effects of genotype and age on tibial bone to EDL muscle ratios.

	wt-7wk	*mdx*-7wk	wt-24mo	*mdx*-24mo	P-Values for Two-Way ANOVA			*dko*-7wk	P-Values for One-Way ANOVA
					Main effect of genotype	Main effect of age	Interaction (genotype x age)		
Body mass (g)	24.0^a (0.5)	26.1^a (0.9)	39.7^b (1.1)	32.2^c (0.5)	-	-	< 0.001	14.2*† (1.4)	< 0.001
EDL peak isometric tetanic force (mN)	362.9^a (13.8)	212.6^b (16.5)	394.7^a (11.9)	313.2^c (17.0)	-	-	0.028	117.1*† (11.8)	< 0.001
EDL peak eccentric force (mN)	492.1 (16.0)	325.1 (18.7)	588.0 (21.4)	460.3 (22.2)	< 0.001	< 0.001	0.336	188.3*† (15.1)	< 0.001
EDL mass (mg)	10.4^a (0.4)	10.1^a (0.4)	12.4^b (0.2)	19.5^c (0.4)	-	-	< 0.001	6.0*† (0.8)	0.002
EDL isometric force normalized to CSA (N/cm^2)	19.3 (0.6)	11.5 (0.8)	18.7 (0.6)	9.5 (0.5)	< 0.001	0.052	0.284	9.4*† (0.5)	< 0.001

*Values are means (SE). The main effects of genotype (wt vs mdx mice) and age (7wk vs 24mo) are listed in the sixth and seventh columns, respectively. When the interaction between genotype and age was significant, the p-value is given in the eighth column and the results from Holm-Sidak post hoc tests ($p<0.05$) are indicated using the superscript lowercase letters; values with the same letter are not significantly different. The p-values in the last column pertain to the one-way ANOVA results across the three groups of 7-wk old mice, and significant findings from Holm-Sidak post hoc tests ($p<0.05$) are indicated by: * Significantly different from wt-7wk and †mdx-7wk.*

wt, wild-type; EDL, extensor digitorum longus muscle; CSA, cross sectional area; 7wk, 7-week old mice; 24mo, 24-month old mice.

Data were not statistically different between male and female *dko* mice for any of the muscle or bone parameters measured (i.e., independent t-tests $P \geq 0.221$) with the greatest difference between genders being 21%. Therefore all muscle and bone results for the two genders were collapsed into a single *dko* group. Comparisons of EDL muscle from 7-week-old *dko* mice to those of age-matched, wild-type and *mdx* mice show that *dko* mice have functional deficits that are even greater than those of *mdx*. *Dko* mice had 42-67% lower peak isometric and eccentric forces relative to *mdx* and wild-type mice (Table 5.1). Unlike *mdx* mice, *dko* mice had decrements in both muscle size and muscle quality (Table 5.1), confirming that *dko* mice have a more severe phenotype than *mdx* mice in terms of muscle function.

3.4.2 Effect of genotype on tibial bone functional capacity

In general, the functional capacity of tibial bone was affected by both genotype and age. Figure 3.1B shows exemplar load-displacement curves from wild-type, *mdx* and *dko* tibia during the three-point bending test. Ultimate loads for tibia of *mdx* mice were 19 and 36% lower than those for wild-type mice at 7 weeks and 24 months, respectively (Figure 3.2A). The larger difference in ultimate load between *mdx* and wild-type mice at 24 months was attributed to an improvement with age in wild-type mice that did not occur in *mdx* mice. For bone stiffness, there were both significant genotype and age effects (Figure 3.2B). Tibial stiffness in *mdx* mice was 15-20% lower than wild-type mice, indicating that *mdx* bone was less resistant to bending. Additional functional properties, including energy absorbed to ultimate load and deflection to ultimate load, also reveal that *mdx* tibia are compromised. Both of these properties were 36-60% lower in 24 month-old *mdx* mice compared to those in 24 month-old wild-type mice (Table 3.2). Collectively, these results indicate that functional deficits are apparent in the tibial bones of *mdx* mice, confirming that bone strength is compromised.

The tibia of *dko* mice had even lower functional capacity. For example, bone from these mice had 34-50% lower values for ultimate load and stiffness compared to those of *mdx* and wild-type mice (Figure 3.2A and B). Energy absorbed to ultimate load and deflection to ultimate load were also smaller in *dko* mice than wild-type mice (61 and 17% respectively, Table 3.2), indicating that *dko* are less able to withstand loading.

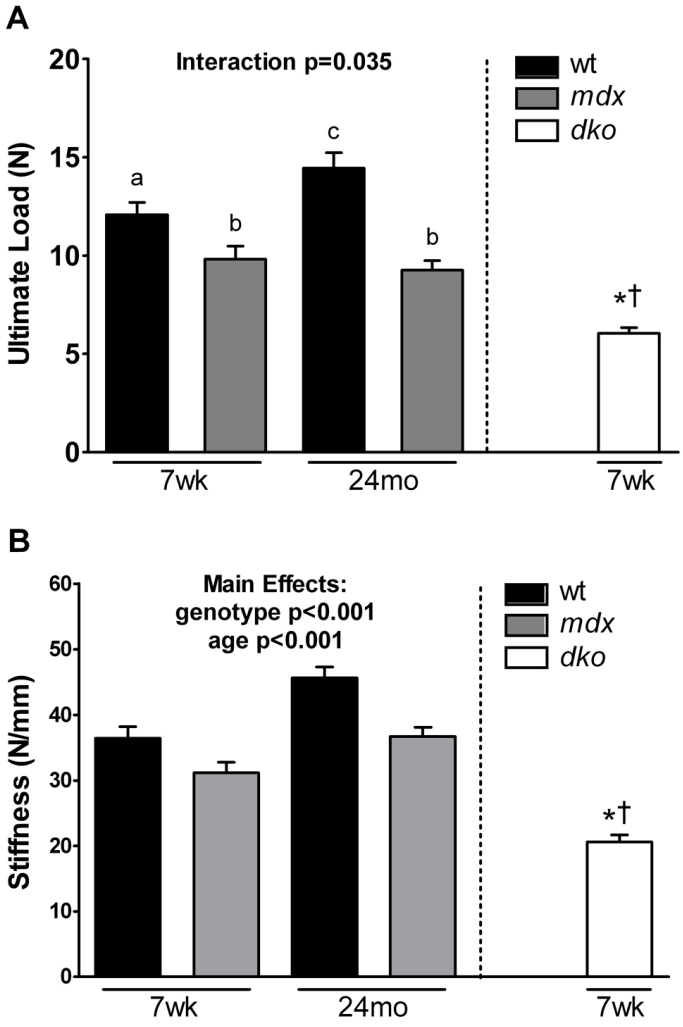

Figure 3.2: Effects of genotype (wild-type, *mdx* and *dko*) and age (7wk vs. 24mo) on tibial bone (A) ultimate load and (B) stiffness. Values are mean ± SE. When significant main effects of two-way ANOVA ($p<0.05$) were present, the corresponding p-values are listed above the bars. When interactions between genotype and age were significant, results Holm-Sidak post hoc tests ($p<0.05$) are indicated using the lowercase letters above the bars; values with the same letter are not significantly different. Significant one-way ANOVA results across the three groups of 7-wk old mice, and significant findings from Holm-Sidak post hoc tests ($p<0.05$) are indicated by: * Significantly different from wt-7wk; † Significantly different from *mdx*-7wk.

3.4.3 Effect of genotype on tibial bone geometry

μCT was utilized to determine if properties reflecting bone geometry at the mid-shaft of the tibia were affected by genotype and thus potentially could account for the differences in bone mechanical properties observed among genotypes. For CSMI at the tibial mid-shaft, which reflects the moment of inertia during three-point bending, independent age and genotype effects were detected. *Mdx* bones had CSMI values that were approximately 25% lower than wild-type bones (Figure 3.3). Because cortical cross-sectional area usually parallels CSMI, it was not surprising to find that cortical cross-sectional area was correspondingly 6-17% smaller in *mdx* mice (Table 3.2). Specifically for the 24 month-old *mdx* mice, the smaller cross-sectional area can be largely attributed to reduced cortical wall thickness (Table 3.2). Body mass can influence bone geometry, therefore two-way ANCOVAs with body mass as the covariate were conducted. Results from those analyses were similar to those presented in Table 3.2, with the exception of periosteal diameter in which significant interactions between genotype and age were found (p=0.002). Specifically, with body mass as a covariate, periosteal diameters were smaller in 7-week old *mdx* mice (i.e., estimated marginal means for a body mass of 30.97 g was 1.25 mm vs 1.38 mm) and larger in 24 month-old *mdx* mice (1.26 mm vs 1.19 mm) compared to wild-type mice.

Tibial bones from 7 week old *dko* mice were smaller than wild-type and *mdx* bones for all geometric properties at the tibial midshaft (Table 3.2 and Figure 3.2). For example *dko* mice had 38-57% smaller CSMI and cross-sectional area values compared to *mdx* mice, further highlighting the impact of disease severity on tibial bone. These collective results indicate that alterations in bone geometry contribute to the compromised tibial bone strength in dystrophic mice.

μCT was also used to determine if trabecular bone morphometry in the tibial metaphysis was affected by genotype. For trabecular bone volume fraction (i.e., trabecular bone volume per total volume of interest), independent genotype and age effects were present (Table 3.2). *Mdx* mice had at least 27% less trabecular bone than wild-type mice. In 7 week-old *mdx* mice, the reduction in bone volume fraction was largely attributed to having 17% fewer trabeculae of equivalent thickness, whereas in 24 month-old *mdx* mice, the number of trabeculae was not different from wild-type mice, yet the trabeculae were 19% thinner (Table 3.2). Consequent to these alterations in trabecular

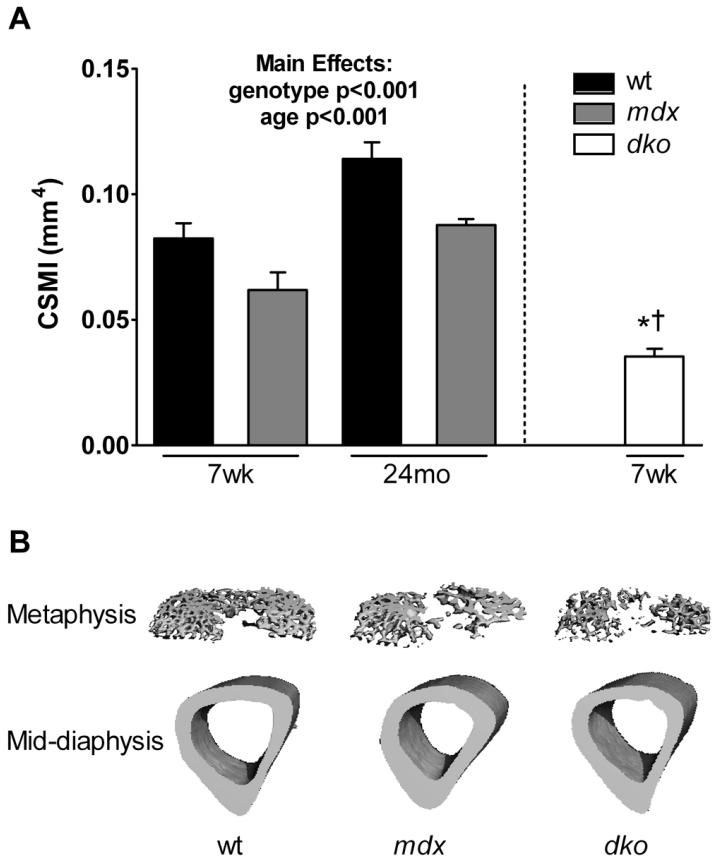

Figure 3.3: A) Effects of genotype (wild-type, *mdx* and *dko*) and age (7wk vs. 24mo) on tibial bone cross sectional moment of inertia (CSMI). Values are mean ± SE. Significant main effects of two-way ANOVA ($p<0.05$) and the corresponding p-values are listed above the bars. Significant one-way ANOVA results across the three groups of 7-wk old mice, and significant findings from Holm-Sidak post hoc tests ($p<0.05$) are indicated by: * Significantly different from wt-7wk; †Significantly different from *mdx*-7wk. (B) Exemplar μCT images from 7-wk old wild-type, *mdx* and *dko* mice.

bone, the trabecular spacing was consistently 6-23% higher in *mdx* mice (Table 3.2).

Trabecular bone morphometry in the proximal tibial bone of 7 week-old *dko* mice was different from those of wild-type and *mdx* mice (Table 3.2). *Dko* mice had 78% lower bone volume fractions compared to wild-type mice, which was primarily due to having 34% fewer and 22% thinner trabeculae. These data for trabecular bone morphometry combined with the alterations seen in cortical bone geometry confirm that bone geometry is compromised in dystrophic mice.

Table 3.2: Effects of genotype and age on tibial bone mechanical function, cortical bone geometry and trabecular bone morphometry.

	wt-7wk	*mdx*-7wk	wt-24mo	*mdx*-24mo	P-Values for Two-Way ANOVA: Main effect of genotype	Main effect of age	Interaction (genotype x age)	*dko*-7wk	P-Values for One-Way ANOVA
Mechanical Functional Properties									
Energy absorbed to ultimate load (mJ)	3.15^{a} (0.24)	$2.32^{a,b}$ (0.28)	4.17^{a} (0.57)	1.69^{b} (0.25)	-	-	0.038	1.23*† (0.09)	< 0.001
Deflection to ultimate load (mm)	0.45^{a} (0.01)	$0.42^{a,b}$ (0.02)	0.51^{a} (0.06)	0.33^{b} (0.02)	-	-	0.047	0.37*† (0.02)	< 0.017
Geometric Properties: Mid-diaphysis									
Cortical cross-sectional area (mm^2)	0.69 (0.03)	0.65 (0.04)	0.75 (0.03)	0.62 (0.01)	0.003	0.499	0.101	0.43*† (0.02)	< 0.001
Cortical wall thickness (mm)	0.202^{a} (0.004)	0.210^{a} (0.007)	0.192^{a} (0.007)	0.159^{b} (0.004)	-	-	< 0.001	0.145*† (0.004)	< 0.001
Periosteal diameter (mm)	1.23 (0.03)	1.15 (0.04)	1.38 (0.02)	1.29 (0.02)	0.003	< 0.001	0.911	1.00*† (0.03)	< 0.001
Trabecular Morphometry: Metaphysis									
Bone Volume Fraction	0.092 (0.013)	0.059 (0.005)	0.030 (0.003)	0.022 (0.002)	0.007	< 0.001	0.087	0.020*† (0.002)	0.000
Trabecular Number (mm^{-1})	5.10^{a} (0.13)	4.23^{b} (0.10)	2.97^{c} (0.03)	2.76^{c} (0.04)	-	-	< 0.001	3.35*† (0.10)	0.000
Trabecular Thickness (mm)	0.041^{a} (0.002)	0.038^{a} (0.002)	0.062^{b} (0.003)	0.050^{c} (0.001)	-	-	0.036	0.032*† (0.001)	0.002
Trabecular Spacing (mm)	0.192 (0.006)	0.237 (0.008)	0.355 (0.007)	0.377 (0.005)	< 0.001	< 0.001	0.090	0.305*† (0.009)	0.000

*Values are means (SE). The main effects of genotype (wt vs mdx mice) and age (7wk vs 24mo) are listed in the sixth and seventh columns, respectively. When the interaction between genotype and age was significant, the p-value is given in the eighth column and the results from Holm-Sidak post hoc tests ($p<0.05$) are indicated using the superscript lowercase letters; values with the same letter are not significantly different. The p-values in the last column pertain to the one-way ANOVA results across the three groups of 7-wk old mice, and significant findings from Holm-Sidak post hoc tests ($p<0.05$) are indicated by: * Significantly different from wt-7wk and †mdx-7wk.*

wt, wild-type; 7wk, 7-week old mice; 24mo, 24-month old mice.

3.4.4 Effect of genotype on tibial bone extrinsic and intrinsic material properties

Extrinsic material properties of the tibia, beyond geometry, were quantified by wet and dry tibial masses, and intrinsic material properties were quantified by vBMD, ultimate stress, modulus of elasticity and bone hydroxyproline concentration. Tibial bone wet and dry masses were lower in *mdx* mice relative to wild-type mice (Table 3.3); however after accounting for body mass as a covariate, tibial dry mass was similar between groups (p=0.053) . Similarly, vBMD at both the tibial mid-shaft and tibial metaphysis was not different between the two genotypes (Table 3.3). Bone hydroxyproline concentration (i.e., hydroxyproline content relative to dry tibial mass) revealed that the concentration of collagen was higher in 24 month-old *mdx* mice compared to 24 month-old wild-type mice (Table 3.3). While ultimate stress values were similar between *mdx* and wild-type mice at 7 weeks of age, aged *mdx* mice had ultimate stress values that were 22% lower than wild-type mice at 24 months of age (Table 3.3). The modulus of elasticity within the tibial bone tended to be higher in *mdx* mice compared to wild-type mice (i.e., main effect of genotype was p=0.051) (Table 3.3). Combined, these data confirm that compared to wild-type mice, *mdx* mice have smaller sized bones of similar density. With age however, *mdx* mice developed higher hydroxyproline concentrations with a trend towards higher modulus of elasticity values while ultimate stress values were diminished.

Extrinsic tibial bone material properties (i.e., wet and try tibial mass) of *dko* mice were much lower compared to both *mdx* and wild-type mice (Table 3.3). Despite the small bone size in *dko* mice, they had similar values for two of the intrinsic material properties, i.e., trabecular vBMD, hydroxyproline concentration and ultimate stress, compared to wild-type and *mdx* mice. Unlike *mdx* mice, *dko* mice had lower cortical vBMD values and higher modulus of elasticity compared to wild-type mice. In summary *dko* mice, the more severe model of DMD, have significant deficits in bone size and cortical vBMD but their modulus of elasticity was higher than that of wild-type mice.

Table 3.3: Effects of genotype and age on tibial bone extrinsic and intrinsic material properties.

	wt-7wk	*mdx*-7wk	wt-24mo	*mdx*-24mo	P-Values for Two-Way ANOVA: Main effect of genotype	Main effect of age	Interaction (genotype x age)	*dko*-7wk	P-Values for One-Way ANOVA
Extrinsic Material Properties									
Tibial wet mass (mg)	60.80 (1.71)	54.38 (2.76)	59.64 (3.52)	49.34 (0.85)	0.002	0.217	0.436	38.41*† (2.20)	< 0.001
Tibial dry mass (mg)	31.97 (1.01)	29.07 (1.12)	35.46 (1.48)	31.16 (0.51)	0.003	0.017	0.528	18.30*† (1.23)	< 0.001
Intrinsic Material Properties									
Cortical vBMD (mg/cm^3)	1346.45 (7.05)	1334.97 (8.72)	1493.03 (11.44)	1470.96 (8.62)	0.081	< 0.001	0.566	1310.17*† (8.19)	0.013
Trabecular vBMD(mg/cm^3)	1077.11 (6.74)	1055.80 (11.51)	1184.85 (12.16)	1201.15 (7.20)	0.799	< 0.001	0.063	1059.06 (15.11)	0.360
Bone hydroxyproline content (% dry bone mass)	1.96^a (0.05)	1.94^a (0.06)	1.66^b (0.05)	1.96^a (0.05)	-	-	0.004	1.92 (0.03)	0.862
Ultimate stress(MPa)	227.68^a (5.25)	233.34^a (8.01)	218.56^a (7.50)	170.13^b (7.91)	-	-	< 0.001	217.26 (11.69)	0.428
Modulus of elasticity (GPa)	9.37 (0.38)	10.95 (0.81)	8.45 (0.30)	8.72 (0.31)	0.051	0.002	0.161	12.35* (0.57)	0.007

*Values are means (SE). The main effects of genotype (wt vs mdx mice) and age (7wk vs 24mo) are listed in the sixth and seventh columns, respectively. When the interaction between genotype and age was significant, the p-value is given in the eighth column and the results from Holm-Sidak post hoc tests ($p<0.05$) are indicated using the superscript lowercase letters; values with the same letter are not significantly different. The p-values in the last column pertain to the one-way ANOVA results across the three groups of 7-wk old mice, and significant findings from Holm-Sidak post hoc tests ($p<0.05$) are indicated by: * Significantly different from wt-7wk and †mdx-7wk.*

wt, wild-type; 7wk, 7-week old mice; 24mo, 24-month old mice; vBMD, volumetric bone mineral density.

3.4.5 Bone and muscle relationships

Ratios that were calculated between the functional properties of the tibia and the EDL muscle of 7-week old *mdx* mice were up to 1.44 fold of those for 7-week old wild-type mice (Figure 3.4 and Table 3.4). These data indicate that at this younger age in *mdx* mice, the functional capacity of the tibial bone is relatively high compared to that of the adjacent, diseased EDL muscle. As the mice aged to 24 months the functional relationships between bone and muscle in *mdx* mice became undistinguishable from those of wild-type mice. This observation can be attributed to two factors. First, there were greater EDL strength gains by *mdx* than wild-type mice with age (i.e., EDL muscles from 24-month *mdx* mice generated 47% more peak isometric force than those from 7-week *mdx* mice while wild-type muscle only improved by 9% with age; Table 5.1). Second, tibia ultimate load improved with age among wild-type (i.e., by 20%) but not *mdx* mice (Figure 3.2). The bone-to-muscle ratios in 7-week old *dko* mice were at least 1.33 fold of those for wild-type mice of the same age, again indicating that the functional capacity of *dko* tibial bone was relatively high compared to that of the neighboring muscle (Figure 3.4 and Table 3.4)

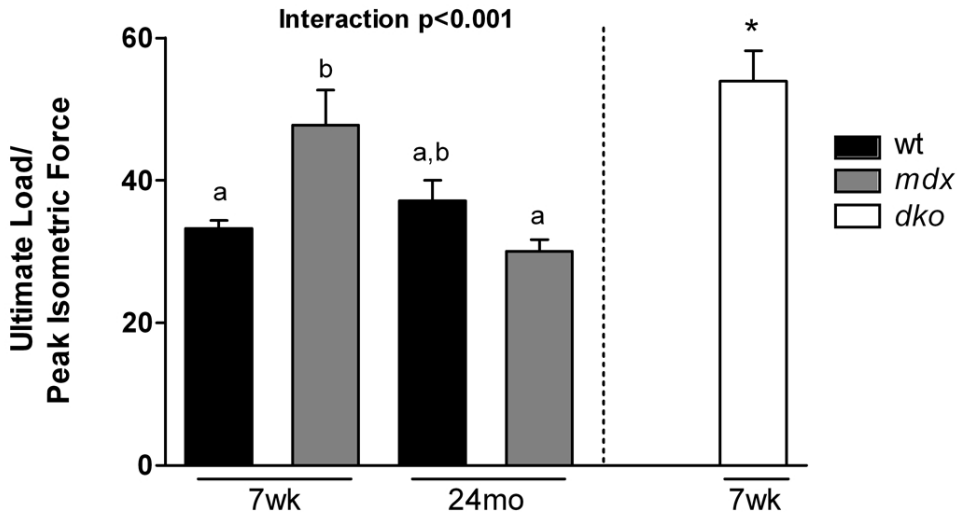

Figure 3.4: Effects of genotype (wild-type, *mdx* and *dko*) and age (7wk vs. 24mo) on tibial bone to EDL muscle ratios. Values are mean ± SE. Statistically significant effects are indicated above the bars. Significant interactions between genotype and age detected by Holm-Sidak post hoc tests ($p<0.05$) are indicated by the lowercase letters above the bars; values with the same letter are not significantly different. Significant one-way ANOVA results across the three groups of 7-wk old mice, and significant findings from Holm-Sidak post hoc tests ($p<0.05$) are indicated by: * Significantly different from wt-7wk.

Table 3.4: Effects of genotype and age on tibial bone to EDL muscle ratios.

	wt-7wk	***mdx*-7wk**	**wt-24mo**	***mdx*-24mo**	**P-Values for Two-Way ANOVA**			***dko*-7wk**	**P-Values for One-Way ANOVA**
					Main effect of genotype	**Main effect of age**	**Interaction (genotype x age)**		
Ultimate load/peak eccentric force	24.56^{a} (1.10)	30.77^{b} (2.93)	$24.98^{a,b}$ (1.98)	20.38^{a} (1.05)	-	-	0.005	32.73* (1.64)	0.003
Stiffness/peak isometric tetanic force, mm^{-1}	100.37^{a} (2.44)	151.66^{b} (14.87)	$116.94^{a,b}$ (6.78)	119.84^{a} (7.82)	-	-	0.006	182.90* (13.70)	0.001
Stiffness/peak eccentric force, mm^{-1}	74.08^{a} (2.68)	97.59^{b} (8.32)	$78.64^{a,b}$ (4.60)	81.01^{a} (4.64)	-	-	0.043	111.24* (5.53)	0.004

*Values are means (SE). The interaction p-values are given in the eighth column and the results from Holm-Sidak post hoc tests ($p<0.05$) are indicated using the superscript lowercase letters; values with the same letter are not significantly different. The p-values in the last column pertain to the one-way ANOVA results across the three groups of 7-wk old mice, and significant findings from Holm-Sidak post hoc tests ($p<0.05$) are indicated by: * Significantly different from wt-7wk.*

wt, wild-type; 7wk, 7-week old mice; 24mo, 24-month old mice.

3.5 Disscusion

We had three primary results from our study. First, mechanical testing of the tibia directly showed that tibial bones from dystrophic mice possess only 50-80% of the strength of that from wild-type mice, illustrating that the muscle disease has downstream functional effects on an associated tissue. Second, this low bone strength in dystrophic mice was mostly attributed to altered extrinsic material properties (i.e., bone geometry and bone mass) more so than alterations in bone mineral density or other intrinsic material properties. Third, the functional capacity of the tibial bone of young *mdx* and *dko* mice is greater than that of the adjacent EDL muscle as indicated by high bone-to-muscle functional capacity ratios relative to wild-type mice, but following improvements in muscle function in *mdx* mice with age the bone-to-muscle relationships in *mdx* mice become equivalent to those in wild-type mice. Combined, these data highlight that there are clear decrements in both bone and muscle tissues of dystrophic mice, as well as a distinct relationship between muscle disease and overall bone health.

In the past decade, the necessity of muscle force application for overall bone health has received increasing attention. Evidence from a hip prosthetic study suggested that 70% of the bending moments placed on bone originated from force produced via muscle contractions rather than from external reaction forces [93]. As a result, it has been hypothesized that muscular contractions produce the majority of mechanical load-induced stimuli sensed by bones mechanosensory cells, which elicit adaptations in bone stiffness and strength if warranted. Several prospective studies have provided indirect evidence in favor of this hypothesis, by showing that bone loss followed muscle atrophy and conversely, that bone was regained after muscle mass recovered [41, 40].

In muscular degenerative diseases that are progressive such as DMD, declines in bone strength and stiffness should theoretically follow decrements in muscle function (i.e., the magnitude and frequency of force production). This reduction in muscle load placed on bone in DMD is the combined effects of loss of contractile strength [49, 94] and the progressive inability to perform activities of daily living [53, 52, 44]. In line with this, recent clinical evidence has shown that boys with DMD lose the greatest amount of bone following the loss of ambulation [2, 55]. While this loss of bone mass is expected to be appropriate for the loss of muscle function, it likely increases the bones propensity to

fracture. This highlights the necessity of muscle-induced loading for proper maintenance of the skeleton in effort to prevent fractures. The present study, consistent with previous work in *mdx* and *dko* mice [86, 49], confirmed that dystrophic muscle generated 20-60% lower levels of force compared to that from wild-type mice. This reduction in force generating capacity in 24 month-old *mdx* mice may appear surprising due to their larger sized EDL muscles; however we are not the first to report this. Between the ages of 6 to 28 months, Lynch et al. [49] has shown that *mdx* mice have larger sized EDL and soleus muscles compared to wild-type mice, which is likely attributed to a lifelong accumulation of fibrosis within the muscle. The greatest deficits in muscle function we found were found in *dko* mice, which have been shown to have a more severe phenotype (i.e., lacking both dystrophin and its homolog utrophin) suggesting to better mimic muscle deterioration in boys with DMD. Likewise, we predicted and our data support that tibia from *mdx* mice were functionally compromised and those from *dko* mice were worse yet.

Our findings confirm and extend the work of Anderson et al. [7], showing that tibial bones from dystrophic mice are indeed functionally weakened. Specifically, we found that the tibial bone from *mdx* and *dko* mice were up to 50% lower for ultimate loads and 44% lower for stiffness than those of wild-type mice. These results are in parallel with the mechanostat theory, that is, one would have predicted that the progressive reductions in the magnitude and frequency of mechanical loading of dystrophic mice (i.e. weakened muscle contractions and reduced physical activity levels [88]) would translate to lower bone strength and stiffness compared to non-diseased mice. Contrary to the mechanostat theory, our bone-to-muscle ratios were not equivalent across genotypes in young mice, suggesting that the functional capacities of bone and muscle were not appropriately matched. Specifically, young dystrophic mice had up to 50% higher ratios compared to wild-type mice, implying that the tibial bone of these young mice was over-adapted relative to the function of the diseased muscle. Adaptations in bone are known to lag those of muscle, and because we selected the 7-week time point, *mdx* muscle had reached its peak rate of muscle deterioration (i.e., 3-4 weeks after weaning [95]); however, appropriate alterations to bone function had likely only been initiated. Alternatively, it is plausible that the lack of dystrophin caused a subtle prenatal bone effect that was apparent in the young, 7-week old *mdx* mice, but had resolved in the

older *mdx* mice. This is speculation because how bone develops during the first three weeks of life in dystrophic mice has not been investigated. By 24 months of age, *mdx* mice muscle strength had increased by 45% while their bone strength had remained unchanged, thereby resulting in bone-to-muscle ratios that were equivalent to those of wild-type mice. This improvement in muscle function likely reversed deleterious adaptations to bone which thereby preserved, but did not improve, its function between 7-weeks and 24-months of age. In summary, tibial bones from *mdx* and *dko* mice were found to be functionally impaired compared to wild-type mice, which was partially attributed to altered muscle contractile function; however, beyond the role of muscle-induced loading, it remains necessary to investigate other contributing factors of bone strength and function.

The skeletal factors that contribute to reductions in bone mechanical strength, namely bone geometry and material properties of the bone, have been minimally assessed in *mdx* mice previously [7, 8]. Our data show that dystrophic tibial bones had smaller cortical cross-sectional area as well as reduced cortical wall thickness, both of which presumably contribute to their compromised bone strength. More importantly however, we found that dystrophic tibia have smaller CSMI compared to tibia from wild-type mice. Of the aforementioned parameters, CSMI is the most important determinant of a bones mechanical properties when subjected to 3-point bending. We found CSMI to be reduced by 24-43% in dystrophic mice compared to wild-type mice. Montgomery et al. reported that *mdx* mice had higher femur bone strength presumably due to larger periosteal diameters, and equivalent cortical thickness and CSMI relative to wild-type mice *mdx* [8]. However after accounting for the larger body mass in *mdx* mice (i.e., performing ANCOVA with body mass as the covariate), differences between genotypes for periosteal diameter were eliminated in that study. Because body mass also varied among groups of mice in our study, we performed similar two-way ANCOVAs with body mass held as the covariate. Our results on bone geometry indicate that muscular dystrophy independent of body mass was a detriment to bone geometry in *mdx* mice. The exception was periosteal diameter in the 24 month-old mice. The results of the two-way ANCOVA indicated that older *mdx* mice actually had higher periosteal diameters after adjusting for body mass compared to wild-type mice, which was dissimilar to the aforementioned findings of Montgomery et al.

These somewhat contrary findings for the *mdx* tibia and femur may be the result of either site-specific differences in bone geometry or due to the sensitivity of the techniques utilized to quantify geometry. μCT was used in the present study, and this technique computationally assesses bone geometry by accounting for the contribution of each voxel and its position in bone, whereas Montgomery et al. utilized a caliper to quantify geometry. Thus, μCT measurements provide greater sensitivity and precision when measuring bone geometry. Further studies utilizing μCT are warranted to discern whether regional differences in geometry exist between *mdx* tibia and femur. Even less is known about geometric or material properties of bone from DMD patients. Consistent with our work on dystrophic mice, preliminary results on bone geometry in boys with DMD suggest that total cross-sectional areas are smaller than controls at various locations along the radial and tibial length [5, 6].

In addition to altered bone geometry contributing to functionally weakened bone, it was important to determine if the muscle disease impacted other extrinsic as well as intrinsic material properties of bone. We found that dystrophic mice had reduced extrinsic material properties (i.e., tibial dry and wet mass). 24-month old *mdx* mice had alterations in two intrinsic material properties, i.e., hydroxyproline content and ultimate stress, which indicated that these mice have more collagen content (i.e., less mineralized bone tissue compared to wild-type mice) along with reduced whole bone strength. These data are in agreement with our results of tibial bone stiffness which, suggest that the stiffness of the tibia from 24-month old wild-type mice increases with their declining collagen content. Based on overwhelming evidence that boys with DMD undergo loss of areal bone mineral density [2, 1, 55, 54, 56], it may seem surprising that tibial cortical and trabecular vBMD was not different between *mdx* and wild-type mice, but this result is in agreement with findings from Montgomery et al [8]. They reported no differences in bone mineral density at the femur or spine between *mdx* and wild-type mice [8]. In addition, preliminary data from a DMD clinical trial showed that cortical vBMD, measured near the mid-diaphysis of the forearm and tibia, was actually higher in boys with DMD than age-matched controls, while significant deficits in vBMD were only apparent in distal regions of these bones [5, 6]. In summary, the notion that overall vBMD is low as a result of dystrophin deficiency should be taken cautiously since four different bone sites of *mdx* mice and two bone sties of DMD patients do not show this.

Despite the alterations in bone strength and geometry of *mdx* and *dko* tibia, a limitation in using these animals models is that dystrophic mice do not experience fractures like boys with DMD. A known short-coming of the *mdx* mouse model is that they have a mild phenotype relative to boys with DMD both in terms of disease progression and muscle weakness, so it is not surprising that *mdx* mice do not experience fractures. The lack of clinical similarities between boys with DMD and *mdx* mice is attributed in part to elevated expression of utrophin by *mdx* mice [96]. *Dko* mice on the other hand, do not have this recovery due to the lack of utrophin, which translates to a progressive disease including truncated growth, limited physical abilities and muscle function, development of cardiomyopathies, and ultimately the mice suffer premature death better paralleling boys with DMD. *Dko* mice also have skeletal problems, the most notable being kyphosis of the spine [86]. Thus, utilization of the *dko* mouse for further bone investigations in relation to muscular dystrophy is reasonable and will likely prove very informative.

In summary, the present study has established that dystrophic mice, *mdx* and *dko*, do in fact have lower tibial bone strength along with deficits in muscle contractile functional capacity. Our findings indicate that bone weakness was predominately the result of adversely affected extrinsic material properties of bone (i.e., bone geometry and mass) rather than alterations to the bones density or other intrinsic material properties. These mouse models of DMD provide a feasible approach for future research to test therapeutic regimens that ideally aim to simultaneously improve both skeletal and muscle tissues without causing further injury to either tissue.

Chapter 4

Prednisolone treatment and restricted physical activity further compromise bone of *mdx* mice

Susan A. Novotny[1], Gordon L. Warren[2], Angela S. Lin[3], Robert E. Guldberg[3], Kristen A. Baltgalvis[4], and Dawn A. Lowe[5]

[1]Department of Kinesiology, University of Minnesota, Minneapolis, Minnesota

[2]Division of Physical Therapy, Georgia State University, Atlanta, Georgia

[3]Institute for Bioengineering and Bioscience, Georgia Institute of Technology, Atlanta Georgia

[4]Department of Biochemistry, Molecular Biology, and Biophysics, University of Minnesota, Minneapolis, Minnesota

[5] Program in Physical Therapy and Rehabilitation Sciences, University of Minnesota, 420 Delaware Street SE, Minneapolis, Minnesota 55455, USA

4.1 Abstract

Objectives The purpose of this study was to determine the extent to which prednisolone treatment and restricted physical activity caused deleterious changes in inherently compromised *mdx* bone. Methods Four week-old male *mdx* mice (n=36) were treated for 8-wk either with or without prednisolone (0.8-1.3 mg/kg/d) and were housed in traditional or small cages (restricted activity). Tibial bone strength, geometry, and intrinsic material properties were assessed at the mid-shaft by three-point bending and micro-computed tomography (μCT). Results Three-point bending results showed that both prednisolone and restricted activity reduced bone strength (7%), however stiffness was only reduced in restricted-activity mice. μCT analyses showed that cortical bone area and cortical thickness were 13% smaller in restricted-activity mice, and may have accounted for their compromised bone strength. Intrinsic material properties, including volumetric bone mineral density (vBMD) and modulus of elasticity, were not impacted by either treatment, however, vBMD tended to be lower in restricted-activity mice (p=0.06). Conclusions These data show that prednisolone treatment and restricted physical activity independently accentuate reductions in the strength and geometry of *mdx* bone, but do not influence intrinsic material properties.

4.2 Introduction

Bone health is compromised secondarily to many diseases. One example of this is Duchenne muscular dystrophy (DMD), an X chromosome-linked neuromuscular disease that has a prevalence of 1.3 to 1.8 per 10,000 males aged 5-24 years [97]. DMD is characterized by progressive muscle weakness that leads to physical inactivity and inevitably causes patients to become non-ambulatory by their early teenage years [52, 98]. Consequently, as dystrophic muscle becomes weaker, not only are there less forceful contractions applying lower loads on bone, fewer muscle-induced loads to bone are applied. As a result, bone is continually adjusting its material and geometric properties to its current loading environment [93] and disuse-mediated bone loss can be initiated [99]. The bone loss that results may largely explain the declines in areal bone mineral density that has been shown in boys with DMD as they age [2, 55].

Another insult to bone health is chronic usage of glucocorticoids such as prednisone,

prednisolone and deflazacort, which are prescribed to improve muscle strength and performance in DMD patients [58, 59, 100, 60]. For example, prednisone has been shown to thwart muscle deterioration, improve physical endurance, decrease falls, improve stair climbing, and prolong independent ambulation in patients with DMD [58, 59, 100, 60]. In parallel with these benefits to muscle tissue, glucocorticoids induce osteoporosis and increase fracture risk by increasing osteocyte and osteoblast apoptosis as well as extending the lifespan of osteoclasts [63, 61, 62]. Specific to DMD, the use of glucocorticoids has been shown to accentuate reductions in bone mass and density [1, 64, 55], increase the incidence of long bone fractures by nearly three-fold [64], and provoke the emergence of vertebral compression fractures which do not occur in patients with DMD whom are not treated with glucocorticoids [65, 64]. These results suggest that altered osteoblast and osteoclast viability disrupt the homeostasis of bone remodeling and therefore may translate to compromised bone structure and strength. Considering that bone is inherently compromised in strength and has altered geometry in individuals with DMD [7, 4, 5, 6, 8, 66, 13], the addition of reduced physical activity and the use of a glucocorticoid may cause further decrements to the structural and material integrity of bone, but contributions of these combined insults have not been thoroughly investigated.

The *mdx* mouse is an animal model of DMD that can be utilized to investigate the musculoskeletal system because the mice display muscle weakness [101], reduced physical activities [88], and compromised bone structure and function compared to wildtype mice [8, 66, 13]. The deficits in muscle function and physical activity in *mdx* mice are less severe relative to patients with DMD and theoretically would have lesser impacts on bone loading. Therefore, an additional intervention was utilized in the current study to amplify reductions in mechanical loading of hindlimb bone in *mdx* mice. Traditional approaches for reducing mechanical loading in rodent models include denervation, hindlimb suspension and casting [102, 103]. These models however, drastically disrupt the ability of mice to ambulate, and therefore would not appropriately model reductions in physical activity in DMD patients. We used the approach of housing *mdx* mice in cages that were 80% smaller in volume than typical mouse cages to restrict physical activities while still permitting the mice some movement. We theorized that this approach would better mimic boys with DMD who are physically inactive yet retained some ambulation, standing, and activities of daily living.

Quantifying the functional capacity of bone is a good predictor of fracture risk. This requires *ex vivo* analyses of bone and thus is not possible to directly study in boys with DMD following glucocorticoid treatment and in response to reduced physical activity. Therefore, the primary objective of this study was to use the *mdx* mouse model of DMD to determine the extent to which a glucocorticoid and restricted physical activity alter the functional capacity of the tibia as well as determine if alterations in functional capacity are explained by changes in geometric and/or intrinsic material properties. Based on glucocorticoids resorptive effects on bone, we hypothesized that tibial bones from prednisolone-treated *mdx* mice would have diminished bone strength and altered bone geometry compared to placebo-treated *mdx* mice. We also sought to determine if restrictions on cage activities (i.e., to mimic limited physical activity in boys with DMD) exacerbated the deleterious effects of disease and prednisolone treatment on tibial bone in *mdx* mice. We hypothesized that imposing restrictions on cage activity of *mdx* mice would be detrimental to tibial bone functional capacity and cortical bone geometry and further that reduced physical activity coupled with prednisolone treatment would be the most detrimental to bone structure and function.

4.3 Methods

4.3.1 Animals

Male *mdx* mice aged 4 week (n=36) were purchased from Jackson Laboratories. Mice were housed in groups of four on a 12:12 hour light-dark cycle at 20-23 ^{o}C and were provided food and water ad libitum. At 5 weeks of age, mice were anesthetized for pellet implantation using fentanyl citrate (10 mg/kg body weight (BW)), droperidol (0.2 mg/kg BW) and diazepam (5 mg/kg BW). At the age of 12-13 weeks, mice were sacrificed with an overdose of sodium pentobarbital (200 mg/kg BW). Animal care and use procedures were approved by the Institutional Animal Care and Use Committee at the University of Minnesota.

4.3.2 Experimental design

At 5 weeks of age, *mdx* mice were randomly assigned to one of four conditions, either without (placebo) or with prednisolone treatment and either housed in normal sized cages (placebo: n=8; prednisolone: n=10) or small cages (i.e., placebo restricted activity, n=8 and prednisolone restricted activity, n=10). At this same age, placebo or prednisolone treatment was initiated and continually administered over a period of 60 days via implanted time-released pellet as previously described [90]. Mice that were assigned to restricted activity groups were placed individually in small cages (plastic inserts sized length x width x height: 11.8 cm x 9.0 cm x 10.7 cm) to limit horizontal physical activities, namely ambulation.

Cage physical activity of each mouse was measured over a 24-hour period, approximately 35 days after pellet implantation. At 12-13 weeks of age, mice were sacrificed and tibial bones were excised. Bones were stored in phosphate-buffered saline at -20 ^{o}C until the time of analysis. A subset of the physical activity data have been published previously. Specifically, cage activity monitoring for the *mdx* placebo and prednisolone groups were reported in Study 2 of Baltgalvis et al. [90]. All data pertaining to mice with restricted activity, as well as all bone data have not been previously published.

4.3.3 Prednisolone pellet implantation and dosage

As previously described, mice were anesthetized using fentanyl citrate, droperidol and diazepam and the pellets were implanted on the dorsal side of the neck using a trochar [90]. The 1.5 mg, 60-day slow-release pellet (Innovative Research of America) is designed to release a constant daily dosage of drug (approximately 0.8-1.3 mg/kg/day of prednisolone). This dosage approximates the most effective dose of prednisone (0.75 mg/kg/day) prescribed to DMD patients (reviewed in [100]) and has also been shown to improve muscle performance in *mdx* mice [104, 105, 106, 107, 108]. We chose to treat mice with the glucocorticoid, prednisolone, as it eliminates the need for hepatic conversion of prednisone into its active form prednisolone and also because deflazacort was not available to us. Placebo pellets contained the same matrix-driven delivery system as the prednisolone pellets, but did not contain the glucocorticoid.

4.3.4 Physical activity monitoring

Physical activity of individual mice was monitored for 24 hours using an open-field activity chamber and Activity Monitor software, version 5 (Med Associates Inc.) as previously described [109]. Briefly, the chamber contains an array of infrared beams, in which the software monitors activity counts every time an infrared beam is interrupted, along with how long the beam is interrupted. The methods used to discern the different types of physical activity are defined in Greising et al., and include active time, resting time, ambulatory distance, rearing counts, and stereotypic (i.e., eating or grooming) counts [109]. *Mdx* mice randomized to the restricted activity groups remained housed in small-sized cages (11.8 cm x 9.0 cm) within the activity chamber during physical activity monitoring, and *mdx* mice randomized to full activity groups had access to the entire area of the activity chamber (27.1cm x 27.9 cm).

4.3.5 Mechanical testing of tibial mid-diaphysis

The procedures used to assess the functional capacities of the mouse tibia have been described in detail previously [13, 11, 12]. Briefly, tibial bones were placed on their lateral side in a Mecmesin MultiTest 1-D test machine and underwent three-point bending at the mid-diaphysis using a Mecmesin AFG-25 load cell (Mecmesin). Functional measures of the tibial bone were quantified by ultimate load, stiffness, and deflection and energy absorbed to ultimate load using custom designed TestPoint software (TestPoint version 7; Measurement Computing Corp.) as previously described [13]. Upon completion of mechanical testing, bones were refrozen in PBS and stored at -80 ^{o}C until the time they underwent micro computed tomography (μCT) scanning. Intrinsic material properties for each tibia (i.e., ultimate stress and modulus of elasticity) were derived from three-point bending and μCT outcome measures as previously described [13, 11, 12].

4.3.6 μCT of the tibial diaphysis

Following mechanical testing, a region near the mid-diaphysis of the tibia was scanned with a μCT system (Scanco Medical μCT 40) to quantify cortical bone geometry and volumetric bone density (vBMD). The μCT was set to a voltage of 55 kVp and a current of 145 μA, and bones were scanned using an isotropic 12 μm voxel size with a 250-ms

integration time. For diaphyseal scanning, the distal half of the tibiae was positioned vertically in a scan tube and its length measured on the scout view image. Start position was set at 85% of the total length in the proximal direction from the distal-most point of the tibia (i.e., slightly distal to where the bone broke during three-point bending), and 66 slices (∼0.8 mm) distal to this point were scanned. Outcome measures for cortical bone at the tibial diaphysis include cortical bone cross-sectional area, cortical thickness, periosteal diameter, cross-sectional moment of inertia (CSMI) and vBMD. Each of these outcomes measures were assessed independently at each of the 66 slices, and the average of all 66 slices was calculated and used for statistical analyses. As previously noted, the minimum principal CSMI ($CSMI_min$) was utilized in the present study due to its correspondence with the CSMI about the bone bending axis during three-point bending testing [13].

4.3.7 Statistical Analyses

To analyze the effects of drug (placebo vs. prednisolone) and physical activity (normal cage size activity vs. small cage size activity), 2-way ANOVAs were utilized. When interactions were significant ($p<0.05$), Holm-Sidak post-hoc tests were performed to determine which combinations of conditions were different from each other. Pearson correlations were also calculated between tibial bone length and other geometric properties to provide insight into the influence of longitudinal growth on the bone cross-sectional geometry. All statistical analyses were carried out using SigmaStat version 3.5 (Systat Software Inc.).

4.4 Results

4.4.1 Physical activity levels and body masses

Twenty-four-hour activity monitoring was performed to confirm that housing *mdx* mice in small cages decreased physical activity, thus mirroring the reductions seen in ambulatory distance in DMD patients. There was no effect of prednisolone on any parameter of cage activity monitored ($p\geq0.154$; Figure 4.1). There was also no effect of cage size

on active time (Figure 4.1A). All groups of *mdx* mice spent ∼4 hours per day being active; however, the types of activities performed during this time were different between activity groups. *Mdx* mice housed in small cages ambulated 84% less distance than traditionally housed *mdx* mice (76 ± 27 vs. 463 ± 27 m/24 hr, respectively; p<0.001; Figure 4.1B), which equated to the mice in small cages spending 87 minutes less per day ambulating. Subsequently, those restricted-activity mice spent more time grooming, as indicated by 40% more stereotypic counts (p<0.001; Figure 4.1C).

Body masses were not different among the four groups of *mdx* mice at 5 weeks of age (21.0 ± 0.2 g; p¿0.061). However at 12 weeks of age, prednisolone-treated mice weighed 4% less than placebo-treated mice (29.9 ± 0.3 vs. 31.1 ± 0.4 g, respectively; p=0.018) and restricted-activity mice weighed 7% less than those housed in normal-sized cages (29.3 ± 0.3 vs. 31.6 ± 0.5 g, respectfully; p<0.001).

4.4.2 Effects of prednisolone and restricted activity on tibial bone mechanical functional capacity

In general, the functional capacity of the tibial bone was negatively affected by both prednisolone and restricted activity. Ultimate loads for the tibia of prednisolone-treated and restricted activity *mdx* mice were low (Figure 4.2A and Table 4.1), demonstrating that both treatments independently compromise bone strength. Restricted activity also affected tibial bone stiffness (Figure 4.2B and Table 4.1), indicating the bones ability to resist bending was reduced. The combination of reductions in tibial bone ultimate load and stiffness in restricted activity mice translated to the 15% increase in deflection to ultimate load (Table 4.1). Energy absorbed to ultimate load, however, was not impacted by either prednisolone or physical activity level (p≥0.081). Collectively, these results indicate that restrictions on physical activity cause further decrements in the functional capacities of the *mdx* tibial bone compared to disease progression alone, while prednisolone appears to negatively impact only the bones bending strength.

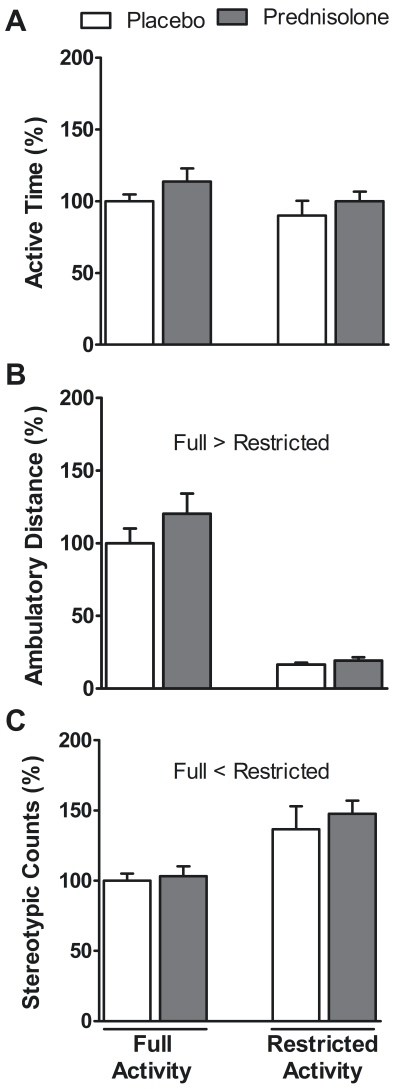

Figure 4.1: Effects of prednisolone and restricted activity on 24-hour physical activity measures including (A) active time, (B) ambulatory distance and (C) stereotypic counts. Values are mean ± SE. Data are normalized to the values of placebo-treated *mdx* mice housed in normal-sized cages that permitted full activity. Restricted Activity refers to *mdx* mice housed in 80% smaller cage by volume. Significant main effects of two-way ANOVA ($p<0.05$) are indicated above the bars.

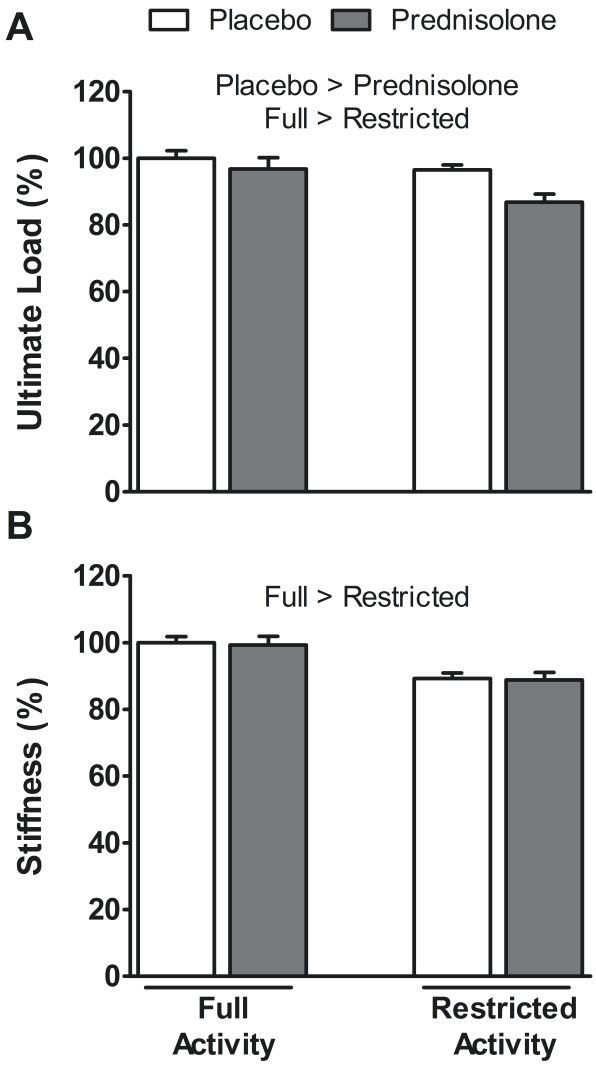

Figure 4.2: Effects of prednisolone and restricted activity on tibial bone (A) ultimate load and (B) stiffness. Values are mean ± SE. Data are normalized to the values of placebo-treated *mdx* mice housed in normal-sized cages to permit full activity. Restricted Activity refers to *mdx* mice housed in 80% smaller cage by volume. Significant main effects of two-way ANOVA ($p<0.05$) are indicated above the bars.

Table 4.1: Effects of prednisolone and restricted activity on tibial bone mechanical function, geometric properties and intrinsic material properties in *mdx* mice.

	Placebo	Placebo + Restricted Activity	Prednisolone	Prednisolone + Restricted Activity	P-Values for Two-Way ANOVA		
					Main effect of Prednisolone	Main effect of Restricted Activity	Interaction (Prednisolone x Restricted Activity)
Mechanical Functional Properties							
Ultimate Load (N)	13.72 (0.32)	13.24 (0.21)	13.29 (0.46)	11.91 (0.34)	0.022	0.016	0.227
Stiffness (N/mm)	41.66 (0.78)	37.20 (0.71)	41.39 (1.08)	37.02 (0.94)	0.810	<0.001	0.963
Deflection to Ultimate Load (mm)	0.41 (0.02)	0.51 (0.04)	0.41 (0.01)	0.44 (0.03)	0.196	0.017	0.184
Energy Absorbed to Ultimate Load (mJ)	3.12 (0.020)	3.42 (0.32)	3.01 (0.10)	2.74 (0.23)	0.081	0.938	0.193
Geometric Properties							
Tibial Length (mm)	18.51 (0.08)	17.74[a] (0.18)	18.04[a] (0.07)	18.14[b] (0.12)	-	-	<0.001
Cortical Cross-sectional Area (mm^2)	0.74 (0.02)	0.67 (0.02)	0.71 (0.02)	0.60 (0.02)	0.015	<0.001	0.381
Cortical Thickness (mm)	0.25 (0.005)	0.22 (0.004)	0.23 (0.004)	0.20 (0.003)	<0.001	<0.001	0.878
Periosteal Diameter (mm)	1.08 (0.01)	1.05 (0.01)	1.08 (0.02)	1.05 (0.01)	0.880	0.041	0.980
CSMI (mm^4)	0.070 (0.003)	0.053 (0.002)	0.061 (0.003)	0.052 (0.002)	0.255	<0.001	0.551
Intrinsic Material Properties							
Ultimate Stress (MPa)	284.8 (9.5)	327.2[a] (5.5)	294.8 (8.0)	302.1[b] (8.5)	-	-	0.039
Modulus of Elasticity (GPa)	13.8 (0.5)	14.7 (0.5)	14.3 (0.4)	15.0 (0.5)	0.396	0.112	0.871
vBMD (mg/cm^3)	1317.0 (6.1)	1312.1 (4.7)	1325.5 ((5.4)	1309.6 (4.9)	0.582	0.061	0.311

Values are means (SE). CSMI, cross-sectional moment of inertia. vBMD, volumetric bone mineral density. [a] *Significantly different from Placebo.* [b] *Significantly different from Placebo + Restricted Activity.*

4.4.3 Effects of prednisolone and restricted activity on tibial bone geometry

μCT was utilized to determine if tibial bone geometry near the mid-shaft was impacted by prednisolone or restricted activity, which may have contributed to the alterations in mechanical functional capacity. For prednisolone-treated *mdx* mice, the area of the cortical bone was 8% smaller, which resulted from 6% smaller cortical thickness(Table 4.1). These deficits likely contributed to the reduction in ultimate load seen in prednisolone-treated mice. Additional measures of cortical bone geometry, including periosteal diameter and CSMI, were not affected by prednisolone treatment (p¿0.26). Restricted activity consistently showed a detrimental influence on bone geometry. Specifically, *mdx* mice that were restricted had 13% smaller cortical cross-sectional area, 13% smaller cortical thickness and 3% smaller periosteal diameter, and 17% lower CSMI (i.e., reflection of the moment of inertia during three-point bending), compared to *mdx* mice with non-restricted activity (Table 4.1). Tibial bone length (Table 4.1), however was positively correlated with cortical cross-sectional area, cortical thickness and CSMI (r= 0.37 to 0.48; p<0.03) but not periosteal diameter (p=0.21). Combined, these reductions in cortical bone geometry in *mdx* mice with restricted activity indicate that reductions in physical activity resulted in smaller sized tibial bones and thus may have contributed to the differences in tibial bone mechanical properties.

4.4.4 Effects of prednisolone and restricted activity on tibial bone intrinsic material properties

Intrinsic material properties of the tibia were quantified by ultimate stress, modulus of elasticity and vBMD. Ultimate stress values were 15% higher in placebo-treated mice with restricted activity compared to placebo mice (i.e., significant interaction; Table 4.1). The combination of prednisolone and restricted activity blunted this increase, such that ultimate stress values were similar to placebo mice but 8% lower than restricted-activity placebo mice (Table 4.1). Differences among groups were not apparent for modulus of elasticity and vBMD, although vBMD tended to be lower in restricted activity mice (i.e., p=0.06 main effect of activity).

4.5 Discussion

We had two primary findings from our study. First, mechanical testing of tibial bones from *mdx* mice showed that both prednisolone treatment and restricted physical activity independently reduced the ultimate load (Figure 4.2A and Table 4.1). Secondly, reductions in tibial bone strength and stiffness were primarily attributed to having smaller bone geometry at the tibial midshaft, rather than alterations in the intrinsic material properties, such as vBMD (Table 4.1). Combined, these data indicate that prednisolone treatment and restricted physical activity independently augment the deleterious effects associated with DMD disease progression on the bones functional capacity and geometry, and may therefore further predispose bone to fracture.

Our previous work confirmed that *mdx* mice have inherently weak tibial bones (e.g., 20-50% lower ultimate loads) relative to wildtype mice [13], and the present study extends these findings using clinically-relevant conditions. Specifically, prednisolone treatment and restricted physical activity each resulted in a 7% reduction in ultimate load (Figure 4.2A). Similar 9% declines in bone strength have been realized in rats after 8 weeks of prednisone treatment [110]; however up to 50% reductions in mouse femur bone strength have been realized with high doses of prednisone (i.e., 1.4 mg/kg/day) [111]. Additional evidence implicating glucocorticoids role in altering bone strength arises from the occurrence of vertebral compression fractures that are present in DMD patients only after taking prednisone in excess of three years [65, 64]. Compression tests performed on vertebrae have confirmed these clinical observations suggesting bone strength is indeed compromised following the use of glucocorticoids such as prednisone [112, 61, 113]. Combined, these data highlight the deleterious effect of this class of drugs on the strength of various bones. The declines in mechanical function following restricted physical activity are in accordance with other forms of severe immobilization (i.e., denervation, fixation, or hindlimb suspension), in which bone strength is reduced 10-20% [102, 103]. Reductions in tibial bone stiffness, however, were only apparent in mice with restricted activity (-11%, Figure 4.2B), highlighting the importance of dynamic loading (e.g. ambulation) rather than static loads (i.e., grooming) for the preservation of bones mechanical strength and stiffness in dystrophic mice.

The mechanical strength of bone is largely dependent upon the geometry, or shape,

of the bone as well as its material properties. Therefore, to determine the extent to which cortical bone geometry was affected by prednisolone treatment and restricted activity, μCT was performed. Our present work confirms previous studies suggesting that glucocorticoid treatment and reduced physical activity have the capacity to negatively alter bone geometry [114, 64, 115], as well as expands our previous work showing that the bone of dystrophic mice has altered bone geometry [13]. Specifically, prednisolone treatment and restricted physical activity independently caused up to 12% further decrements in tibial bones cortical cross-sectional area and cortical thickness compared to disease progression alone (Table 4.1). These data are in agreement with preliminary pQCT findings in boys with DMD, which suggest that cross-sectional areas of the tibia and radius are reduced, and following the loss of ambulation, the areas become further reduced [4, 5, 6]. CSMI, which is the most precise determinant of bones mechanical properties during three-point bending, was not affected by prednisolone treatment, but was lower in *mdx* mice with restricted activity (Table 4.1). Preliminary pQCT data show that boys with DMD have 32% lower strength-strain index (i.e., a pQCT-derived surrogate for polar CSMI) compared to healthy boys [4, 5, 6]. Further, those findings suggest that differences were accentuated in non-ambulatory boys, but congruent with the present study, were not influenced by the use of glucocorticoid. It is possible that in our study differences in the rates of longitudinal bone growth among groups of mice may partially or totally account for the observed differences in bone cross-sectional geometry. To probe this idea, we calculated correlations and found that cortical cross-sectional area, cortical thickness and CSMI (but not periosteal diameter) were modestly correlated with tibial bone length. Despite these positive associations, the among-group statistical comparison findings for cortical cross-sectional area and CSMI do not match those for tibial bone length (Table 4.1), suggesting that differential longitudinal bone growth rates do not completely explain the differences among groups in bone cross-sectional geometry. Combined, these results indicate that glucocorticoids and restricted physical activity both have deleterious effects on bone cross-sectional area; however, physical activity alone has a negative impact on CSMI.

Beyond investigating the role of prednisolone and restricted activitys capacity to alter bone geometry, we also investigated the impact that these factors have on the tibial bones intrinsic material properties. Neither modulus of elasticity nor vBMD were

impacted by prednisolone use or restricted activity; however, there was a trend toward *mdx* mice with restricted activity having lower vBMD (p=0.06, Table 4.1). Declines in bone mass following reductions in physical activity [116, 37], as well as with DMD disease progression [56, 2, 117] have been well documented. In the present study, the effect of restricted activity on tibia vBMD may have been minimized because mice engaged in some weight-bearing activities that loaded the hindlimb bones (i.e., rearing while doing stereotypic activities), which may have blunted loss of bone mass. Preliminary pQCT studies in boys with DMD show that vBMD is not affected by prednisone use [4] and cortical vBMD at the mid-diaphysis may actually be higher than age-matched controls [5, 6], suggesting that bones intrinsic material properties are also minimally affected by glucocorticoids.

In summary, the present study has established that prednisolone treatment and restrictions on physical activity negatively and independently accentuate reductions in the strength of cortical bone of *mdx* mice. Tibia from mice that were treated with prednisolone and were restricted in their physical activity had the lowest values of function and structure (e.g., ultimate load, cortical bone cross-sectional area, and cortical thickness). The reductions in bone strength are attributed to alterations in bone geometry rather than altered intrinsic material properties. These results indicate prednisolone and restrictions of physical activity have detrimental affects on skeletal health, and may possibly contribute to the development of bone fragility and heightened fracture risk in boys with DMD.

Chapter 5

Musculoskeletal response of dystrophic mice to short term, low intensity, high frequency vibration

Susan A. Novotny[1], Michael D. Eckhoff[2], Brian C. Eby[2], Jarrod A. Call[2], David Nuckley[2] and Dawn A. Lowe[2]

[1]Department of Kinesiology, University of Minnesota, Minneapolis, Minnesota [2]Programs in Physical Therapy and Rehabilitation Sciences, University of Minnesota, Minneapolis, Minnesota

5.1 Abstract

Objectives: This study aimed to identify parameters of low intensity vibration that initiated the greatest osteogenic response in dystrophin-deficient mice and confirm that vibration is not deleterious to diseased skeletal muscle. **Methods:** *Mdx* mice were randomized to one of seven vibration treatments and after 14 days, plasma osteocalcin levels and osteogenic gene expression in tibia were compared. Muscle torque and expression of genes associated with inflammation and myogenesis were also assessed in hindlimb muscles. *Mdx* mice vibrated for 3d were compared to control mice as well as other modalities known to elicit muscle injury, and a 7d vibration study included dystrophic mice with more severe phenotypes due to altered utrophin. **Results:** Two sets of vibration parameters (45Hz at $0.6g$ and 90Hz at $0.6g$) evoked an osteogenic response. 45Hz upregulated alkaline phosphatase and tended to upregulate osteoprotegerin without altering RANKL levels, and 90Hz simultaneously upregulated osteprotegerin and RANKL. Thus, subsequent muscle studies utilized the 45Hz setting. Vibration for 3 or 7d was not injurious to dystrophic muscle as shown by the lack of differences between vibrated and non-vibrated mice in torque production and gene expression. **Conclusions:** These data indicate that vibration at 45Hz and $0.6g$ is safe for dystrophic muscle and may be a potential therapeutic modality to improve musculoskeletal health in DMD. These data indicate that vibration at 45Hz and $0.6g$ is safe for dystrophic muscle and may be a potential therapeutic modality to improve musculoskeletal health in DMD.

5.2 Introduction

Bone and muscle are biomechanically and biochemically linked at many levels. As such, bone strength, shape, and mass are largely determined by the mechanical influences of its associated muscles. In muscle diseases, such as Duchenne muscular dystrophy (DMD), decrements in bone mass are apparent in various skeletal regions as a result of muscle weakness and the consequential reductions in mechanical loading [2, 55, 6, 5]. The loss of bone mass appears to compromise the strength of the bone, as indicated by the prevalence of fragility fractures, which occur after falling from standing or sitting heights [2, 3, 1, 118, 57]. The primary determinant of bone strength is shape, or geometry, and this is altered in several skeletal regions of both patients and mouse models of DMD [6, 5, 13, 66]. Exercise regimens such as running and jumping are typically prescribed to improve bone strength and geometry in healthy populations, however these activities are ill advised in patients with DMD due to their high susceptibility to fragility fractures in bone [2, 3, 1, 57] and concern for exercise-induced muscle damage [119]. Therefore, an alternative bone-sparing strategy is needed for DMD, one which is affective at improving bone strength and geometry, but also safe for muscle.

Low intensity vibration (i.e., less than 1 g of acceleration, where 1 g is equivalent to gravity) has been shown to have an anabolic effect on bone as well as prevent disuse-mediated bone loss [81, 120, 82, 80]. However, some studies have failed to replicate these findings when utilizing similar acceleration and frequency parameters of vibration [121, 122, 123, 124, 125]. The conflicting results suggest that these parameters may need to be customized to the population of interest. That is, the optimal mechanical signal delivered by vibration to stimulate bone formation that is required to improve geometry and strength may differ depending on the underlying status of the bone and condition(s) that precipitated its decline.

Thus, prior to considering vibration as a bone-sparing modality for muscular dystrophy, our first study was designed to identify parameters of vibration that increased circulating osteocalcin levels and initiated the greatest osteogenic response in tibia of *mdx* mice. *Mdx* mice were selected because they have a bone phenotype similar to patients with DMD including bone strength, geometry and trabecular architecture that are

reduced up to 78% compared to wildtype mice [13, 66, 7]. We chose circulating osteocalcin and specific genes along the osteoblastic lineage as well as genes associated with the inhibition and activation of osteoclasts based on previous work [124, 126, 127, 128]. In Study 1, we tested the hypothesis that *mdx* mice exposed to 14 daily bouts of low intensity vibration would have increased osteogenic gene expression and elevated circulating levels of osteocalcin compared to non-vibrated *mdx* mice.

After identifying the parameters of vibration that appeared to be most anabolic for bone of *mdx* mice, our next objective was to assess short-term responses of dystrophic skeletal muscle to those specific vibration-induced mechanical signals. Our previous work on wildtype mice showed that low intensity vibration training improved muscle contractility. Specifically, up to 20% improvements in strength and maximal rate of relaxation occurred following 6 wk of training, with no indication of adverse effects to muscle function [129]. However, the efficacy and impact of vibration training on dystrophic muscle is unknown and is critical to determine because the lack of dystrophin renders skeletal muscle vulnerable to mechanical stress [130]. Consequently, we performed Studies 2 and 3 to determine the extent to which low intensity vibration impacted skeletal muscle contractility and altered the expression of genes associated with inflammation and myogenesis. Study 2 tested the general hypothesis that three daily bouts of vibration would not be injurious to *mdx* muscle. The study was designed so that vibration-induced responses of hindlimb muscles could be directly compared with those from muscles of *mdx* mice that completed 3 d of voluntary wheel running or were subjected to a bout of injurious eccentric contractions. This was done in attempt to place vibration training on a continuum with other physical interventions known to elicit relatively minor and major muscle injury, that is, acute response to wheel running [131] and eccentric contractions, respectively [130, 90]. The specific hypothesis tested in Study 2 was that contractility and gene expression of muscles from vibrated *mdx* mice would not be different than those from control *mdx* mice, but would be different than those from *mdx* mice that wheel ran or were subjected to eccentric contraction-induced injury.

A subsequent study tested the general hypothesis that seven daily bouts of low intensity vibration would not be deleterious to muscle of dystrophic mice, even those with phenotypes substantially more severe than the *mdx* mouse. Mice lacking both

dystrophin and utrophin (*dko* mice;[86]) and mice lacking dystrophin that are haploinsufficient for utrophin (*het*; [68, 132]) as well as *mdx*, were subjected to seven daily bouts of vibration or a sham vibration intervention. The specific hypothesis tested in Study 3 was that contractility and gene expression of hindlimb muscles from vibrated *dko*, *het*, and *mdx* mice would not be different than those from littermates that were subjected to the sham vibration protocol. Support of hypotheses in Studies 2 and 3 would endorse the premise that low intensity vibration is not harmful to dystrophic muscle and that vibration therapy could be considered as a bone-sparing strategy in patients with DMD.

5.3 Methods

Animals

Five wk-old male *mdx* mice (C57Bl/10ScSn-DMD^{mdx}) were obtained from Jackson Laboratories (Bar Harbor, ME) for Study 1. For Studies 2 and 3, dystrophic mice were obtained from our breeding colony at the University of Minnesota [133], with the exception of being backcrossed onto a pure C57Bl/10 background, which was verified by The Jackson Laboratory. Study 2 utilized male *mdx* mice aged 8 wk because peak muscle pathology occurs in the *mdx* mouse from about 5-10 wk of age. Study 3 utilized 3 wk-old *mdx*, *het*, and *dko* littermates of both sexes. Relatively younger mice were selected for this study in order to determine the impact of vibration at the onset of disease pathology. All mice were housed on a 12:12-h light-dark cycle at 20-23 ^{o}C and were provided food and water ad libitum. Mice in Study 1 were killed by sodium pentobarbital overdose (200 mg/kg body mass) and exsanguination. Immediately following *in vivo* contractility testing, mice in Studies 2 and 3 were further anesthetized with sodium pentobarbital (75 mg/kg body mass), muscles were dissected, and then mice were euthanized by exsanguination. All animal care and use procedures were approved by the Institutional Animal Care and Use Committee at the University of Minnesota.

Experimental Design

The purpose of Study 1 was to determine the parameters of vibration (i.e., acceleration and frequency) that increased circulating osteocalcin levels and initiated the greatest osteogenic response in tibia of *mdx* mice. To do this, *mdx* mice were randomly assigned

to one of seven vibration treatments; non-vibrated control (n=8), 30 Hz at 0.3 *g* (n=6), 30 Hz at 0.6 *g* (n=6), 45 Hz at 0.3 *g* (n=8), 45 Hz at 0.6 *g* (n=8), 90 Hz at 0.3 *g* (n=6), or 90 Hz at 0.6 *g* (n=6). At 6 wk of age, *mdx* mice began daily bouts of vibration (7 d/wk for 15 min/d) for 14 d. For this and all subsequent studies, non-vibrated control mice (i.e., 0 Hz at 0 g) were placed on a vibration platform while the system was turned off. Approximately 1 hr following the last bout of vibration, mice were anesthetized and plasma was collected via cardiac puncture to assess the impact vibration training had on a circulating marker of bone formation. Tibial bones were removed, flash frozen in liquid nitrogen, and then stored at -80 C until the time of RNA isolation.

The purpose of Study 2 was to determine if vibration was injurious to *mdx* muscle by placing it along a continuum with other physical interventions that are known to elicit minimal or major muscle injury in mice (i.e., acute wheel running and eccentric contractions, respectfully). To do this, *mdx* mice were randomly assigned to one of four groups; control (n=10), vibration (n=11), wheel running (n=8), or eccentric contractions (n=8). Cage activities were also monitored in control, vibration and wheel running groups to determine whether vibration was stressful to *mdx* mice [134]. Following the third daily bout of vibration (15 min/d, using 45 Hz and 0.6 g), 3 d of voluntary wheel running, or 3 d after a single bout of injurious eccentric contractions, plasma was collected from the retro-orbital cavity to assess creatine kinase (CK) activity and stored at -80 ^{o}C. Contractility of the posterior crural muscle group (gastrocnemius, plantaris, soleus muscles) was then tested *in vivo*. Immediately following contractility testing, gastrocnemius muscles were excised, flash frozen in liquid nitrogen, and stored at -80 ^{o}C. Subsequently, these muscles were used to determine the relative potential of low intensity vibration to increase expression of genes associated with muscle inflammation and myogenesis.

The purpose of Study 3 was to extend the evaluation of short-term responses of dystrophic muscle to vibration by lengthening the duration of vibration exposure to 7 d and by using dystrophic mouse models that have more severe phenotypes than *mdx* mice. To do this, *mdx*, *het* and *dko* mice were randomly assigned to vibration training (n= 8, 8 and 7, respectfully) or non-vibrated control groups (n= 9, 12 and 7, respectfully) at 3 wk of age. Twenty-four hours after the seventh bout of vibration (15 min/d at 45 Hz and 0.6 g), plasma was collected from the retro-orbital cavity to assess CK, and

then posterior crural muscle contractility was assessed *in vivo*. Immediately following testing, tibialis anterior (TA) muscles were excised, flash frozen in liquid nitrogen, and stored at -80 ^{o}C until RNA was isolated to assess gene expression.

Vibration Training

Our low intensity vibration device was designed after the work of Fritton et al. [135] with minor modifications that improve device performance and ensure fidelity [173]. Briefly, the circular vibration platform is driven by a centrally-mounted linear actuator (Moog CSA Engineering, Mountain View, CA) on the underside of the platform. A custom-designed program created with LabVIEW software (National Instruments, Austin, TX) controls and modulates the linear actuator based on continual accelerometer feedback. Mice were placed into one of four individual compartments of the centrally-mounted cage (See Figure 5.1 of [173]). The height of the cage was set to 5 cm to limit rearing and jumping by the mice.

Wheel Running

Mice were individually housed in cages containing running wheels (Single Activity Wheel Chambers, Model 80820, Lafayette Instruments Co., Lafayette, IL). One gram of resistance was applied to each wheel using resistance brakes (Model 86070-B1, Lafayette Instruments). Total distance run over the 3-d study was measured using the manufacturers software (Model 86065, Lafayette Instruments).This 72-hr of distance recording excluded the 30 min during which cage activity was monitored.

Eccentric Contractions

In effort to compare vibration training to a relatively major muscle injury intervention, the posterior crural muscles of anesthetized *mdx* mice underwent a series of 100 eccentric contractions as previously described [136].

Cage Activity Monitoring

As a means of determining if vibration was stressful, as shown to occur with mild exercise in *mdx* mice [137], cage activities were monitored in vibrated mice and compared to non-vibrated control and wheel-running mice. Cage activity was not measured in the

mice that performed the eccentric contractions because of the lingering effects of anesthesia. Active time, ambulatory distance, and stereotypic time (i.e., eating or grooming) were measured for 30 min immediately after a bout of vibration (Med Associates Inc., St. Albans, VT) [109].

Plasma Osteocalcin and CK Activity

Circulating levels of osteocalcin were assessed in plasma using an ELISA assay (Biomedical Technologies Inc., Stoughton, MA). The assay was performed in duplicate using 1:10 dilution of plasma and following manufacturer specifications. Data for the standards were fit using a 4-parameter logistic curve fit.

Plasma CK activity was determined in duplicate with plasma diluted 1:2 in PBS. Activity was measured using a kinetic assay (Creatine Kinase, C7512-300, Pointe Scientific, Inc., Canton, MI) and a Spectramax Plus 384 spectrophotometer with Softmax Pro v5 (Molecular Devices, Sunnyvale, CA) [138].

In vivo Posterior Crural Muscle Function

Contractile function of the posterior crural muscles was tested as previously reported [139]. After severing the peroneal nerve, the sciatic nerve was stimulated at 250 Hz for 150 ms to elicit maximal isometric torque. Torque production as a function of stimulation frequency was measured as described previously [133], with the addition of measurements at 200 and 250 Hz.

RNA Isolation and Real-Time RT-PCR

RNA was isolated from the left tibial bones of mice in Study 1 by homogenizing in liquid nitrogen using a mortar and pestle and then transferring the powdered bone to TRI reagent (Applied Biosystems, Austin, TX). Phases were separated by centrifugation and RNA was precipitated by ethanol addition and then applied to RNA clean-up spin columns (Qiagen, Valencia, CA). DNA contaminates were removed by RNase-Free DNase treatment (Promega, Madison, WI) and total RNA concentration was quantified on a Nanodrop spectrophotometer (Nanodrop, Wilmington, DE). One microgram of cDNA was then diluted, synthesized and reverse transcribed using High Capacity cDNA Reverse Transcription (Applied Biosystems). cDNA samples were stored at -20

^{o}C until RT-PCR was performed. cDNA at 1:100 dilutions were then combined with TaqMan Universal PCR Master mix (Applied Biosystems, Carlsbad, CA) and TaqMan gene expression assays (Applied Biosystems), and were then run on a Biorad MyiQ thermocycler (Hercules, CA). Genes of interest associated with osteoblast cell activation, differentiation, signaling and bone formation included: alkaline phosphatase (ALP), runt related transcription factor 2 (Runx2), bone morphogenetic protein 2 (BMP2), and collagen type-1 α-1. Gene expression associated with the inhibition and activation of osteoclasts (i.e., Osteoprotegerin (OPG) and activator for nuclear factor κB ligand (RANKL), respectively) were also quantified.

The effects of short term vibration on gene expression associated with muscle inflammation (macrophage-1 antigen, (MAC-1) and the chemokine ligand 2 (MCP-1)) and myogenesis (Paired box gene-7 (Pax-7), Myogenic differentiation-1 (MyoD), and Myogenin) were assessed in gastrocnemius and TA muscles from mice in Studies 2 and 3, respectively. RNA was isolated by homogenizing muscles in TRI reagent. One μg of RNA was reverse transcribed and used for RT-PCR at a dilution of 1:100. For all analyses, triplicates were run for each mouse and the average crossing threshold for each gene of interest and the housekeeping gene (i.e., GAPDH or 18s) were used to make comparisons against non-vibrated control mice using Rest 2009 software, described below.

Statistical Analyses

To examine if vibration was stressful for dystrophic mice or altered circulating osteocalcin levels in Study 1, one-way ANOVAs were used to compare body mass and osteocalcin levels across groups. To determine optimal parameters of vibration on bone in Study 1, the combined effects of acceleration (0.3 and 0.6) and frequency (30, 45 and 90 Hz) were analyzed for tibial bone gene expression data using two-way ANOVAs (i.e., main effects of acceleration and frequency).

For Study 2, one-way ANOVAs were used to compare body mass, plasma CK activity, cage activities and *in vivo* muscle function across treatments (i.e., controls, vibration, wheel running, and eccentric contractions). When assumptions of normality or equal variance were violated, Kruskal-Wallis One Way Analysis of Variance on Ranks was performed along with Dunns post-hoc tests. For Study 3, two-way ANOVAs were

used to analyze the effects of treatment (non-vibrated controls vs. vibrated) and genotype (*mdx*, *het* and *dko*) on body mass, CK activity, and *in vivo* muscle function. For all ANOVAs, when significant main effects or interactions were present (i.e., $P<0.05$), Holm-Sidak post hoc tests were performed to determine which conditions were different from each other. These statistical analyses were carried out using SigmaStat version 3.5 (Systat Software Inc; Point Richmond, CA).

To examine the effect of vibration on gene expression profiles compared to non-vibrated control mice, in all studies, real time RT-PCR data were analyzed with REST 2009 Software (Qiagen). Data are expressed as relative expression compared to non-vibrated mice with 95% confidence intervals [140]. Note that the 95% confidence intervals represent data that has an exponential distribution, and therefore the data are more heavily distributed on the lower bound making the mean closer to the lower bound than the upper bound. As such, the length of the 95% confidence interval is smaller below the mean than above.

5.4 Results

Study 1, Osteogenic responses: In general, vibration treatment was well tolerated by *mdx* mice and did not appear to be stressful as indicated by the preservation of body mass (25.1 ± 0.4 g in vibrated vs. 24.4 ± 0.1 g in control mice at the end of the study, $P=0.978$). In addition, behavior of the mice did not appear to be affected during or immediately after a bout of vibration.

Parameters of vibration that resulted in the greatest increase in circulating osteocalcin and osteogenic mRNA expression in the tibial bone in response to 14 d of 15-min bouts of vibration were sought. However, circulating plasma osteocalcin levels were not different among the seven groups of mice, suggesting that vibration did not alter osteoblast activity (59.2 ± 2.2 ng/ml, $P \geq 0.354$).

Result of REST 2009 analyses revealed that osteoprotegerin mRNA expression was significantly upregulated in *mdx* mice vibrated at 90 Hz and 0.6 *g* and modestly upregulated at 45 Hz and 0.6 *g* ($P=0.109$) compared to non-vibrated *mdx* mice (Figure 5.1A). RANKL mRNA expression was 1.24 fold higher at 90 Hz and 0.6 g, and equivalent to control *mdx* mice at 45 Hz and 0.6 *g* (Figure 5.1B), suggesting that the osteoprotegerin

to RANKL ratio is more osteogenic at 45 Hz and 0.6 g. In addition, alkaline phosphatase mRNA expression at 45 Hz at 0.6 g was increased, but this increase was not apparent at 90 Hz at 0.6 g (Figure 5.1C). There were no detectable differences in mRNA expression for Runx2, collagen type I-α- I, or BMP-2 at any of the six parameters of vibration utilized compared to the non-vibrated condition (range of fold change 0.837-1.44, $P \geq 0.156$).

Results of two-way ANOVAs showed no main effects of acceleration and frequency ($P \geq 0.181$), with the exception of osteoprotegerin, which had a trend toward upregulation at higher frequencies ($P = 0.052$). Due to the relative elevations of alkaline phosphatase and osteoprotegerin mRNA expression at 45 Hz at 0.6 g those parameters were used for subsequent muscle-specific studies in dystrophic mice.

Study 2, Contractility: To determine whether vibration was deleterious to muscle lacking dystrophin, *mdx* mice were exposed to three daily bouts of vibration and then their hindlimb muscle function was compared to control *mdx* mice, as well as to *mdx* mice that engaged in other forms of physical activities. Specifically, *mdx* mice in the wheel running group voluntarily ran 17.5 $\pm$ 2.0 km over the 3-d study and *mdx* mice in the eccentric group performed 100 eccentric contractions resulting in an immediate 79% loss in eccentric torque.

Following three days of normal cage activity (i.e., controls), vibration, wheel running, or a bout of eccentric contractions, peak isometric torque produced by the posterior crural muscles was significantly different between groups (Figure 5.2A). Vibrated mice were equivalent to both control and wheel running mice. As hypothesized, *mdx* mice that performed eccentric contractions had up to 37% lower isometric torque values, though post-hoc testing did not detect a significant difference between any of the groups (Figure 5.2A). CK activity levels were different among groups ($P = 0.020$), with eccentric mice having 24% higher plasma CK activity levels than controls (2829.5 $\pm$ 95.2 U/L vs 2278.9 $\pm$ 122.1 U/L). There were no differences in CK activity levels between vibrated, wheel running and control mice.

Additional measures of posterior crural muscle contractile function assessed in Study 2 including maximal rates of contraction and relaxation during isometric contractions and isometric torque as a function of stimulation frequency confirm that vibration was not injurious to *mdx* muscle (Figure 5.2). Muscles of vibrated mice generated equivalent

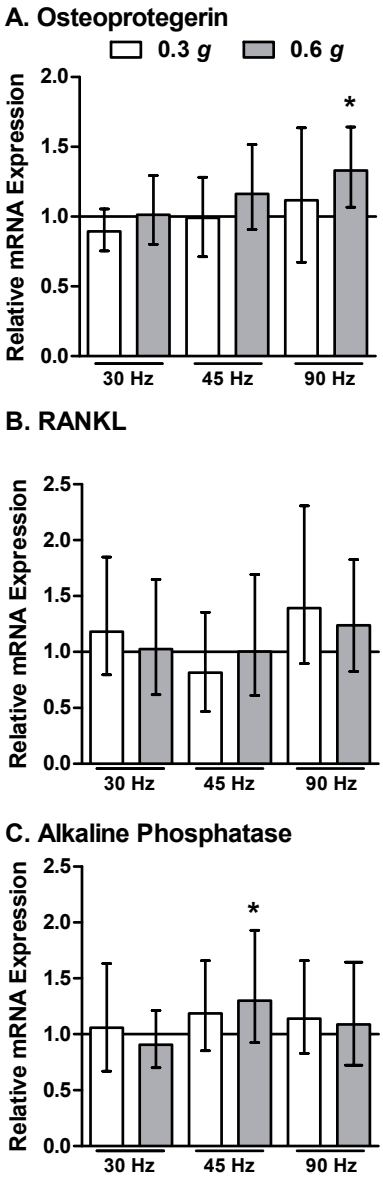

Figure 5.1: Six different permutations of low-intensity vibration parameters had minimal effects on tibial bone osteogenic mRNA expression following 14 days of daily vibration exposure. The height of the bars indicate the fold change mRNA expression (i.e., delta-delta CT) above non-vibrated *mdx* mice (represented by the horizontal gray line) and the error bars indicate the 95% confidence intervals. *Significantly different from non-vibrated *mdx* mice as determined by REST, 2009 software ($P<0.05$).

torque compared to control mice and greater torque compared to eccentrically-injured muscles at both 10 and 30 Hz (Figure 5.2B). Combined, these data indicate that muscle contractile function was not compromised by vibration in *mdx* mice, as was shown with eccentrically-injured muscle of *mdx* mice.

In addition, cage activity levels were not reduced during the 30 min immediately following vibration, and in fact, these mice tended to be 7% more active than non-vibrated controls (Figure 5.1). This increase in cage activity corresponded to ∼70 sec, and was primarily spent ambulating (11.6 ± 0.5 min in vibrated mice and 10.2 ± 0.5min in control mice, P=0.107). Despite the increase in active time, vibrated mice traveled equivalent total distances (Figure 5.1). These results support the contention that vibration is not detrimental to *mdx* mice.

Table 5.1: Comparison of 30-minute cage activity levels between *mdx* mice in typical mouse cages (control), following vibration, or wheel running.

	Control	**Vibrated**	**Wheel Running**	**One Way ANOVA P-value**
Active Time (min)	17.1 (0.6)	18.3 (0.4)	16.0 (0.9)	0.054
Stereotypic time (min)	10.2 (0.5)	11.6 (0.6)	9.2 (1.0)	0.111
Ambulatory distance (m)	49.3 (2.5)	55.3 (2.3)	45.8 (5.0)	0.157

Values are means (SE).

Study 3, Contractility: To further assess if vibration could be injurious to dystrophic mice, we extended the vibration exposure time to 7 d and utilized *het* and *dko* mice in addition to *mdx* mice. These mice represent a range of dystrophic phenotypes of DMD where *dko* mice in particular are very susceptible to muscle injury. Body mass did not significantly differ among the groups following 7 d of vibration exposure (14.5 ± 0.5 g, P≥0.429).

In vivo contractile testing of the posterior crural muscles showed that vibration had no deleterious consequences on muscle function, however, by design, genotypic differences in contractile function were apparent. Peak isometric torque was not influenced by vibration, while *dko* mice had up to 38% lower torque and rates of contraction and relaxation compared to both *mdx* and *het* mice (Figure 5.3A). Similar patterns were seen for isometric torque as a function of stimulation frequency. Vibration had no effect

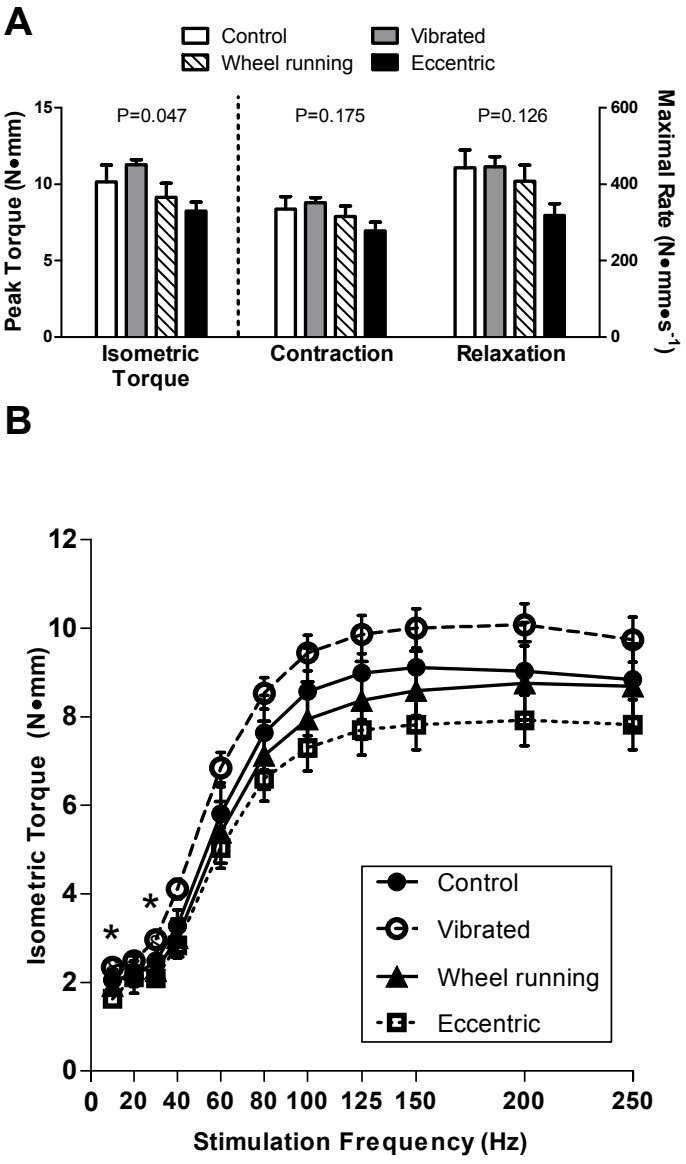

Figure 5.2: Three daily bouts of low intensity vibration on *mdx* mouse posterior crural muscle contractility compared to other exercise modalities. Data are mean, SE. A: Peak isometric torque and rates of contraction and relaxation were not detrimentally affected by vibration. Main effect P-values from one-way ANOVA's are indicated above each set of bars. Despite the significant main effect for peak isometric torque, post hoc testing did not detect a significant difference among any of the four groups. B: Isometric torque as a function of stimulation frequency for non-vibrated control, vibrated, wheel running and eccentrically injured *mdx* mice. *Significant difference determined from post hoc testing with torque by vibrated mice greater than that by eccentric mice.

on submaximal torques and *dko* mice had lower isometric torque values at all frequencies above 80 Hz (Figure 5.3B). CK activity was measured to assess if vibration was more injurious to models of DMD that are more susceptible to injury. There was no effect of genotype or 7 d of vibration on plasma CK activity (1354 ± 34 U/L for all groups; P≥0.514).

Studies 2 and 3, Gene Expression

mRNA expression profiles were assessed in two muscles to determine if early markers of muscle inflammation and myogenesis were affected by short-term vibration training. Vibration had no impact on any of the genes assessed in the gastrocnemius muscle following 3 d of exposure (P≥0.126), however, wheel running and eccentric injured muscles had a nearly 7-fold upregulation of MAC-1 and MCP-1 mRNA expression compared to control muscles (Figure 5.4A). Extending vibration training out to 7 d and using the most severe model of DMD (i.e., *dko* mice) did not evoke changes in tibialis anterior muscle mRNA expression levels in genes associated with muscle inflammation or myogenesis (Figure 5.4B, P≥0.192). *Het* mice, however did have a small but statistically significant 1.4 fold increase in Pax-7 mRNA when vibrated (Figure 5.4B, P=0.044). Combined, these data suggest that vibration is not injurious to dystrophic muscle in terms of eliciting an inflammatory response and also showed little evidence for initiating myogenesis.

5.5 Discussion

We had three primary findings from our project. First, low intensity vibration was well tolerated in each of the three dystrophic mouse models utilized (i.e., *mdx*, *het* and *dko* mice) and at two ages in the *mdx* mice. It also did not appear to be stressful based on preservation of cage activities and body mass. Second, in response to 14 d of low intensity vibration training, 45 Hz and 0.6 g was identified as the set of parameters that tended to be the most osteogenic in *mdx* mice. As such, subsequent studies on muscle responses to vibration were performed using these parameters of vibration. Third, vibration was consistently shown to be non-injurious to dystrophic muscle of various disease severity. Contractile function of the posterior crural muscles was not different

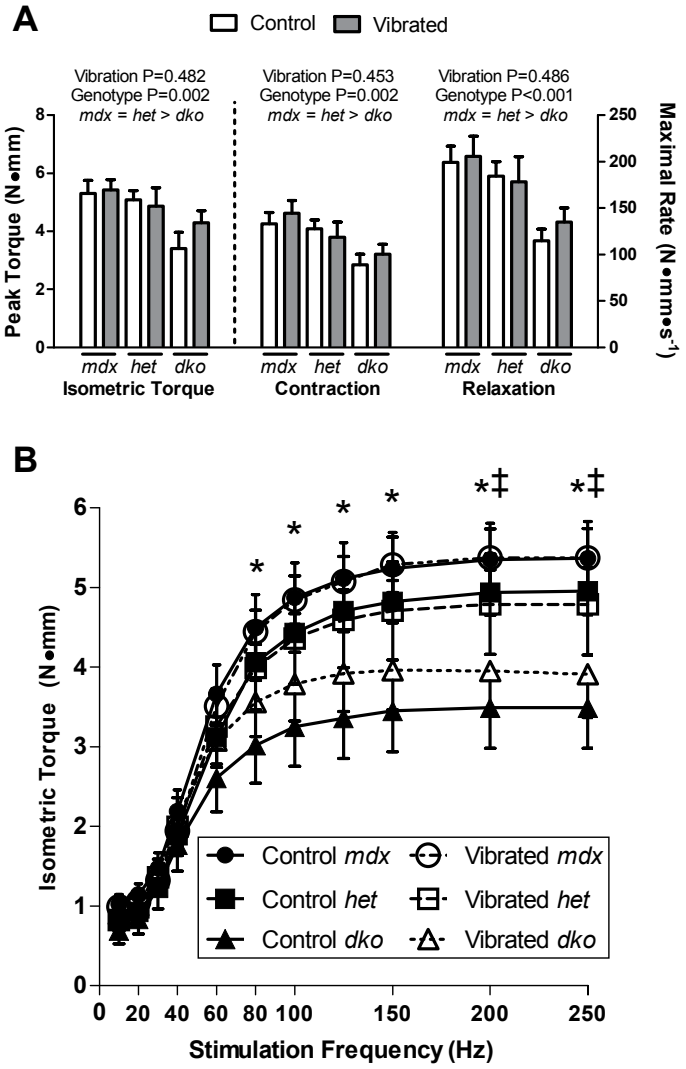

Figure 5.3: Seven daily bouts of low intensity vibration training on posterior crural muscle contractility in three mouse models of DMD which vary in their disease severity. Data are mean, SE. A: Peak isometric torque and rates of contraction and relaxation were not different between control and vibrated mice. *Dko* mice consistently had lower contractility than both *mdx* and *het* mice. Main effect P-values from two-way ANOVA's are indicated above each set of bars with post-hoc results in words immediately below the genotype main effects. B: Isometric torque production as a function of stimulation frequency indicated that vibration did not impact torque production at any frequency; however *dko* mice had lower torque production at frequencies above 80 Hz. Only main effects of genotype were detected, and therefore only post hoc testing results are displayed: *Significant difference between *mdx* and *dko*; ‡Significant difference between *het* and *dko*.

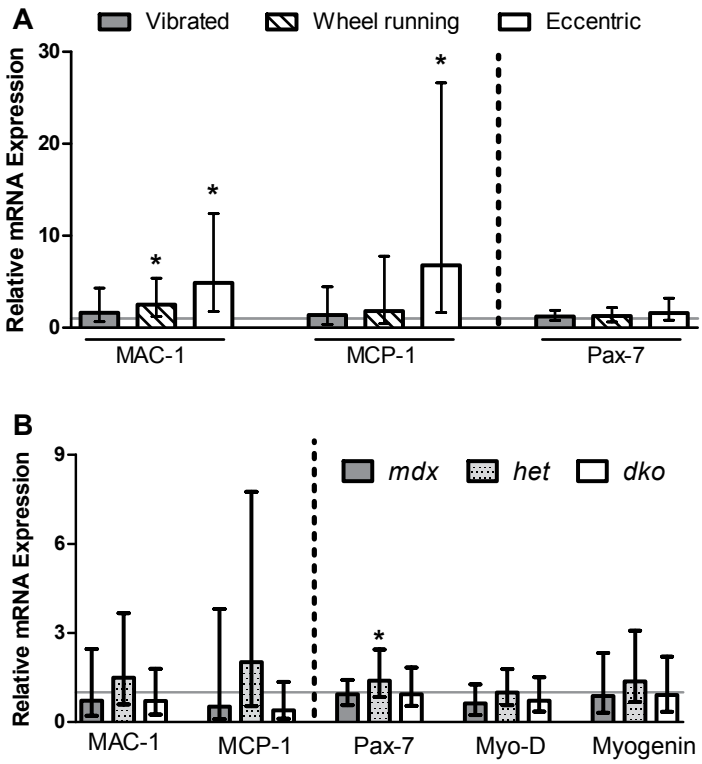

Figure 5.4: Low intensity vibration training for three or seven days did not affect muscle mRNA expression of genes associated with inflammation or myogenesis. RNA was isolated from A: gastrocnemius muscles of *mdx* mice three days following interventions of vibration, wheel running, or eccentric contractions and compared to those of control *mdx* mice (indicated by the solid gray line) and B: tibialis anterior muscle from *mdx*, *het* and *dko* mice that were vibrated for seven days and compared to genotype-matched, non-vibrated controls (indicated by the solid gray line). The height of the bars indicate the fold change in mRNA expression (i.e., delta-delta CT) above controls and the error bars indicate the 95% confidence intervals. *Significantly different from respective, non-vibrated *mdx* mice as determined by REST, 2009 software ($P<0.05$).

between non-vibrated and vibrated dystrophic mice, and plasma CK activity and expression levels of genes associated with muscle inflammation also were not affected by vibration. The long term goal that this study begins to address is the potential of low intensity vibration as a therapeutic modality for DMD. The utility of vibration has received increasing attention in recent years due to its ability to improve musculoskeletal health [72, 78, 70], especially in disabled children and women with low bone mass [81, 82, 80, 141]. Theoretically, vibration would mechanically load bone to maintain bone health yet would be safe for the adjacent diseased muscle, and results of our study support this theory.

Results from our first study identified two sets of vibration parameters (i.e., 90 Hz at 0.6 g and 45 Hz at 0.6 g) that evoked an osteogenic response (Figure 5.1). The 45 Hz and 0.6 g setting increased both osteoprotegerin and alkaline phosphatase mRNA levels up to 30%, but did not impact RANKL (Figure 5.1). Similar fold-change increases in alkaline phosphatase mRNA expression have been reported following 2-4 d of a known anabolic stimulus (i.e., four-point bending) [124, 142]. The 90 Hz and 0.6 g setting upregulated osteoprotegerin and RANKL to similar extents, and therefore the increase in RANKL could potentially have negated any osteoprotegerin-induced osteogenic effects. Similar upregulation of RANKL has also been reported in mice vibrated for 21 d [126], however in cells, vibration decreased RANKL mRNA expression up to 55% with no change in osteoprotegerin [143]. Consistent with our findings, others have shown no change in mRNA expression following vibration for Collagen type I [126], BMP-2 [126, 124], and Runx-2 [124]. Consequently, our subsequent studies were performed utilizing 45 Hz and 0.6 g because that pair of parameters tended to increase osteoprotegerin expression with no change in RANKL and also elicited a 1.4 fold increase in of alkaline phosphatase mRNA expression, which is involved with matrix maturation and mineralization.

The results of our second and third studies consistently showed that vibration was not injurious to inherently fragile dystrophic muscle. The most crucial pieces of evidence to support this statement are the functional results. That is, there was no indication that strength (submaximal or maximal isometric torque) or contractility rates (contraction or relaxation) of the posterior crural muscles were affected by 3 or 7 of vibration treatment in dystrophic mice. This was in contrast to other interventions, such as eccentric contractions, that did cause loss of strength (Figure 5.2). This was substantiated

in the traditional *mdx* mouse at a younger age, as well as in more severe dystrophic mouse models *het* and *dko* mice (Figure 5.3).

The expression profiles of genes associated with muscle inflammation and recovery from injury further support our hypothesis that vibration is not injurious. MAC-1 and MCP-1 are genes that meditate the recruitment and activation of inflammatory cells following muscle damage and these genes were not upregulated after either 3 or 7 d of vibration but were increased by wheel running or eccentric contractions (Figure 5.4). These data indicated that vibration is on the low end of the continuum of exercises that cause damage in dystrophic mice. Specifically, eccentrically-injured muscles had 5-7 fold increases in MAC-1 and MCP-1 similar to previous reports [144, 145]. Interestingly, *het* mice had modest increases in MAC-1 and MCP-1 following 7 d of vibration, supporting the notion that *het* mice may be better models of inflammation and fibrosis in DMD [68].

Genes associated with myogenesis were also not affected by vibration, with the exception of upregulated Pax-7 gene following 7 d of vibration in *het* mice (Figure 5.4). Vibration of cultured C2C12 myoblasts has previously shown a vibration dose-dependent increase in MyoD and myogenin expression [146]. High intensity vibration training for two weeks in young mice induced muscle hypertrophy that was attributed to enhanced fusion and differentiation of satellite cells, and muscle fiber number and cross-sectional area [147, 148]. Vibration-induced muscle hypertrophy has also been associated with the inhibition of muscle atrophy pathways by downregulating myostatin gene expression [149]. On the contrary, our previous work showed that eight weeks of low intensity vibration training in wildtype mice improved muscle functional capacity in the absence of hypertrophy [129]. Specifically, muscle strength improved by 14% but muscle mass, protein content, and fiber cross-sectional areas were not affected [129]. Given these improvements in the muscle function of wildtype mice, a future goal is to determine if similar improvements are attainable in dystrophic mice and DMD patients. Reyes et al. [141] has applied vibration directly to the elbow of children with motor disabilities (including patients with DMD) and realized a 65% increase in muscle force compared to a 20% decline in control patients, however the improvements in DMD patients muscle function was not specifically stated.

The present studies thoroughly characterized dystrophic muscle function following

short-term vibration training, after determining the vibration parameters that evoked the greatest osteogenic response in mouse models of DMD. The results suggest that vibration at 45 Hz and 0.6 g has the potential to have anabolic impact on bone health, while not causing injury to inherently fragile dystrophic muscle. Additional long-term treatment studies are needed to determine the efficacy of vibration to improve both bone and muscle in dystrophic mice and to improve musculoskeletal health in DMD.

Chapter 6

Low intensity, high frequency vibration to improve musculoskeletal function in a mouse model of muscle disease

Susan A. Novotny[1], Tara L. Mader[2],Angela G. Greising[2], Angela S. Lin[3], Robert E. Guldberg[3], Gordon L. Warren[4], and Dawn A. Lowe[2]

[1] Department of Kinesiology, University of Minnesota, Minneapolis, Minnesota [2] Program in Physical Therapy and Rehabilitation Sciences, University of Minnesota [3] Institute for Bioengineering and Bioscience, Georgia Institute of Technology, Atlanta Georgia [4] Division of Physical Therapy, Georgia State University, Atlanta, Georgia

6.1 Abstract

The objective of the study was to determine if low intensity, high frequency vibration training impacted the musculoskeletal system in the *mdx* mouse model of DMD. Three-week old wildtype and *mdx* mice were randomized to control (n=12 and 11) or vibrated (n=14 and 11, 45Hz and 0.6g, 15min/d, 5d/wk) groups. *Mdx* mice were injected 5 and 1 day prior to sacrifice with Calcein and Xylenol. *In vivo* and *ex vivo* contractile function of the anterior crural and extensor digitorum longus muscles were assessed following 8wks of vibration and then mice were sacrificed. Muscles were prepared for histological analyses and subcutaneous and visceral fat pads were excised and weighed. Tibia were dissected and analyzed by micro-computed tomography for trabecular architecture at the metaphysis and cortical geometry and density at the mid-diaphysis. Three-point bending measured bone strength and a subset of tibia were processed for dynamic histomorphmetry. Vibration training for 8wk did not alter trabecular architecture, dynamic histomorphometry, cortical geometry, or whole bone strength ($P \geq 0.34$). Vibration did not alter any measure of muscle contractile function in either genotype ($P \geq 0.12$); however the preservation of muscle function and morphology in *mdx* mice suggests vibration is not deleterious to muscle lacking dystrophin. Vibrated mice had smaller subcutaneous fat pads ($P=0.03$) and tended to have smaller visceral fat pads ($P=0.08$). These data suggest that vibration training at 45Hz and 0.6g does not significantly impact musculoskeletal function but may influence fat in mice.

6.2 Introduction

Duchenne muscular dystrophy (DMD) is an X chromosome-linked disease characterized by progressive muscle weakness [50, 45, 51]. Bone strength is compromised in these patients as evident by the occurrence of fragility fractures upon falling from sitting or standing height [2, 3, 1, 118, 57]. Compromised bone strength in DMD is multi-factorial, likely including combined effects of the failure to accumulate peak bone strength during growth and declines in bone health secondary to the muscle disease. Furthermore, patients are recommended to avoid moderate- to high-intensity physical activity to prevent accelerating the muscle disease [130, 150], and consequent to the absence of exercise the bone may fail to increase in width, also impacting bone strength. Preliminary data suggest that bone size is reduced in various skeletal sites in boys with DMD [5, 6], and those data are supported by reports that that these patients have low bone mass across the lifespan [2, 55]. Paralleling suboptimal attainment of bone strength, continual declines in muscle function (i.e., the magnitude and frequency of muscle-induced mechanical loads) likely initiate disuse-mediated bone remodeling. This is supported by evidence that the discrepancies in bone mass between boys with DMD and their age-matched peers are accentuated with age, especially following the loss of ambulation where skeletal regions such as the hip and calcaneous experience drastic bone loss [2, 55]. Therefore, effective bone-sparing training modalities are warranted to thwart declines in bone health of boys with DMD in effort to preserve bone strength and prevent fractures.

Major determinants of bone health and training modalities to preserve bone are related to mechanical loading [76]. Bones response to mechanical loading is governed by an inverse-frequency law, which suggests that applying low-intensity loads thousands of times per day may be just as effective as applying few high-intensity loads per day to maintain bone health [77].Thus in the case of DMD, where high-intensity loads ($\geq$1500 $\mu\epsilon$) may be injurious to the inherently fragile muscle, utilizing low-intensity loads ($\sim$5-10 $\mu\epsilon$) more often may be a feasible approach to maintain bone health. Low intensity, high frequency vibration applies non-invasive stimulus to bone, and is attractive as a training modality due to evidence indicating that vibration initiates an anabolic bone response [151], slows bone loss [72, 71], and improves bone strength [74]. Activation patterns of postural muscles during vibration are similar to those produced during

standing [77], and thus, the efficacy of vibration in older adults and disable children may be attributed to the preservation of these low intensity muscle-induced stimuli. For example, the activation of postural muscles are known to decrease three-fold with aging [76], so vibration may be acting as a surrogate for muscle loading and stave off disuse-mediated bone resorption. If vibration acts as a surrogate for postural muscle activation, it may potentially explain why healthy adults do not glean beneficial effects following chronic vibration training [152]. This suggests that vibration would be most effective under conditions in which the magnitude and/or spectrum of mechanical loads applied to the bone are reduced or physical inactivity is apparent. Accordingly, vibration has been shown to be quite effective at preventing bone loss associated with bed rest [153], as well as improving skeletal health in disabled children [82]. Consequently, vibration may be efficacious for patients with a muscle disease, such as DMD.

The *mdx* mouse is a widely used model of DMD and like patients has alterations in bone health [7, 66, 13, 154], and is relatively physically inactive [88]. *Mdx* mice, therefore, provide a feasible model to determine the efficacy of vibration to improve musculoskeletal function in the presence of reduced muscle strength and physical activity. The extent of bones response to vibration in mice is influenced by various factors including transmissibility of the vibration stimulus, the parameters of vibration used (i.e., acceleration and frequency), as well as genetic background of the mice [155, 154, 156]. This suggests that parameters of vibration are not universally effective across all mice, and therefore, optimization may be necessary specific to the model of interest to maximize musculoskeletal benefits. Recently, we compared six different pairs of vibration parameters, and identified 45 Hz at 0.6 g to best initiate an osteogenic response in *mdx* mice at the mRNA level Chapter 5. It remains to be determined if those acute improvements in gene expression at 45 Hz at 0.6 g would translate to improved bone structure and function with prolonged vibration training in dystrophic mice.

Therefore, the objective of the present study was to determine if vibration therapy translated to preservation of *mdx* mouse tibial bone trabecular architecture, cortical geometry and whole bone strength, compared to non-vibrated mice. Previous studies in mice have indicated that 3-6 weeks of vibration training is necessary to quantify structural adaptations within bone [127, 157, 156, 158, 159]. Consequently, we hypothesized that 8 weeks of vibration would improve tibial bone. Specifically, three point bending

was utilized to detect improvements in bone strength and micro-computed tomography (μCT) was performed to elucidate the possible underlying mechanical determinants of improved strength (i.e., geometry and intrinsic material properties). Dynamic histomorphometry was also used as a direct measure of osteoblastic activity in tibia from *mdx* mice. In addition, we hypothesized that vibration training would not be injurious to dystrophic muscle as indicated by anterior crural muscle strength, contractility of extensor digitorum longus (EDL) muscles, muscle morphology, and plasma creatine kinase activity.

6.3 Methods

Animals

Three-week old male wildtype mice (C57Bl/10, n=26) and *mdx* mice (n=22) were obtained from our breeding colony at the University of Minnesota. At 11 wk of age, mice were anesthetized using sodium pentobarbital (37.5 mg/kg body mass (BM)), and while under anesthesia, mice were euthanized by exsanguination. Mice were housed on a 12:12-h light-dark cycle at 20-23 ^{o}C and were provided food and water ad libitum. All animal care and use procedures were approved by the Institutional Animal Care and Use Committee at the University of Minnesota.

Experimental Design

Mice were randomly assigned to either a control group (wildtype control n=12, *mdx* control n=11) or vibration group (wildtype vibrated n=14, *mdx* vibrated n=11). Mice allocated to the vibration groups were exposed to 15 min bouts of vibration 5 d/wk for 8 wk (range 55-58 d) starting at 3 wk of age. The vibration stimulus consisted of a 45 Hz stimulus with 0.6 g of acceleration (where 1 g is equivalent to gravity) based our on preliminary work in *mdx* mice Chapter 5. Mice in the control group were placed on the vibration platform for the same duration of time, but with the machine turned off. Body mass was recorded weekly. To quantify dynamic trabecular bone histomorphometry, *mdx* mice were injected subcutaneously with 15 mg/kg BM Calcein (Sigma, St. Louis, MO) 5 days prior to sacrifice, and again one day prior to sacrifice with 90 mg/kg BM Xylenol orange (Sigma), as adapted from [160].

After 8 wk of vibration, mice were anesthetized for blood collection, muscle functional testing, and tissue excision. Plasma was collected via retro-orbital bleed and flash frozen in liquid nitrogen to assess creatine kinase activity. Anterior crural muscle function was then assessed *in vivo* by quantifying passive and active torques and susceptibility to contraction-induced injury. The EDL muscle from the contralateral limb was then excised and used to assess *ex vivo* force production. The same two investigators performed all *in vivo* and *ex vivo* measurements and they were blinded to the mouses genotype and vibration group. Prior to exsanguination, the subcutaneous and visceral fat pads were excised and weighed, as consistent reductions in fat pad masses have been reported following long-term vibration training [127, 161]. The tibialis anterior, EDL, gastrocnemius, and soleus muscles were dissected and snap frozen in liquid nitrogen or mounted in OTC. Tibial bones were removed and stored in either phosphate-buffered saline at -20 ^{o}C until the time of mechanical testing or in 70% alcohol at -4 ^{o}C until the time of dynamic histomophometric processing.

μCT of Tibial Bone Metaphysis and Mid-diaphysis

A μCT system (Scanco Medical micrCT 40, Bruttisellen, Switzerland) was used to quantify trabecular morphometry in the tibial metaphysis as well as cortical bone geometry and volumetric bone density (vBMD) at the tibial mid-diaphysis [13].Trabecular bone morphometry was assessed in the proximal tibial metaphysis (50 slice region of interest, starting 5 slices distal to the last image containing the growth plate, using 12 um voxel size) as previously described [13]. Bone volume fraction (BV/TV), trabecular thickness, trabecular number, trabecular spacing and trabecular vBMD were determined for each slice and the average value across each of the 50 slices was used for statistical analyses.

For a $\sim$0.8 mm region of the tibial mid-diaphysis, the following outcome measures were assessed: cortical cross-sectional area, cortical thickness, periosteal diameter, cross-sectional moment of inertia (CSMI), and vBMD. These measures were assessed for each of the 66 slices within the region of interest, and the average for all 66 slices was used for statistical analyses. Following the completion of imaging, tibial bones were refrozen in PBS until the time they underwent mechanical testing.

Mechanical Testing of the Tibial Mid-diaphysis

Mechanical testing procedures for assessing the functional capacity of the mouse tibial bone has previously been described in detail [13, 12, 11]. Briefly the left tibial bone of each mouse was placed on its lateral side in a Mecmesin MultiTest 1-D test machine, and was loaded in three-point bending at the mid-diaphysis using a Mecmesin AFG-25 load cell (Mecmesin, West Sussex, UK). The functional capacity of the tibial bone was quantified by ultimate load, stiffness, and deflection and energy absorbed to ultimate load using custom designed TestPoint software (TestPoint version 7; Measurement Computing Corp.) [13].

Trabecular Bone Dynamic Histomorphometry

A subset of tibia were dehydrated and embedded without demineralization in methylmethacrylate (Polysciences, Warrington, PA) as previously described [162]. Briefly, 5 μm thick longitudinal sections were cut on a microtome (Leica, Heidelberg, Germany) and mounted unstained. Flurochrome labels were visualized at 20x, and dynamic histomrophometric measures were made using OsteoMeasure image analyzer (OsteoMetric, Atlanta, GA) in a region $\sim$60 μm distal to the proximal growth plate. Outcome measures of interest include mineralized surface per bone surface (MS/BS), mineral apposition rate (MAR), and bone formation rates relative to bone surface or total volume (BFR/BS and BFR/TV, respectively). All parameters were measured and expressed according to standardized nomenclature [163]. A single investigator performed all histological preparations and another investigator performed all the analyses; both were blinded to the genotype and treatment.

In vivo Measurements of Anterior Crural Muscle Function

Mice underwent *in vivo* contractile testing of the anterior crural muscles of the left hind limb while anesthetized (cocktail containing: fentanyl citrate (0.2 mg/kg BM), droperidol (10 mg/kg BM), and diazepam (5 mg/kg BM)) [90]. Outcome measures of interest included: : passive torque about the ankle [164], susceptibility to eccentric contraction-induced injury [119] and peak-isometric torque (pre- and post-injury) [90, 165]. Torque loss was then calculated as the difference between pre- and post-isometric torque values.

Ex Vivo Measurements of EDL Muscle Contractility

The contractile function of EDL muscle of *mdx* mice was investigated as it is sensitive to disease progression, contraction-induced injury, and can adapt in response to treatment [90, 89]. Measurements included: peak twitch force, time-to-peak twitch force, twitch one half-relaxation time, peak isometric tetanic force (P_o), maximal rates of tetanic force production and relaxation, eccentric force, and percent decline in isometric tetanic force following eccentric contractions [91]. EDL muscles were trimmed, blotted and weighed following the measurements. Physiological cross-sectional area was calculated using EDL muscle mass, anatomical muscle length (i.e., L_o), and a fiber length-to-muscle length ratio of 0.44, and this calculated value was used to adjust peak isometric tetanic force to determine specific P_o [91, 166].

Muscle Morphology

Altered vascularity has been noted as a possible contraindication of vibration [167], therefore we measured capillary density at the distal end and mid-belly of the soleus muscle using a periodic acid-Schiff reaction [168]. Capillary density was quantified by counting the number of capillaries surrounding a fiber. Central nucleated fibers (i.e., a marker of muscle regeneration) were also assessed in both regions of the soleus as well as the mid-belly of the tibialis anterior muscle. The number of central nucleated fibers present per 300 fibers was counted in each of these regions from hematoxylin and eosin-stained sections [88]. A single investigator performed all histological preparations and another investigator performed all the analyses; both were blinded to the genotype and treatment.

Statistical Analyses

The effects of vibration (45 Hz at 0.6 *g* vs. non-vibrated control) and genotype (wild-type vs. *mdx*) were assessed by two-way ANOVAs with vibration and genotype as the fixed factors. When significant interactions were present, Holm-Sidak post-hoc measures were used to determine differences among the groups. When assumptions of normality or equal variance were violated, Kruskal-Wallis One Way Analysis of Variance on Ranks was performed along with Dunns post-hoc measures. Dynamic histomorphometry measures of the tibia were only performed on *mdx* mice, and therefore the data were assessed by t-tests. All statistical analyses were carried out using SigmaPlot version 11.0 (Systat

Software Inc; Point Richmond, CA).

6.4 Results

Tibial Bone Trabecular Morphometry and Cortical Geometry

μCT was performed at the proximal metaphysis and mid-diaphysis of the tibia to determine the extent to which vibration and genotype influenced trabecular bone morphometry and cortical bone geometry, respectively. In the proximal metaphysis of the tibia, vibration did not influence trabecular morphometry, though differences between *mdx* and wildtype were detected (Figure 6.1A). Specifically, bone volume fractions, trabecular thickness, number, and spacing did not differ between control and vibrated mice (Figure 6.1A). The lack of improved trabecular morphometry in the metaphysis of *mdx* mice following vibration was confirmed by dynamic histomorphometry (Figure 6.1B). Overall, vibration had no impact on bone formation in *mdx* mice as indicated by MS/BS (34.1%, P=0.989), MAR (1.06 μm/d, P=0.373), BFR/BS (0.36 $\mu m^3/\mu m^2$/d, P=0.633) or BFR/TV (0.193 %/d, P=0.908). For the differences in trabecular bone morphometry across genotype, bone volume fraction showed that *mdx* mice had 17% less bone than wildtype, which was attributed having 12% thinner trabeculae (Figure 6.1A). Trabecular number (Figure 6.1A) and spacing (0.185 mm +/- 0.004, P=0.559) were not influenced by genotype.

Neither vibration nor genotype influenced any parameter of cortical geometry at the tibial mid-shaft (Table 6.1 and Figure 6.2A). These data suggest that the shape of the bone was similar across all groups, despite the tendency of *mdx* mice to have longer tibial lengths (Table 6.1).

Tibial Bone Functional and Intrinsic Material Properties

Three point bending tests were performed at the mid-shaft of the tibial diaphysis to determine if whole bone strength was affected, even in the absence of change in bone geometry. The strength and stiffness of tibial bones were not different between vibrated and non-vibrated, control mice (Figure 6.2B and C). The lack of difference was extended to variables derived from ultimate load and stiffness including energy and deflection to ultimate load (Table 6.1). Comparisons across genotypes confirmed that bone strength

was compromised in *mdx* mice, as indicated by 9% smaller ultimate loads and a trend toward lower tibial stiffness (Figure 6.2B and C), as well as lower energy to ultimate load compared to wildtype mice (Table 6.1).

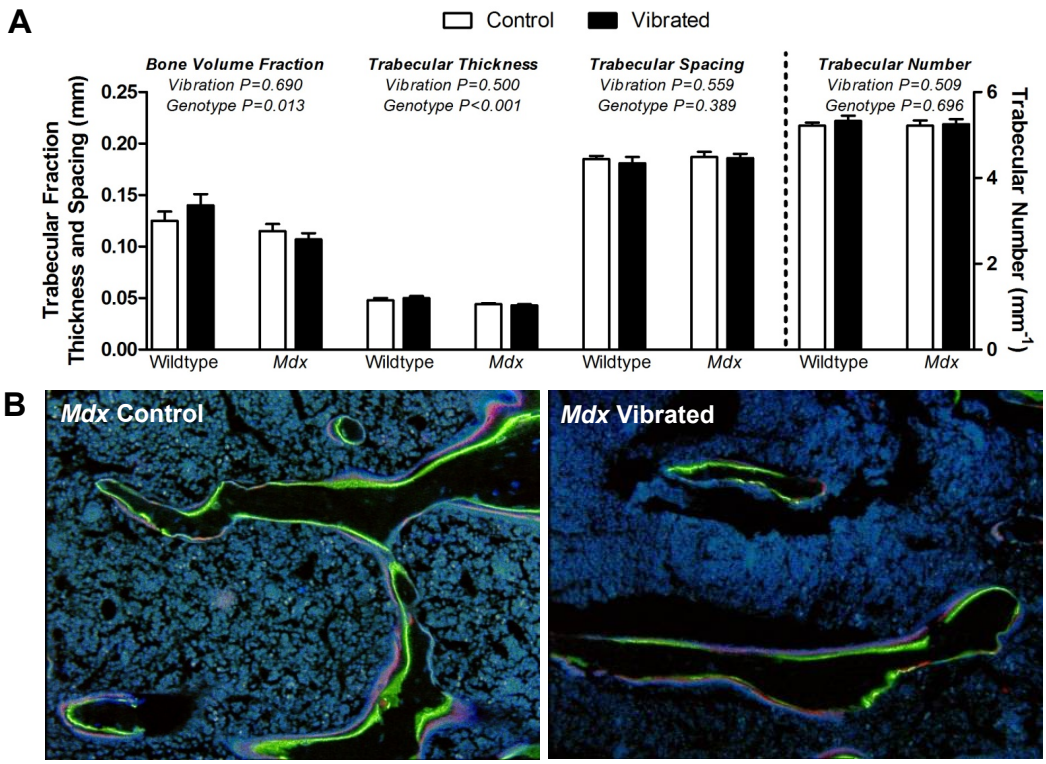

Figure 6.1: Effect of 8 weeks of low-intensity vibration on trabecular architecture and dynamic histomorphometry in the proximal tibial metaphysis of *mdx* and wildtype mice. A) Vibration training did not influence trabecular bone volume fractions, thickness, spacing or number. B) Measures of dynamic histomorphometry were also not influenced by vibration (exemplar images from two *mdx* mice) compared to non-vibrated mice. As expected, *mdx* mice had lower values for trabecular bone volume fraction and thickness compared to wildtype mice. Data are mean, SE. Main effect P-values from two-way ANOVA's are indicated above each set of bars in Panel A.

Table 6.1: Effects of low intensity vibration training on tibial bone cortical geometry, mechanical function, and intrinsic material properties in wildtype and *mdx* mice.

					P-Values for Two-Way ANOVA		
	Wildtype Control	**Wildtype Vibrated**	***Mdx* Control**	***Mdx* Vibrated**	**Main effect of Vibration**	**Main effect of Genotype**	**Interaction (Vibration x Genotype)**
Cortical Geometric Properties							
Tibial Length (mm)	17.73 (0.08)	17.89 (0.07)	17.96 (0.06)	17.92 (0.05)	0.409	0.059	0.154
Cortical Cross-Sectional Area (mm^2)	0.76 (0.03)	0.79 (0.02)	0.77 (0.02)	0.75 (0.02)	0.818	0.610	0.274
Cortical Thickness (mm)	0.22 (0.01)	0.23 (0.00)	0.23 (0.00)	0.23 (0.00)	0.336	0.495	0.429
Mechanical Functional Properties							
Energy to Ultimate Load (mJ)	4.05 (0.28)	4.26 (0.10)	3.53 (0.11)	3.59 (0.27)	0.521	0.005	0.720
Deflection to Ultimate Load (mm)	0.45 (0.01)	0.48 (0.02)	0.43 (0.01)	0.45 (0.03)	0.148	0.142	0.921
Intrinsic Material Properties							
Ultimate Stress (MPa)	282.8 (5.3)	279.9 (3.5)	273.6 (6.4)	280.0 (5.2)	0.746	0.397	0.385
Modulus of Elasticity (GPa)	10.7 (0.3)	10.6 (0.3)	10.8 (0.4)	10.9 (0.3)	0.945	0.620	0.713
Cortical vBMD ($mg*cm^{-3}$)	1345.1 (17.7)	1351.8 (9.0)	1303.7 (13.9)	1313.2 (10.8)	0.543	0.004	0.918
Trabecular vBMD ($mg*cm^{-3}$)	1095.6 (3.1)	1094.1 (4.1)	1077.8 (3.3)	1079.4 (4.3)	0.986	<0.001	0.679

Values are means (SE). vBMD, volumetric bone mineral density

Overall, vibration had no impact on any measure of intrinsic material properties of the tibia (Table 6.1). While ultimate stress and modulus of elasticity values were similar across genotypes, μCT revealed differences in vBMD between *mdx* and wildtype mice at both the tibial proximal metaphysis and the cortical midshaft with *mdx* mice having up to 3% lower vBMD (Table 6.1).

Anterior Crural Muscle Function

To determine if vibration training affected musculature in close proximity to the vibrating platform, passive and active torques about the ankle were assessed. Passive torque was unaffected by vibration training at each of the nine joint angles measured (data not shown, $P \geq 0.087$). *Mdx* mice had greater passive torque at 20 degrees of dorsiflexion compared to wildtype mice but there was no difference between control and vibrated groups (Table 6.2) suggesting that vibration did not alter muscle or joint stiffness.

Overall, the active measures of anterior crural muscle contractile function showed no effect of vibration. Absolute and normalized maximal isometric toques were not impacted by vibration (Table 6.2 and Figure 6.3A, respectively), indicating that muscle strength was not altered following vibration training. Genotypic differences in isometric torque were only apparent after accounting for increased body mass of the *mdx* mice (Figure 6.3A). Susceptibility to contraction-induced injury, as indicated by declines in eccentric torque over a series of contractions (Figure 6.3B) and isometric torque loss (Table 6.2), were not affected by vibration. *Mdx* mice had a substantial loss of anterior crural muscle function reflected by 42% lower isometric torque after the eccentric contractions compared to that before (0.79 N*mm vs. 1.3 N*mm, $P<0.001$), and ~70% loss of eccentric torque (Figure 6.3B). These data indicate that lack of dystrophin but not vibration is detrimental to muscle function. Similarly, plasma creatine kinase activity did not differ between vibration and control groups ($P=0.974$), but was 4-fold higher in *mdx* than wildtype mice (4507 U/L vs. 1055 U/L, $P<0.001$).

EDL Muscle Contractile Function

Force-generating capacity of the EDL muscle was not affected by 8 weeks of vibration training. Vibration had no impact on peak twitch force, maximal isometric tetanic force, specific P_o, peak eccentric force, and eccentric or isometric force loss due to

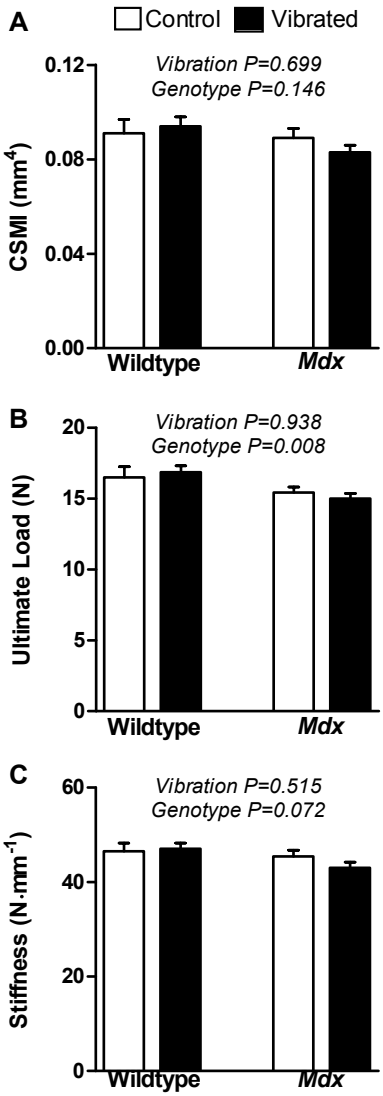

Figure 6.2: Effect of 8 weeks of low-intensity vibration on tibial bone cross-sectional moment of inertia, ultimate load and stiffness in *mdx* and wildtype mice. Vibration training did not influence tibial bone A) cross-sectional moment of inertia, B) ultimate load, or C) stiffness compared to non-vibrated control mice. *Mdx* mice had lower values for ultimate load and trends for lower stiffness compared to wildtype mice. Data are mean, SE. Main effect P-values from two-way ANOVA's are indicated above each set of bars, where the P-values associated with the main effect of vibration and genotype are listed above the bars.

contraction-induced injury (Figure 6.4 and Table 6.2). Characteristics relating to speed of EDL muscle contraction, including time-to-peak twitch force, half-relaxation time of twitch force, and maximal rates of tetanic force development and relaxation were also not effected by vibration (Table 6.2). Most of the EDL contractile measures were different between wildtype and *mdx* mice, reflecting the expected pathology of the muscle disease (Figure 6.4 and Table 6.2).

Muscle Morphology

Tibialis anterior, soleus, and gastrocnemius muscle masses and central nucleated fibers were not impacted by vibration (Table 6.3). Vibrated mice had 5% smaller EDL muscles, primarily due to vibrated *mdx* mice having 9% smaller EDL muscles compared control *mdx* mice (Table 6.3). *Mdx* mice had greater muscle masses and increased central nucleated fibers compared to wildtype (Table 6.3).

Fat and Body Masses

At the start of the study, body mass did not differ between vibration and control groups (P=0.654), though *mdx* mice weighed less than wildtype (9.0 $\pm$ 0.3 g vs 10.7 $\pm$ 0.7 g, P=0.005). Eight weeks later *mdx* mice were 12% heavier than wildtype mice and vibrated mice tended to have reduced body mass (Figure 6.5). Vibrated mice also had significantly smaller subcutaneous fat pads and tended to have lower visceral fat pad masses compared to controls (Figure 6.5). Main effects of genotype were consistently present for fat and muscle masses with *mdx* mice having up to 47% less fat pad masses (Figure 6.5).

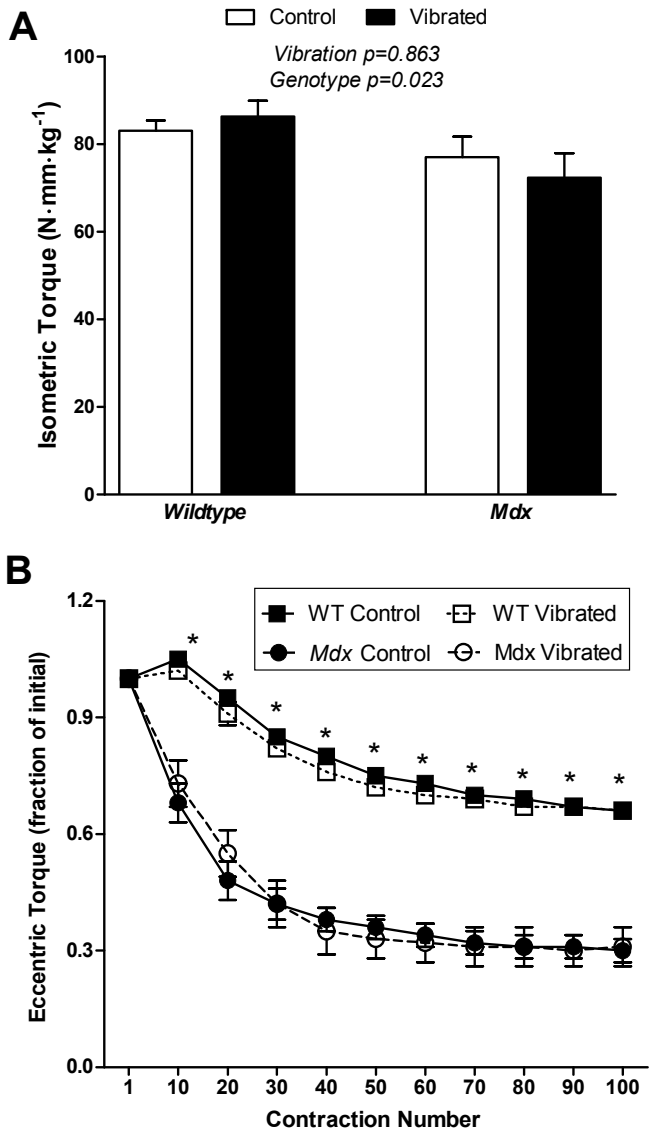

Figure 6.3: Effect of 8 weeks of low-intensity vibration on *in vivo* anterior crural muscle isometric torque and susceptibility to eccentric contraction-induced injury in *mdx* and wildtype mice. A: *in vivo* testing of anterior crural muscle function showed that maximal isometric torque were not different in mice subjected to vibration compared to non-vibrated control mice. B: Vibration training did not alter susceptibility to eccentric contraction-induced injury in vibrated mice compared to control mice. As expected, *mdx* mice had lower isometric torque values and greater susceptibility to eccentric injury (i.e., greater decrements in eccentric torque production). Data are mean, SE. Main effect P-values from two-way ANOVA's are indicated above each set of bars in Panel A, where the P-values associated with the main effect of vibration and genotype are listed above the bars. In panel B, only a main effect of genotype was present, where the * signifies a significant difference between *mdx* and wildtype mice.

Table 6.2: Muscle contractile function following 8 weeks of low intensity vibration training in wildtype and *mdx* mice.

	Wildtype Control	Wildtype Vibrated	*Mdx* Control	*Mdx* Vibrated	P-Values for Two-Way ANOVA		
					Main effect of Vibration	Main effect of Genotype	Interaction (Vibration x Genotype)
***In Vivo* function of Anterior Crural Muscles**							
Passive Torque at 20^o Dorsiflexion (N*mm)	1.24 (0.10)	1.42 (0.09)	1.65 (0.20)	1.55 (0.11)	0.767	0.044	0.313
Maximal Isometric Torque (N*mm)	2.3 (0.1)	2.4 (0.1)	2.5 (0.2)	2.2 (0.2)	0.526	0.714	0.164
Isometric Torque Loss (%)	42.3 (1.9)	41.5 (1.7)	71.9 (5.1)	61.6 (6.9)	0.192	<0.001	0.257
***Ex Vivo* function of EDL Muscles**							
Peak Twitch Force (mN)	99.3 (3.5)	94.0 (2.2)	94.4 (3.1)	90.2 (3.1)	0.118	0.150	0.860
Time-to-Peak Twitch Force (ms)	19.0 (0.3)	18.8 (0.3)	19.1 (0.5)	20.1 (0.5)	0.276	0.071	0.108
Half-Relaxation Time of Twitch Force (ms)	15.0 (0.4)	13.9 (0.4)	17.8 (0.3)	18.3 (0.7)	0.558	< 0.001	0.133
Peak Eccentric Force (mN)	639.0 (13.3)	629.6 (15.1)	549.2 (19.2)	517.6 (22.7)	0.253	<0.001	0.533
Isometric Force Loss (%)	4.1 (1.0)	3.8 (1.4)	63.1 (5.5)	67.5 (5.7)	0.617	<0.001	0.553
Maximal Rate of Tetanic Force Development (N*s^{-1})	10.9 (0.4)	10.9 (0.3)	10.2 (0.4)	10.4 (0.5)	0.784	0.167	0.738
Maximal Rate of Tetanic Force Relaxation (N*s^{-1})	22.6 (0.4)	23.4 (0.7)	18.5 (1.0)	16.5 (1.2)	0.477	<0.001	0.116

Values are means (SE). Isometric torque loss was calculated as the percent difference between isometric torque measured before and after the 100 eccentric contractions. Isometric force loss was calculated as the percent difference between peak isometric tetanic force measured before and after the 5 eccentric contractions

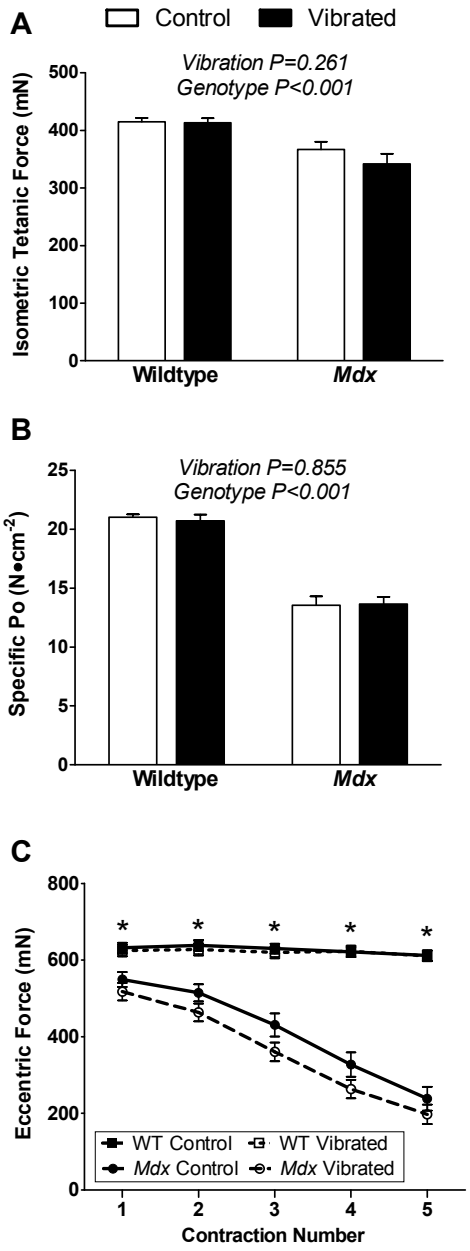

Figure 6.4: Effect of 8 weeks of low-intensity vibration on *Ex vivo* Extensor Digitorum Longus (EDL) muscle isometric tetanic force, specific force (P_o), and susceptibility to eccentric contraction-induced injury in *mdx* and wildtype mice. Vibration training did not influence EDL muscle A) maximal isometric tetanic force production, B) Specific force, or susceptibility to eccentric contraction-induced injury compared to non-vibrated control mice. As expected, *mdx* mice had lower values for each of the thee measured of EDL muscle function compared to wildtype mice. Data are mean, SE. Main effect P-values from two-way ANOVA's are indicated above each set of bars in Panel A and B, where the P-values associated with the main effect of vibration and genotype are listed above the bars. In panel C, only a main effect of genotype was present, where the * signifies a significant difference between *mdx* and wildtype mice.

Table 6.3: Effects of low intensity vibration training and genotype on muscle and fiber characteristics

	Wildtype Control	**Wildtype Vibrated**	***Mdx* Control**	***Mdx* Vibrated**	**P-Values for Two-Way ANOVA**		
					Main effect of Vibration	**Main effect of Genotype**	**Interaction (Vibration x Genotype)**
EDL Muscle							
EDL Muscle Mass (mg)	11.6 (0.3)	11.6 (0.2)	16.2 (0.6)	14.7 (0.4)	0.045	<0.001	0.054
EDL Anatomical Muscle Length (mm)	12.6 (0.1)	12.5 (0.1)	12.7 (0.1)	12.6 (0.1)	0.516	0.411	0.811
Tibialis Anterior Muscle							
Tibialis Anterior Muscle Mass (mg)	45.3 (1.2)	48.0 (1.3)	78.1 (2.9)	75.4 (3.3)	0.991	<0.001	0.238
Centrally Nucleated Fibers, Mid-belly (%)	1.6 (0.6)	3.3 (0.9)	71.2 (1.5)	70.3 (1.2)	0.741	<0.001	0.298
Soleus Muscle							
Soleus Muscle Mass (mg)	6.7 (0.4)	7.0 (0.3)	9.3 (0.6)	8.3 (0.4)	0.405	<0.001	0.183
Centrally Nucleated Fibers, Mid-belly (%)	2.5 (0.4)	5.0 (1.7)	63.6 (2.2)	64.2 (2.7)	0.457	<0.001	0.636
Isometric Force Loss (%)	4.1 (1.0)	3.8 (1.4)	63.1 (5.5)	67.5 (5.7)	0.617	<0.001	0.553
Centrally Nucleated Fibers, Distal (%)	8.7 (7.2)	8.3 (5.5)	62.4 (6.7)	62.7 (3.2)	0.991	<0.001	0.950
Gastrocnemius Muscle							
Gastrocnemius muscle mass (mg)	125.9 (5.2)	128.6 (4.2)	173.0 (9.0)	164.8 (4.3)	0.654	<0.001	0.363

Values are means (SE). EDL, extensor digitorum longus

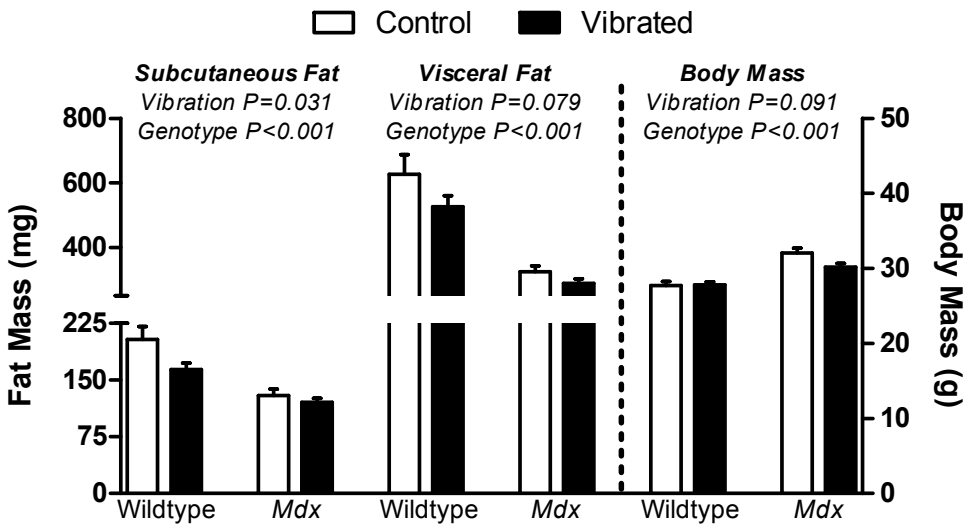

Figure 6.5: Effect of 8 weeks of low-intensity vibration on fat pad masses and body mass in *mdx* and wildtype mice. Vibrated mice had lower subcutaneous fat pads and a trend for lower visceral fat pad masses. *Mdx* mice were larger in body mass, but had lower fat pad masses compared to wildtype mice. Body masses were not different in mice subject to vibration compared to non-vibrated control mice. Data are mean, SE. Data were analyzed by two-way ANOVA's and the P-values associated with the main effects of vibration and genotype are indicated above each set of bars.

6.5 Discussion

Vibration training has been reported to enhance bone and muscle in humans and rodent models. Our study, however, failed to show any enhancement in those tissues. First, 8 weeks of low intensity vibration training did not alter trabecular architecture, cortical bone geometry, or whole bone strength in tibia of wildtype mice or mice with a muscle disease. Secondly, vibration did not alter any of our measures of contractile function of hindlimb muscles. Despite the lack of benefit, the preservation of muscle function in *mdx* mice indicates that vibration is a safe training modality for dystrophic muscle. Lastly, mice that were vibration-trained had smaller subcutaneous fat pads and tended to have smaller visceral fat pads compared to non-vibrated mice. Combined, these data suggest that in mice vibration training at 45 Hz and 0.6 g does not significantly impact

musculoskeletal function, but does affect fat pads.

Trabecular bone

We hypothesized that 8 weeks of low intensity vibration training would improve trabecular architecture. Vibration training, however, did not affect any measure of trabecular architecture or dynamic histomorphometry in the proximal tibial metaphysis (Figure 6.1 and Table 6.1). The anticipation of alterations in trabecular bone architecture was based on several reports of improved bone health in the proximal tibia of healthy mice following vibration training. Specifically, improvements in trabecular thickness [79, 156], trabecular number [127], bone volume fraction [79, 127, 156], dynamic rates of bone formation [79, 158], and decrease trabecular spacing [127] have been reported in response to 3 to 6 weeks of vibration training that had used similar low intensity parameters. In addition to these beneficial adaptations in healthy mice, vibration has also been shown to preserve or improve trabecular bone in mice modeling disuse [120, 151], and in patients with childhood diseases [141, 82]; thus making vibration training an attractive therapeutic modality for DMD. The lack of alterations in trabecular bone in our study is corroborated by one other study using *mdx* and wildtype mice and similar parameters of vibration [169], as well as other mouse models associated with physical inactivity and muscle weakness [121, 125].

Cortical Bone

Reductions in *mdx* tibial bone strength and stiffness compared to wildtype mice (Figure 6.2) are consistent with previous reports [66, 13] and have previously been attributed to altered bone geometry [13]. We hypothesized that 8 weeks of vibration training would improve cortical bone geometry and whole bone strength. Cortical bone, however, was not altered by vibration as indicated by the lack of differences in cortical bone geometry or bone strength between vibrated and control groups (Table 6.1 and Figure 6.2). These data are corroborated by evidence from others indicating that low intensity vibration did not alter bone geometry at the midshaft of the tibial [157, 170] and femur [76]. Improvements in periosteal BFR and MAR at the tibial midshaft following vibration have been noted, however this increase in bone growth did not translate to improvements in cortical bone area or whole bone strength or stiffness [157]. Cortical bone dynamic

histomorphometry was not measured in the present study due to the lack of functional improvements in cortical bone geometry and whole bone strength.

The lack of anabolic bone response in the present study may be attributed to multiple possible factors including 1) transmissibility of the vibration stimuli, 2) suboptimal parameters of vibration, 3) the high fidelic function of our vibration platform, or 4) the mild skeletal phenotype in *mdx* mice. First, bones response to vibration is dependent upon transmissibility of the vibration stimuli, such that skeletal regions closest to the source have more robust responses [155] compared to distal sites where transmissibility is diminished [171]. Transmission of the vibration stimuli is influenced by muscle activation patterns and joint angles [171, 172], so it is possible that in mice a higher intensity vibration (i.e., accelerations exceeding 1 g) would better amplify transmission and provoke an osteogenic response as previously shown [157]. Second, the parameters of vibration utilized in the present study may be suboptimal for long-term training. Bones response to vibration is not universally effective and has been shown to preferentially respond to certain vibration stimuli [13, 155, 157, 156, 158]. We previously identified two sets of potentially osteogenic vibration parameters in *mdx* mice (i.e., 45 Hz and 0.6 g and 90 Hz at 0.6 g) following 14 d of vibration, based on subtle alterations in alkaline phosphatase, osteoprotegerin and RANKL expression [13]. Bone in rats is capable of differentiating and preferentially responding to vibration stimuli at 90 Hz rather than 45 Hz [155], thus, it is plausible that vibration using 90 Hz at 0.6 g may have initiated an anabolic response. The third potential reason vibration didnt cause an anabolic bone response may be due to the continually-persistent vibration stimuli produced by our device (i.e., intra-trial and intra-animal variability was $<4\%$ at frequencies greater than 20 Hz [173]). Others who have gleaned vibration-induced anabolic responses report that variability of their device is as high as 21% and 48% for 45 Hz and 90 Hz, respectively [155]. Therefore, our highly-fidelic device may cause bone cells to desensitize within a few cycles as shown with other forms of loading [174, 175]. Lastly, the mild phenotype of *mdx* mice may result in insufficiently compromised bone to benefit from vibration training, and therefore the vibration stimuli may have been redundant, rather than osteogenic in these mice. Vibration has been proposed to act as a surrogate for muscle [76], as it produces bone strains equivalent to those of postural muscles during standing [77, 74, 176]. *Mdx* mice, unlike DMD patients, retain the ability to independently stand

and ambulate throughout life, and therefore, muscle-induced low level strains are likely preserved.

Muscle Function

Eight weeks of vibration training did not alter any measure of hindlimb muscle function (Figures 6.3 and 6.4 and Table 6.2). The overall efficacy of low intensity vibration to improve muscle function in humans remains controversial [78, 70], with various reports of beneficial effects [82, 141, 80, 177, 178, 153] and several reporting lack of alterations. Few studies have used mouse models to investigate vibration and skeletal muscle and those reports are also inconsistent in regard to effects on muscle size [125, 129, 159, 167]. The vibration training protocol used in present study did not improve muscle size or strength in *mdx* or wildtype mice. The lack of vibration-induced improvements in muscle is consistent with a more severe model of weakness and physical inactivity [125], but contradicts our previous vibration work in wildtype mice in which muscle strength improved by 10% despite no effect on muscle mass, size, or protein content [129]. Combined, these data do not support the notion that low intensity vibration induces myogenesis.

Contraindications to muscle have been reported following vibration training [167, 179], and due to the high susceptibility of dystrophic muscle to injury, it was necessary to establish that vibration can be a safe training modality. Our results show that 8 weeks of low intensity vibration training was not deleterious to any measure of muscle function (Figures 6.3 and 6.4 and Table 6.2). The lack of injury with vibration training corroborate our previous study in healthy mice[129], and contradicts the two studies which have reported muscle-specific contraindication of vibration (i.e., reduced vascularity in the distal soleus muscle in response to a low intensity vibration [167], and centrally-located nuclei in muscle fibers following relatively high intensity vibration [179]). Our thorough investigation utilized established recommendations for pre-clinical testing in *mdx* mice including a combination of *in vivo* and *ex vivo* assessment of muscle function providing the most comprehensive evaluation of a training modalitys efficacy and safety [180]. We further complemented these data with histological and plasma CK to confirm that vibration was not injurious to dystrophic muscle. As a result, our results show that low intensity vibration is not injurious to dystrophic mouse muscle, and therefore vibration is most likely a safe training modality for DMD.

Fat Pads

Vibrated mice had smaller subcutaneous and visceral fat pad masses following 8 weeks of training (Figure 6.5). These vibration-induced reduction in fat mass have been consistently reported [127, 129, 161] and vibration training has even been shown to inhibit diet-induced obesity [127]. The proposed mechanism behind these vibration-induced fat reductions is that vibration may drive differentiation of mesenchymal stem cells away from adipocytes toward the osteoblasts linage [127, 75, 151]. It is possible that the continual demand for differentiation of mesenchymal stem cells in *mdx* mice toward muscle precursor cells and fibroblasts may have impeded, or blunted, vibrations ability to drive differentiation toward osteoblasts. *Mdx* mice in the present study indeed had consistently smaller fat pads, independent of vibration (Figure 6.5). Stem cells in *mdx* mice have also been shown to have slower proliferate rates and reduced osteogenic and myogenic differentiation patterns [181]. Similar reductions in osteogenic gene expression have been noted in DMD patients [154]. As a result, the failure to attain vibration-induced osteogenic effects in *mdx* mice may be partially attributed to their inherently slower and inflexible patterns of mesenchymal stem cell differentiation patterns. Despite this possibility, wildtype mice did not respond to vibration either and mesenchymal stem cells differentiate normally and theoretically have plasticity for altering stem cell fate in response to vibration signals in these mice.

In summary, the present study has established that 8 weeks of low intensity vibration training at 45 Hz and 0.6 g did not significantly impact trabecular or cortical bone within the tibia of *mdx* or wildtype mice. Hindlimb muscle function also was not affected; however vibration may aid slowing the acquisition of fat mass. Further research is needed to determine if alternative parameters of vibration can initiate an osteogenic response in patients or animal models of muscle disease such as DMD.

Chapter 7

Summary Statement and Future Directions

The contents of this dissertation add significant findings to the fields of bone health in muscular dystrophy and the efficacy of vibration training. Muscle strength and physical activity are essential contributors to bone health, and decrements in these factors have been associated with deleterious effects. The muscle disease, Duchenne muscular dystrophy (DMD), has hallmark characteristics of progressive muscle weakness and physical inactivity. The two most commonly used mouse models of DMD for pre-clinical testing include the *mdx* and *dko* mice. These models are used because, similar to patients, these mice lack functional dystrophin, display muscle weakness [101], and have reduced physical activity levels [88]. At the start of my dissertation, only two studies had investigated bone health in dystrophic mice, however their evidence was conflicting [7, 8]. Therefore, the first aim of my dissertation was to confirm that skeletal health was altered secondary to the muscle disease in mouse models of DMD and to identify the underlying mechanisms. The second aim was to determine the extent to which physical inactivity and a standard drug treatment for patients with DMD further impact skeletal health. Upon establishing that bone health was altered in dystrophic mice my final dissertation aim was to determine the safety and efficacy of an increasingly popular intervention for bone health. Specifically, I investigated low intensity, high frequency vibration treatment as a potential therapeutic modality to preserve, and potentially improve, dystrophic musculoskeletal health.

My first study established that tibial bones from dystrophic mice were up to 38% weaker in strength and stiffness compared to wildtype mice, which was attributed to reductions in bone geometry rather than material properties (Chapter 3). Trabecular bone health was also compromised in dystrophic mice, as indicated by up to 78% reduction in trabecular morphometry. Combined, the results of this study established that dystrophic mice (i.e., *mdx* and *dko*) have an altered bone health secondary to their muscle disease, and therefore are an appropriate model to use in pre-clinical trials for identifying potential therapeutic regimens to improve bone health in DMD.

Upon establishing that bone health was compromised in DMD, my second study examined the extent to which prednisolone treatment and restricted physical activity further altered skeletal health in *mdx* mice. Prednisone treatment was investigated because it is standard of care for patients with DMD due to its ability to improve muscle strength, but it has known catabolic effects on bone. My results showed that both

prednisolone and restricted physical activity negatively and independently accentuate reductions in bone strength and geometry in *mdx* mice (Chapter 4). The combined effects likely contribute to the development of bone fragility and a heightened fracture risk in boys with DMD.

Due to the beneficial effects of prednisolone to thwart muscle deterioration, improve physical endurance, and prolong independent ambulation in patients with DMD [60, 59, 58, 100], I focused my remaining studies on identifying a safe therapeutic modality to restore physical activity levels in DMD. Low intensity vibration (i.e., less than 1 g of acceleration, where 1 g is equivalent to gravity) has been shown to have an anabolic effect on bone as well as prevent disuse-mediated bone loss [120, 81, 82, 80]. Several studies, however, have failed to replicate findings [121, 122, 123, 124, 125] or have shown differential responses [79] using similar parameters of vibration. Thus, prior to considering vibration as a bone-sparing modality for muscular dystrophy, I attempted to identify parameters of vibration that initiated the greatest osteogenic response in *mdx* mice, yet were safe for the adjacent diseased muscle. In response to 14 d of low intensity vibration training, two sets of parameters (i.e., 90 Hz at 0.6 g and 45 Hz at 0.6 g) were identified to be the most osteogenic based on the expression of osteoprotegerin and alkaline phosphatase (Chapter 5). Vibration was well tolerated by dystrophic mice and was consistently shown to be non-injurious to dystrophic muscle of various disease severities. The results suggest that longer term vibration training at 45 Hz and 0.6 g may have the potential to have an anabolic impact on bone health, while not causing injury to inherently fragile dystrophic muscle.

In my final study, I investigated the efficacy of long-term low intensity vibration training to improve dystrophic musculoskeletal health. Vibration training for 8 weeks did not alter trabecular architecture, dynamic histomorphometry, cortical geometry, whole bone strength, or any measure of muscle contractile function (Chapter 6). The preservation of musculoskeletal function and histomorphometry in mdx mice suggests vibration is not deleterious. Additionally, vibrated mice had smaller subcutaneous fat pads and tended to have smaller visceral fat pads. Combined, these data suggest that vibration training at 45Hz and 0.6 g does not significantly impact musculoskeletal function but may influence fat.

The lack of vibration-induced alterations in musculoskeletal health in the present

dissertation does not completely negate the potential utility of vibration as a therapeutic modality in DMD or other muscle diseases. It is possible that the musculoskeletal response to vibration may have been blunted in dystrophic mice in my study due to several factors including: 1) low transmissibility of the vibration stimuli, 2) utilization of less than optimal parameters of vibration, and 3) the potential for rapid desensitization of bone cells due to the consistency of the stimuli produced by my vibration device. For example, initial work in Dr. Lowes laboratory using healthy mice vibrated at 45 Hz and 1.0 g demonstrated 14% improvements in muscle strength following 6 weeks of training [129]. The higher acceleration of vibration used in our initial work (1.0 vs 0.6 g) may have improved the transmissibility of the vibration stimuli and therefore the response of the muscle. In addition, the consistency of the stimuli produced by the vibration plate during that initial study was less precise, and therefore the variability of the vibratory stimuli may have contributed to improvements in muscle strength. These factors should be considered in future studies investigating the utility of vibration as a therapeutic modality in DMD, as well as other populations. I would recommend that additional studies investigating dystrophic mice use a mean frequency of 90 Hz with an acceleration ranging between 0.6 to 1.0 g and also lower the precision of vibration device such that the stimulus is more variable. This recommendation is based on evidence indicating that the anabolic response to vibration is more profound with 90 Hz, rather than 45 Hz, and the applied stimulus varied as much as 48% [155]. Further investigations should also consider utilizing the *dko* mouse model of DMD, which has a more severe musculoskeletal phenotype compared to *mdx* mice and better mimics the disease progression seen in patients with DMD.

Additional therapeutic strategies should also be considered to improve bone health in DMD. Low intensity vibration is one of many physical treatment modalities aimed at restoring bone health. It remains possible that other low-intensity physical activities may better evoke an osteogenic response than that seen with vibration. The use of dystrophic mice may aid in identifying such modalities. Clinical research should also consider encouraging patients to continually incorporate physical activity in their daily lives, and aim to prolong the duration of these activities rather than increase the intensity at which activities are preformed. For example, simple activities such as standing may preserve bone health, or thwart bone loss, in advanced stages of the disease if

performed intermittently throughout the day for short durations.

Preservation of mechanical loading may be the key to preserving bone geometry and strength in patients with DMD in effort to reduce the incidence of fragility fractures. In conclusion, my thesis work has identified two mouse models of DMD that may aid in identifying such therapeutic modalities, and as a result, has contributed to the overall advancement within the field of bone health in DMD.

References

[1] M. L. Bianchi, A. Mazzanti, E. Galbiati, S. Saraifoger, A. Dubini, F. Cornelio, and L. Morandi. Bone mineral density and bone metabolism in duchenne muscular dystrophy. *Osteoporos Int*, 14(9):761–7, 2003.

[2] C. M. Larson and R. C. Henderson. Bone mineral density and fractures in boys with duchenne muscular dystrophy. *J Pediatr Orthop*, 20(1):71–4, 2000.

[3] D. G. McDonald, M. Kinali, A. C. Gallagher, E. Mercuri, F. Muntoni, H. Roper, P. Jardine, D. H. Jones, and M. G. Pike. Fracture prevalence in duchenne muscular dystrophy. *Dev Med Child Neurol*, 44(10):695–8, 2002.

[4] NJ Crabtree, KA Ward, H. Roper, Z Mughal, and NJ Shaw. The effect of non-ambulation on bone strength in boys with duchenne muscular dystrophy. In *ASBMR 30th Annual Meeting WG1–WG41. Journal of Bone and Mineral Research*, volume 23, page S506, 2008.

[5] W. King, J. Landoll, V. Matkovic, and JT Kissel. Volumetric radial and tibial bone mineral density in boys with duchenne muscular dystrophy. In *Neurology*, page 72, 2009.

[6] J. Landoll, W. King, JT Kissel, and V. Matkovic. Forearm pqct measurements in males with duchenne muscular dystrophy. In *J Bone Miner Res*, page 23, 2008.

[7] J. E. Anderson, D. L. Lentz, and R. B. Johnson. Recovery from disuse osteopenia coincident to restoration of muscle strength in mdx mice. *Bone*, 14(4):625–34, 1993.

[8] E. Montgomery, C. Pennington, C. M. Isales, and M. W. Hamrick. Muscle-bone interactions in dystrophin-deficient and myostatin-deficient mice. *Anat Rec A Discov Mol Cell Evol Biol*, 286(1):814–22, 2005.

[9] S.C. Cowin. *Mechanical Properties of Bone*, pages 151–184. Elsevier, Philadelphia, 1981.

[10] A. M. Parfitt, M. Kleerekoper, and A. R. Villanueva. *Increased bone age: Mechanisms and consequences*, pages 301–308. Copenhagen, 1987.

[11] G. L. Warren, D. A. Lowe, C. L. Inman, O. M. Orr, H. A. Hogan, S. A. Bloomfield, and R. B. Armstrong. Estradiol effect on anterior crural muscles-tibial bone relationship and susceptibility to injury. *J Appl Physiol*, 80(5):1660–5, 1996.

[12] G. L. Warren, A. L. Moran, H. A. Hogan, A. S. Lin, R. E. Guldberg, and D. A. Lowe. Voluntary run training but not estradiol deficiency alters the tibial bone-soleus muscle functional relationship in mice. *Am J Physiol Regul Integr Comp Physiol*, 293(5):R2015–26, 2007.

[13] S. A. Novotny, G. L. Warren, A. S. Lin, R. E. Guldberg, K. A. Baltgalvis, and D. A. Lowe. Bone is functionally impaired in dystrophic mice but less so than skeletal muscle. *Neuromuscul Disord*, 21(3):183–93, 2011.

[14] C. H. Turner and D. B. Burr. *Experimental Techniques for Bone Mechanics*, pages 7–1–7–35. CRC Press, Boca Raton, 2001.

[15] M. Sato, T. A. Grese, J. A. Dodge, H. U. Bryant, and C. H. Turner. Emerging therapies for the prevention or treatment of postmenopausal osteoporosis. *J Med Chem*, 42(1):1–24, 1999.

[16] Jr. Smith, R. W. and R. R. Walker. Femoral expansion in aging women: Implications for osteoporosis and fractures. *Science*, 145:156–7, 1964.

[17] C. Slemenda. Prevention of hip fractures: risk factor modification. *Am J Med*, 103(2A):65S–71S; discussion 71S–73S, 1997.

[18] J. D. Currey. How well are bones designed to resist fracture? *J Bone Miner Res*, 18(4):591–8, 2003.

[19] H. M. Frost. *Bone Remodeling Dynamics*. Charles C Thomas Company, 1963.

[20] A Ardizzoni. Osteocyte lacunar size-lamellar thickness relationships in human secondary osteons. *Bone*, 28(2):215–219, 2001.

[21] S. Qiu, D. S. Rao, S. Palnitkar, and A. M. Parfitt. Age and distance from the surface but not menopause reduce osteocyte density in human cancellous bone. *Bone*, 31(2):313–8, 2002.

[22] H. M. Frost. Bone's mechanostat: a 2003 update. *Anat Rec A Discov Mol Cell Evol Biol*, 275(2):1081–101, 2003.

[23] C. T. Rubin. Skeletal strain and the functional significance of bone architecture. *Calcif Tissue Int*, 36 Suppl 1:S11–8, 1984.

[24] N. Basso and J. N. Heersche. Characteristics of in vitro osteoblastic cell loading models. *Bone*, 30(2):347–51, 2002.

[25] S. L. Bass, L. Saxon, R. M. Daly, C. H. Turner, A. G. Robling, E. Seeman, and S. Stuckey. The effect of mechanical loading on the size and shape of bone in pre-, peri-, and postpubertal girls: a study in tennis players. *J Bone Miner Res*, 17(12):2274–80, 2002. 0884-0431 (Print) Journal Article.

[26] E. Seeman. Bone quality: the material and structural basis of bone strength. *J Bone Miner Metab*, 26(1):1–8, 2008. Seeman, Ego Review Japan Journal of bone and mineral metabolism J Bone Miner Metab. 2008;26(1):1-8. Epub 2008 Jan 10.

[27] S. Khosla and L.J. Melton III. An introduction to clinical osteoporosis, 2006.

[28] C. H. Turner and A. G. Robling. Designing exercise regimens to increase bone strength. *Exerc Sport Sci Rev*, 31(1):45–50, 2003.

[29] Y. Umemura, T. Ishiko, T. Yamauchi, M. Kurono, and S. Mashiko. Five jumps per day increase bone mass and breaking force in rats. *J Bone Miner Res*, 12(9):1480–5, 1997.

[30] Alexander G Robling, Felicia M Hinant, David B Burr, and Charles H Turner. Improved bone structure and strength after long-term mechanical loading is greatest if loading is separated into short bouts. *J Bone Miner Res*, 17(8):1545–1554, 2002.

[31] A. M. Parfitt. What is the normal rate of bone remodeling? *Bone*, 35(1):1–3, 2004.

[32] H. K. Uhthoff and Z. F. Jaworski. Bone loss in response to long-term immobilisation. *J Bone Joint Surg Br*, 60-B(3):420–9, 1978.

[33] W. Dehority, B. P. Halloran, D. D. Bikle, T. Curren, P. J. Kostenuik, T. J. Wronski, Y. Shen, B. Rabkin, A. Bouraoui, and E. Morey-Holton. Bone and hormonal changes induced by skeletal unloading in the mature male rat. *Am J Physiol*, 276(1 Pt 1):E62–9, 1999.

[34] Z. F. Jaworski, M. Liskova-Kiar, and H. K. Uhthoff. Effect of long-term immobilisation on the pattern of bone loss in older dogs. *J Bone Joint Surg Br*, 62-B(1):104–10, 1980.

[35] W. S. Jee, X.J. Li, and H. Z. Ke. The skeletal adaptation to mechanical usage in the rat. *Cells Mater*, 1(Suppl):131, 1991.

[36] J. Tuukkanen, B. Wallmark, P. Jalovaara, T. Takala, S. Sjogren, and K. Vaananen. Changes induced in growing rat bone by immobilization and remobilization. *Bone*, 12(2):113–8, 1991.

[37] Q. Q. Zeng, W. S. Jee, A. E. Bigornia, Jr. King, J. G., S. M. D'Souza, X. J. Li, Y. F. Ma, and W. J. Wechter. Time responses of cancellous and cortical bones to sciatic neurectomy in growing female rats. *Bone*, 19(1):13–21, 1996.

[38] A. J. Kaneps, S. M. Stover, and N. E. Lane. Changes in canine cortical and cancellous bone mechanical properties following immobilization and remobilization with exercise. *Bone*, 21(5):419–23, 1997.

[39] H. M. Frost. On our age-related bone loss: insights from a new paradigm. *J Bone Miner Res*, 12(10):1539–46, 1997.

[40] J. Rittweger and D. Felsenberg. Recovery of muscle atrophy and bone loss from 90 days bed rest: results from a one-year follow-up. *Bone*, 44(2):214–24, 2009.

[41] H. Sievanen, A. Heinonen, and P. Kannus. Adaptation of bone to altered loading environment: a biomechanical approach using x-ray absorptiometric data from the patella of a young woman. *Bone*, 19(1):55–9, 1996.

[42] Sarah M Greising, Heather M Gransee, Carlos B Mantilla, and Gary C Sieck. Systems biology of skeletal muscle: fiber type as an organizing principle. *Wiley Interdiscip Rev Syst Biol Med*, 4(5):457–473, 2012.

[43] J. M. Ervasti. Costameres: the achilles' heel of herculean muscle. *J Biol Chem*, 278(16):13591–4, 2003.

[44] A.E. Emery and F. Muntoni. *Duchenne Muscular Dystrophy*. Oxford Univ. Press, Oxford, 2003.

[45] D. J. Blake, A. Weir, S. E. Newey, and K. E. Davies. Function and genetics of dystrophin and dystrophin-related proteins in muscle. *Physiol Rev*, 82(2):291–329, 2002.

[46] R. D. Cohn and K. P. Campbell. Molecular basis of muscular dystrophies. *Muscle Nerve*, 23(10):1456–71, 2000.

[47] R. Matsuda, A. Nishikawa, and H. Tanaka. Visualization of dystrophic muscle fibers in mdx mouse by vital staining with evans blue: evidence of apoptosis in dystrophin-deficient muscle. *J Biochem*, 118(5):959–64, 1995.

[48] B. Weller, G. Karpati, and S. Carpenter. Dystrophin-deficient mdx muscle fibers are preferentially vulnerable to necrosis induced by experimental lengthening contractions. *J Neurol Sci*, 100(1-2):9–13, 1990.

[49] G. S. Lynch, R. T. Hinkle, J. S. Chamberlain, S. V. Brooks, and J. A. Faulkner. Force and power output of fast and slow skeletal muscles from mdx mice 6-28 months old. *J Physiol*, 535(Pt 2):591–600, 2001.

[50] F. Cozzi, M. Cerletti, G. C. Luvoni, R. Lombardo, P. G. Brambilla, S. Faverzani, F. Blasevich, F. Cornelio, O. Pozza, and M. Mora. Development of muscle pathology in canine x-linked muscular dystrophy. ii. quantitative characterization of histopathological progression during postnatal skeletal muscle development. *Acta Neuropathol*, 101(5):469–78, 2001.

[51] T.G. Gainer, Q. Wang, C.W. Ward, and R.W. Grange. *Duchenne Muscular Dystrophy*, pages 113–124. Human Kinetics, Champaign, IL, 2008.

[52] D. G. Allen. Skeletal muscle function: role of ionic changes in fatigue, damage and disease. *Clin Exp Pharmacol Physiol*, 31(8):485–93, 2004.

[53] N. Gaudreault, D. Gravel, and S. Nadeau. Evaluation of plantar flexion contracture contribution during the gait of children with duchenne muscular dystrophy. *J Electromyogr Kinesiol*, 19(3):e180–6, 2009.

[54] G. A. Hawker, R. Ridout, V. A. Harris, C. C. Chase, L. J. Fielding, and W. D. Biggar. Alendronate in the treatment of low bone mass in steroid-treated boys with duchennes muscular dystrophy. *Arch Phys Med Rehabil*, 86(2):284–8, 2005.

[55] A. C. Soderpalm, P. Magnusson, A. C. Ahlander, J. Karlsson, A. K. Kroksmark, M. Tulinius, and D. Swolin-Eide. Low bone mineral density and decreased bone turnover in duchenne muscular dystrophy. *Neuromuscul Disord*, 17(11-12):919–28, 2007.

[56] L. F. Aparicio, M. Jurkovic, and J. DeLullo. Decreased bone density in ambulatory patients with duchenne muscular dystrophy. *J Pediatr Orthop*, 22(2):179–81, 2002.

[57] C. S. Straathof, W. C. Overweg-Plandsoen, G. J. van den Burg, A. J. van der Kooi, J. J. Verschuuren, and I. J. de Groot. Prednisone 10 days on/10 days off in patients with duchenne muscular dystrophy. *J Neurol*, 256(5):768–73, 2009.

[58] E. A. Beenakker, J. M. Fock, M. J. Van Tol, N. M. Maurits, H. M. Koopman, O. F. Brouwer, and J. H. Van der Hoeven. Intermittent prednisone therapy in duchenne muscular dystrophy: a randomized controlled trial. *Arch Neurol*, 62(1):128–32, 2005.

[59] R. C. Griggs, 3rd Moxley, R. T., J. R. Mendell, G. M. Fenichel, M. H. Brooke, A. Pestronk, J. P. Miller, V. A. Cwik, S. Pandya, J. Robison, and et al. Duchenne dystrophy: randomized, controlled trial of prednisone (18 months) and azathioprine (12 months). *Neurology*, 43(3 Pt 1):520–7, 1993.

[60] J. R. Mendell, R. T. Moxley, R. C. Griggs, M. H. Brooke, G. M. Fenichel, J. P. Miller, W. King, L. Signore, S. Pandya, J. Florence, and et al. Randomized, double-blind six-month trial of prednisone in duchenne's muscular dystrophy. *N Engl J Med*, 320(24):1592–7, 1989.

[61] N. E. Lane, W. Yao, M. Balooch, R. K. Nalla, G. Balooch, S. Habelitz, J. H. Kinney, and L. F. Bonewald. Glucocorticoid-treated mice have localized changes in trabecular bone material properties and osteocyte lacunar size that are not observed in placebo-treated or estrogen-deficient mice. *J Bone Miner Res*, 21(3):466–76, 2006.

[62] R. S. Weinstein. Clinical practice. glucocorticoid-induced bone disease. *N Engl J Med*, 365(1):62–70, 2011.

[63] D. Jia, C. A. O'Brien, S. A. Stewart, S. C. Manolagas, and R. S. Weinstein. Glucocorticoids act directly on osteoclasts to increase their life span and reduce bone density. *Endocrinology*, 147(12):5592–9, 2006.

[64] W. M. King, R. Ruttencutter, H. N. Nagaraja, V. Matkovic, J. Landoll, C. Hoyle, J. R. Mendell, and J. T. Kissel. Orthopedic outcomes of long-term daily corticosteroid treatment in duchenne muscular dystrophy. *Neurology*, 68(19):1607–13, 2007.

[65] J. E. Bothwell, K. E. Gordon, J. M. Dooley, J. MacSween, E. A. Cummings, and S. Salisbury. Vertebral fractures in boys with duchenne muscular dystrophy. *Clin Pediatr (Phila)*, 42(4):353–6, 2003.

[66] W. R. Nakagaki, C. A. Bertran, C. Y. Matsumura, H. Santo-Neto, and J. A. Camilli. Mechanical, biochemical and morphometric alterations in the femur of mdx mice. *Bone*, 48(2):372–9, 2011.

[67] P. Sicinski, Y. Geng, A. S. Ryder-Cook, E. A. Barnard, M. G. Darlison, and P. J. Barnard. The molecular basis of muscular dystrophy in the mdx mouse: a point mutation. *Science*, 244(4912):1578–80, 1989.

[68] L. Zhou, J. A. Rafael-Fortney, P. Huang, X. S. Zhao, G. Cheng, X. Zhou, H. J. Kaminski, L. Liu, and R. M. Ransohoff. Haploinsufficiency of utrophin gene worsens skeletal muscle inflammation and fibrosis in mdx mice. *J Neurol Sci*, 264(1-2):106–11, 2008.

[69] P. J. Marin and M. R. Rhea. Effects of vibration training on muscle power: a meta-analysis. *J Strength Cond Res*, 24(3):871–8, 2010.

[70] M. Mikhael, R. Orr, and M. A. Fiatarone Singh. The effect of whole body vibration exposure on muscle or bone morphology and function in older adults: a systematic review of the literature. *Maturitas*, 66(2):150–7, 2010.

[71] R. D. Prisby, M. H. Lafage-Proust, L. Malaval, A. Belli, and L. Vico. Effects of whole body vibration on the skeleton and other organ systems in man and animal models: what we know and what we need to know. *Ageing Res Rev*, 7(4):319–29, 2008.

[72] L. Slatkovska, S. M. Alibhai, J. Beyene, and A. M. Cheung. Effect of whole-body vibration on bmd: a systematic review and meta-analysis. *Osteoporos Int*, 21(12):1969–80, 2010.

[73] E. Ozcivici, R. Garman, and S. Judex. High-frequency oscillatory motions enhance the simulated mechanical properties of non-weight bearing trabecular bone. *J Biomech*, 40(15):3404–11, 2007.

[74] C. Rubin, A. S. Turner, S. Bain, C. Mallinckrodt, and K. McLeod. Anabolism. low mechanical signals strengthen long bones. *Nature*, 412(6847):603–4, 2001.

[75] E. Ozcivici, Y. K. Luu, B. Adler, Y. X. Qin, J. Rubin, S. Judex, and C. T. Rubin. Mechanical signals as anabolic agents in bone. *Nat Rev Rheumatol*, 6(1):50–9, 2010.

[76] C. Rubin, A. S. Turner, C. Mallinckrodt, C. Jerome, K. McLeod, and S. Bain. Mechanical strain, induced noninvasively in the high-frequency domain, is anabolic to cancellous bone, but not cortical bone. *Bone*, 30(3):445–52, 2002.

[77] R. P. Huang, C. T. Rubin, and K. J. McLeod. Changes in postural muscle dynamics as a function of age. *J Gerontol A Biol Sci Med Sci*, 54(8):B352–7, 1999.

[78] R. W. Lau, L. R. Liao, F. Yu, T. Teo, R. C. Chung, and M. Y. Pang. The effects of whole body vibration therapy on bone mineral density and leg muscle strength in older adults: a systematic review and meta-analysis. *Clin Rehabil*, 25(11):975–88, 2011.

[79] S. Judex, L. R. Donahue, and C. Rubin. Genetic predisposition to low bone mass is paralleled by an enhanced sensitivity to signals anabolic to the skeleton. *Faseb J*, 16(10):1280–2, 2002.

[80] V. Gilsanz, T. A. Wren, M. Sanchez, F. Dorey, S. Judex, and C. Rubin. Low-level, high-frequency mechanical signals enhance musculoskeletal development of young women with low bmd. *J Bone Miner Res*, 21(9):1464–74, 2006.

[81] C. Rubin, R. Recker, D. Cullen, J. Ryaby, J. McCabe, and K. McLeod. Prevention of postmenopausal bone loss by a low-magnitude, high-frequency mechanical stimuli: a clinical trial assessing compliance, efficacy, and safety. *J Bone Miner Res*, 19(3):343–51, 2004.

[82] K. Ward, C. Alsop, J. Caulton, C. Rubin, J. Adams, and Z. Mughal. Low magnitude mechanical loading is osteogenic in children with disabling conditions. *J Bone Miner Res*, 19(3):360–9, 2004.

[83] A. C. Soderpalm, P. Magnusson, A. C. Ahlander, J. Karlsson, A. K. Kroksmark, M. Tulinius, and D. Swolin-Eide. Bone markers and bone mineral density in duchenne muscular dystrophy. *J Musculoskelet Neuronal Interact*, 8(1):24, 2008.

[84] J. S. Chamberlain, J. Metzger, M. Reyes, D. Townsend, and J. A. Faulkner. Dystrophin-deficient mdx mice display a reduced life span and are susceptible to spontaneous rhabdomyosarcoma. *Faseb J*, 21(9):2195–204, 2007.

[85] G. Bulfield, W. G. Siller, P. A. Wight, and K. J. Moore. X chromosome-linked muscular dystrophy (mdx) in the mouse. *Proc Natl Acad Sci U S A*, 81(4):1189–92, 1984.

[86] R. M. Grady, H. Teng, M. C. Nichol, J. C. Cunningham, R. S. Wilkinson, and J. R. Sanes. Skeletal and cardiac myopathies in mice lacking utrophin and dystrophin: a model for duchenne muscular dystrophy. *Cell*, 90(4):729–38, 1997.

[87] T. S. Gross, S. L. Poliachik, J. Prasad, and S. D. Bain. The effect of muscle dysfunction on bone mass and morphology. *J Musculoskelet Neuronal Interact*, 10(1):25–34.

[88] R. M. Landisch, A. M. Kosir, S. A. Nelson, K. A. Baltgalvis, and D. A. Lowe. Adaptive and nonadaptive responses to voluntary wheel running by mdx mice. *Muscle Nerve*, 38(4):1290–303, 2008.

[89] A. L. Moran, G. L. Warren, and D. A. Lowe. Soleus and edl muscle contractility across the lifespan of female c57bl/6 mice. *Exp Gerontol*, 40(12):966–75, 2005.

[90] K. A. Baltgalvis, J. A. Call, J. B. Nikas, and D. A. Lowe. Effects of prednisolone on skeletal muscle contractility in mdx mice. *Muscle Nerve*, 40(3):443–54, 2009.

[91] G. L. Warren, D. A. Hayes, D. A. Lowe, J. H. Williams, and R. B. Armstrong. Eccentric contraction-induced injury in normal and hindlimb-suspended mouse soleus and edl muscles. *J Appl Physiol*, 77(3):1421–30, 1994.

[92] J. F. Jr. Woessner. he determination of hydroxyproline in tissue and protein samples containing small proportions of this imino acid. *Arch Biochem Biophys*, pages 440–447, 1961.

[93] T. W. Lu, S. J. Taylor, J. J. O'Connor, and P. S. Walker. Influence of muscle activity on the forces in the femur: an in vivo study. *J Biomech*, 30(11-12):1101–6, 1997.

[94] S. G. Aitkens, M. A. McCrory, D. D. Kilmer, and E. M. Bernauer. Moderate resistance exercise program: its effect in slowly progressive neuromuscular disease. *Arch Phys Med Rehabil*, 74(7):711–5, 1993.

[95] J. M. Gillis. Understanding dystrophinopathies: an inventory of the structural and functional consequences of the absence of dystrophin in muscles of the mdx mouse. *J Muscle Res Cell Motil*, 20(7):605–25, 1999.

[96] D. J. Law, D. L. Allen, and J. G. Tidball. Talin, vinculin and drp (utrophin) concentrations are increased at mdx myotendinous junctions following onset of necrosis. *J Cell Sci*, 107 (Pt 6):1477–83, 1994.

[97] Center for Disease Control and Prevention. Prevalence of duchenne/becker muscular dystrophy among males aged 5–24 years — four states, 2007, 10/15/2009 2009.

[98] N. Gaudreault, D. Gravel, S. Nadeau, P. Desjardins, and A. Briere. A method to evaluate contractures effects during the gait of children with duchenne dystrophy. *Clin Orthop Relat Res*, 456:51–7, 2007.

[99] J. M. Hughes and M. A. Petit. Biological underpinnings of frost's mechanostat thresholds: the important role of osteocytes. *J Musculoskelet Neuronal Interact*, 10(2):128–35, 2010.

[100] A. Y. Manzur, T. Kuntzer, M. Pike, and A. Swan. Glucocorticoid corticosteroids for duchenne muscular dystrophy. *Cochrane Database Syst Rev*, (1):CD003725, 2008.

[101] J. F. Watchko, T. L. O'Day, and E. P. Hoffman. Functional characteristics of dystrophic skeletal muscle: insights from animal models. *J Appl Physiol*, 93(2):407–17, 2002.

[102] A. M. Hanson, V. L. Ferguson, S. J. Simske, C. M. Cannon, and S. Stodieck. Comparison of tail-suspension and sciatic nerve crush on the musculoskeletal system in young-adult mice. *Biomed Sci Instrum*, 41:92–6, 2005.

[103] A. Minematsu, H. Imagita, N. Kanemura, and O. Yoshimura. The progression of bone and muscle atrophy in mice hind limb with immobilization. *Hiroshima J Med Sci*, 55(3):79–83, 2006.

[104] A. De Luca, S. Pierno, A. Liantonio, M. Cetrone, C. Camerino, B. Fraysse, M. Mirabella, S. Servidei, U. T. Ruegg, and D. Conte Camerino. Enhanced dystrophic progression in mdx mice by exercise and beneficial effects of taurine and insulin-like growth factor-1. *J Pharmacol Exp Ther*, 304(1):453–63, 2003.

[105] P. T. Golumbek, R. M. Keeling, and A. M. Connolly. Strength and corticosteroid responsiveness of mdx mice is unchanged by rag2 gene knockout. *Neuromuscul Disord*, 17(5):376–84, 2007.

[106] J. A. Granchelli, C. Pollina, and M. S. Hudecki. Pre-clinical screening of drugs using the mdx mouse. *Neuromuscul Disord*, 10(4-5):235–9, 2000.

[107] M. S. Hudecki, C. M. Pollina, J. A. Granchelli, M. K. Daly, T. Byrnes, J. C. Wang, and J. C. Hsiao. Strength and endurance in the therapeutic evaluation of prednisolone-treated mdx mice. *Res Commun Chem Pathol Pharmacol*, 79(1):45–60, 1993.

[108] R. M. Keeling, P. T. Golumbek, E. M. Streif, and A. M. Connolly. Weekly oral prednisolone improves survival and strength in male mdx mice. *Muscle Nerve*, 35(1):43–8, 2007.

[109] S. M. Greising, K. A. Baltgalvis, A. M. Kosir, A. L. Moran, G. L. Warren, and D. A. Lowe. Estradiol's beneficial effect on murine muscle function is independent of muscle activity. *J Appl Physiol*, 110(1):109–15, 2011.

[110] Y. Kozai, R. Kawamata, T. Sakurai, M. Kanno, and I. Kashima. Influence of prednisolone-induced osteoporosis on bone mass and bone quality of the mandible in rats. *Dentomaxillofac Radiol*, 38(1):34–41, 2009.

[111] A. R. Doyon, I. K. Ferries, and J. Li. Glucocorticoid attenuates the anabolic effects of parathyroid hormone on fracture repair. *Calcif Tissue Int*, 87(1):68–76, 2010.

[112] G. Balooch, W. Yao, J. W. Ager, M. Balooch, R. K. Nalla, A. E. Porter, R. O. Ritchie, and N. E. Lane. The aminobisphosphonate risedronate preserves localized mineral and material properties of bone in the presence of glucocorticoids. *Arthritis Rheum*, 56(11):3726–37, 2007.

[113] R. S. Weinstein, R. L. Jilka, M. Almeida, P. K. Roberson, and S. C. Manolagas. Intermittent parathyroid hormone administration counteracts the adverse effects of glucocorticoids on osteoblast and osteocyte viability, bone formation, and strength in mice. *Endocrinology*, 151(6):2641–9, 2010.

[114] Y. Fujita, K. Watanabe, S. Uchikanbori, and K. Maki. Effects of risedronate on cortical and trabecular bone of the mandible in glucocorticoid-treated growing rats. *Am J Orthod Dentofacial Orthop*, 139(3):e267–77.

[115] M. Squire, L. R. Donahue, C. Rubin, and S. Judex. Genetic variations that regulate bone morphology in the male mouse skeleton do not define its susceptibility to mechanical unloading. *Bone*, 35(6):1353–60, 2004.

[116] P. Eser, A. Frotzler, Y. Zehnder, L. Wick, H. Knecht, J. Denoth, and H. Schiessl. Relationship between the duration of paralysis and bone structure: a pqct study of spinal cord injured individuals. *Bone*, 34(5):869–80, 2004.

[117] G. M. Palmieri, T. E. Bertorini, J. W. Griffin, M. Igarashi, and J. G. Karas. Assessment of whole body composition with dual energy x-ray absorptiometry in duchenne muscular dystrophy: correlation of lean body mass with muscle function. *Muscle Nerve*, 19(6):777–9, 1996.

[118] L. A. Landin. Epidemiology of children's fractures. *J Pediatr Orthop B*, 6(2):79–83, 1997.

[119] M. Eagle. Report on the muscular dystrophy campaign workshop: exercise in neuromuscular diseases newcastle, january 2002. *Neuromuscul Disord*, 12(10):975–83, 2002.

[120] C. Rubin, G. Xu, and S. Judex. The anabolic activity of bone tissue, suppressed by disuse, is normalized by brief exposure to extremely low-magnitude mechanical stimuli. *Faseb J*, 15(12):2225–9, 2001.

[121] J. E. Brouwers, B. van Rietbergen, K. Ito, and R. Huiskes. Effects of vibration treatment on tibial bone of ovariectomized rats analyzed by in vivo micro-ct. *J Orthop Res*, 28(1):62–9, 2009.

[122] B. A. Christiansen, A. A. Kotiya, and M. J. Silva. Constrained tibial vibration does not produce an anabolic bone response in adult mice. *Bone*, 45(4):750–9, 2009.

[123] L. Slatkovska, S. M. Alibhai, J. Beyene, H. Hu, A. Demaras, and A. M. Cheung. Effect of 12 months of whole-body vibration therapy on bone density and structure in postmenopausal women: a randomized trial. *Ann Intern Med*, 155(10):668–79, W205, 2010.

[124] A. A. Kotiya, P. V. Bayly, and M. J. Silva. Short-term low-strain vibration enhances chemo-transport yet does not stimulate osteogenic gene expression or cortical bone formation in adult mice. *Bone*, 48(3):468–75, 2011.

[125] S. L. Manske, C. A. Good, R. F. Zernicke, and S. K. Boyd. High-frequency, low-magnitude vibration does not prevent bone loss resulting from muscle disuse in mice following botulinum toxin injection. *PLoS One*, 7(5):e36486, 2012.

[126] S. Judex, N. Zhong, M. E. Squire, K. Ye, L. R. Donahue, M. Hadjiargyrou, and C. T. Rubin. Mechanical modulation of molecular signals which regulate anabolic and catabolic activity in bone tissue. *J Cell Biochem*, 94(5):982–94, 2005.

[127] Y. K. Luu, E. Capilla, C. J. Rosen, V. Gilsanz, J. E. Pessin, S. Judex, and C. T. Rubin. Mechanical stimulation of mesenchymal stem cell proliferation and differentiation promotes osteogenesis while preventing dietary-induced obesity. *J Bone Miner Res*, 24(1):50–61, 2009.

[128] M. J. Patel, K. H. Chang, M. C. Sykes, R. Talish, C. Rubin, and H. Jo. Low magnitude and high frequency mechanical loading prevents decreased bone formation responses of 2t3 preosteoblasts. *J Cell Biochem*, 106(2):306–16, 2009.

[129] J. N. McKeehen, S. A. Novotny, K. A. Baltgalvis, J. A. Call, D. J. Nuckley, and D. A. Lowe. Adaptations of mouse skeletal muscle to low-intensity vibration training. *Med Sci Sports Exerc*, In press, 2012.

[130] B. J. Petrof, J. B. Shrager, H. H. Stedman, A. M. Kelly, and H. L. Sweeney. Dystrophin protects the sarcolemma from stresses developed during muscle contraction. *Proc Natl Acad Sci U S A*, 90(8):3710–4, 1993.

[131] A. Irintchev and A. Wernig. Muscle damage and repair in voluntarily running mice: strain and muscle differences. *Cell Tissue Res*, 249(3):509–21, 1987.

[132] Maaike van Putten, Darshan Kumar, Margriet Hulsker, Willem M H Hoogaars, Jaap J Plomp, Annemarieke van Opstal, Maarten van Iterson, Peter Admiraal, Gert-Jan B van Ommen, Peter A C 't Hoen, and Annemieke Aartsma-Rus. Comparison of skeletal muscle pathology and motor function of dystrophin and utrophin deficient mouse strains. *Neuromuscul Disord*, 22(5):406–17, May 2012.

[133] J. A. Call, J. M. Ervasti, and D. A. Lowe. Tat-muutrophin mitigates the pathophysiology of dystrophin and utrophin double-knockout mice. *J Appl Physiol*, 111(1):200–5, 2011.

[134] K. A. Baltgalvis, J. A. Call, G. D. Cochrane, R. C. Laker, Z. Yan, and D. A. Lowe. Exercise training improves plantarflexor muscle function in mdx mice. *Med Sci Sports Exerc*, 2012.

[135] J. C. Fritton, C. T. Rubin, Y. X. Qin, and K. J. McLeod. Whole-body vibration in the skeleton: development of a resonance-based testing device. *Ann Biomed Eng*, 25(5):831–9, 1997.

[136] J. A. Call, M. D. Eckhoff, K. A. Baltgalvis, G. L. Warren, and D. A. Lowe. Adaptive strength gains in dystrophic muscle exposed to repeated bouts of eccentric contraction. *J Appl Physiol*, 111(6):1768–77, 2011.

[137] Y. M. Kobayashi, E. P. Rader, R. W. Crawford, N. K. Iyengar, D. R. Thedens, J. A. Faulkner, S. V. Parikh, R. M. Weiss, J. S. Chamberlain, S. A. Moore, and K. P. Campbell. Sarcolemma-localized nnos is required to maintain activity after mild exercise. *Nature*, 456(7221):511–5, 2008.

[138] M. Horder, E. Magid, E. Pitkanen, M. Harkonen, J. H. Stromme, L. Theodorsen, W. Gerhardt, and J. Waldenstrom. Recommended method for the determination of creatine kinase in blood modified by the inclusion of edta. the committee on enzymes of the scandinavian society for clinical chemistry and clinical physiology (sce). *Scand J Clin Lab Invest*, 39(1):1–5, 1979.

[139] S. M. Greising, J. A. Call, T. C. Lund, B. R. Blazar, J. Tolar, and D. A. Lowe. Skeletal muscle contractile function and neuromuscular performance in zmpste24 -/- mice, a murine model of human progeria. *Age (Dordr)*, 34(4):805–19, 2012.

[140] Michael W. Pfaffl, Graham W. Horgan, and Leo Dempfle. Relative expression software tool (rest©) for group-wise comparison and statistical analysis of relative expression results in real-time pcr. *Nucleic Acids Research*, 30(9):e36, 2002.

[141] M. L. Reyes, M. Hernandez, L. J. Holmgren, E. Sanhueza, and R. G. Escobar. High-frequency, low-intensity vibrations increase bone mass and muscle strength in upper limbs, improving autonomy in disabled children. *J Bone Miner Res*, 26(8):1759–66, 2011.

[142] C. Kesavan, S. Mohan, S. Oberholtzer, J. E. Wergedal, and D. J. Baylink. Mechanical loading-induced gene expression and bmd changes are different in two inbred mouse strains. *J Appl Physiol*, 99(5):1951–7, 2005.

[143] E. Lau, S. Al-Dujaili, A. Guenther, D. Liu, L. Wang, and L. You. Effect of low-magnitude, high-frequency vibration on osteocytes in the regulation of osteoclasts. *Bone*, 46(6):1508–15, 2010.

[144] G. L. Warren, M. Summan, X. Gao, R. Chapman, T. Hulderman, and P. P. Simeonova. Mechanisms of skeletal muscle injury and repair revealed by gene expression studies in mouse models. *J Physiol*, 582(Pt 2):825–41, 2007.

[145] G. L. Warren, T. Hulderman, D. Mishra, X. Gao, L. Millecchia, L. O'Farrell, W. A. Kuziel, and P. P. Simeonova. Chemokine receptor ccr2 involvement in skeletal muscle regeneration. *Faseb J*, 19(3):413–5, 2005.

[146] C. Z. Wang, G. J. Wang, M. L. Ho, Y. H. Wang, M. L. Yeh, and C. H. Chen. Low-magnitude vertical vibration enhances myotube formation in c2c12 myoblasts. *J Appl Physiol*, 109(3):840–8, 2010.

[147] G. Ceccarelli, L. Benedetti, D. Pre, G. Magenes, and M. G. Cusella De Angelis. An "in vivo" study of high frequency vibration on muscle development. In O. Dössel and W.C. Schlegel, editors, *IFMBE*, volume 25, pages 859–62.

[148] E. Ceccarelli, L. Benedetti, D. Pre, D. Galli, L. Vercesi, G. Magenes, and M. G. Cusella De Angelis. High frequency vibration (hfv) induces muscle hypertrophy in newborn mice and enhances primary myoblasts fusion in satellite cells. In P.D. Bamidis and N. Pallikarakis, editors, *MEDICON 2010, IFMBE*, volume 29, pages 608–11.

[149] G. Ceccarelli, L. Benedetti, D. Galli, D. Pre, G. Silvani, N. Crosetto, G. Magenes, and M. G. Cusella De Angelis. Low-amplitude high frequency vibration down-regulates myostatin and atrogin-1 expression, two components of the atrophy pathway in muscle cells. *J Tissue Eng Regen Med*, 2012.

[150] P. Moens, P. H. Baatsen, and G. Marechal. Increased susceptibility of edl muscles from mdx mice to damage induced by contractions with stretch. *J Muscle Res Cell Motil*, 14(4):446–51, 1993.

[151] E. Ozcivici, Y. K. Luu, C. T. Rubin, and S. Judex. Low-level vibrations retain bone marrow's osteogenic potential and augment recovery of trabecular bone during reambulation. *PLoS One*, 5(6):e11178, 2010.

[152] S. Torvinen, P. Kannus, H. Sievanen, T. A. Jarvinen, M. Pasanen, S. Kontulainen, A. Nenonen, T. L. Jarvinen, T. Paakkala, M. Jarvinen, and I. Vuori. Effect of 8-month vertical whole body vibration on bone, muscle performance, and body balance: a randomized controlled study. *J Bone Miner Res*, 18(5):876–84, 2003.

[153] D. Blottner, M. Salanova, B. Puttmann, G. Schiffl, D. Felsenberg, B. Buehring, and J. Rittweger. Human skeletal muscle structure and function preserved by vibration muscle exercise following 55 days of bed rest. *Eur J Appl Physiol*, 97(3):261–71, 2006.

[154] A. Rufo, A. Del Fattore, M. Capulli, F. Carvello, L. De Pasquale, S. Ferrari, D. Pierroz, L. Morandi, M. De Simone, N. Rucci, E. Bertini, M. L. Bianchi, F. De Benedetti, and A. Teti. Mechanisms inducing low bone density in duchenne muscular dystrophy in mice and humans. *J Bone Miner Res*, 2011.

[155] Stefan Judex, Xin Lei, Daniel Han, and Clinton Rubin. Low-magnitude mechanical signals that stimulate bone formation in the ovariectomized rat are dependent

on the applied frequency but not on the strain magnitude. *J Biomech*, 40(6):1333–1339, 2007.

[156] B. A. Christiansen and M. J. Silva. The effect of varying magnitudes of whole-body vibration on several skeletal sites in mice. *Ann Biomed Eng*, 34(7):1149–56, 2006.

[157] B. S. Oxlund, G. Ortoft, T. T. Andreassen, and H. Oxlund. Low-intensity, high-frequency vibration appears to prevent the decrease in strength of the femur and tibia associated with ovariectomy of adult rats. *Bone*, 32(1):69–77, 2003.

[158] R. Garman, G. Gaudette, L. R. Donahue, C. Rubin, and S. Judex. Low-level accelerations applied in the absence of weight bearing can enhance trabecular bone formation. *J Orthop Res*, 25(6):732–40, 2007.

[159] L. Xie, C. Rubin, and S. Judex. Enhancement of the adolescent murine musculoskeletal system using low-level mechanical vibrations. *J Appl Physiol*, 104(4):1056–62, 2008.

[160] U. T. Iwaniec, T. J. Wronski, J. Liu, M. F. Rivera, R. R. Arzaga, G. Hansen, and R. Brommage. Pth stimulates bone formation in mice deficient in lrp5. *J Bone Miner Res*, 22(3):394–402, 2007.

[161] G. F. Maddalozzo, U. T. Iwaniec, R. T. Turner, C. J. Rosen, and J. J. Widrick. Whole-body vibration slows the acquisition of fat in mature female rats. *Int J Obes (Lond)*, 32(9):1348–54, 2008.

[162] S. Lotinun, G. L. Evans, R. T. Turner, and M. J. Oursler. Deletion of membrane-bound steel factor results in osteopenia in mice. *J Bone Miner Res*, 20(4):644–52, 2005.

[163] A. M. Parfitt, M. K. Drezner, F. H. Glorieux, J. A. Kanis, H. Malluche, P. J. Meunier, S. M. Ott, and R. R. Recker. Bone histomorphometry: standardization of nomenclature, symbols, and units. report of the asbmr histomorphometry nomenclature committee. *J Bone Miner Res*, 2(6):595–610, 1987.

[164] M. W. Garlich, K. A. Baltgalvis, J. A. Call, L. L. Dorsey, and D. A. Lowe. Plantarflexion contracture in the mdx mouse. *Am J Phys Med Rehabil*, 89(12):976–85, 2010.

[165] C. P. Ingalls, G. L. Warren, D. A. Lowe, D. B. Boorstein, and R. B. Armstrong. Differential effects of anesthetics on in vivo skeletal muscle contractile function in the mouse. *J Appl Physiol*, 80(1):332–40, 1996.

[166] S. V. Brooks and J. A. Faulkner. Contractile properties of skeletal muscles from young, adult and aged mice. *J Physiol*, 404:71–82, 1988.

[167] W. L. Murfee, L. A. Hammett, C. Evans, L. Xie, M. Squire, C. Rubin, S. Judex, and T. C. Skalak. High-frequency, low-magnitude vibrations suppress the number of blood vessels per muscle fiber in mouse soleus muscle. *J Appl Physiol*, 98(6):2376–80, 2005.

[168] R. K. Josephson. Contraction dynamics and power output of skeletal muscle. *Annu Rev Physiol*, 55:527–46, 1993.

[169] B.J. Lee, S. Judex, K. Luu, J. Thomas, V. Gilsanz, and C. Rubin. Potential mitigation of the skeletal complications of duchenne's muscular dystrophy with vibration, 2007.

[170] L. Xie, J. M. Jacobson, E. S. Choi, B. Busa, L. R. Donahue, L. M. Miller, C. T. Rubin, and S. Judex. Low-level mechanical vibrations can influence bone resorption and bone formation in the growing skeleton. *Bone*, 39(5):1059–66, 2006.

[171] C. Rubin, M. Pope, J. C. Fritton, M. Magnusson, T. Hansson, and K. McLeod. Transmissibility of 15-hertz to 35-hertz vibrations to the human hip and lumbar spine: determining the physiologic feasibility of delivering low-level anabolic mechanical stimuli to skeletal regions at greatest risk of fracture because of osteoporosis. *Spine (Phila Pa 1976)*, 28(23):2621–7, 2003.

[172] R. Ritzmann, A. Gollhofer, and A. Kramer. The influence of vibration type, frequency, body position and additional load on the neuromuscular activity during whole body vibration. *Eur J Appl Physiol*, 2012.

[173] S. A. Novotny, S. A. Novotny, H. Mehta, D. A. Lowe, and D. J. Nuckley. Vibration platform for mice to deliver precise, low intensity mechanical signals to the musculoskeleton. *Submitted to: Medical Engineering and Physics*, 2013.

[174] A. G. Robling, D. B. Burr, and C. H. Turner. Recovery periods restore mechanosensitivity to dynamically loaded bone. *J Exp Biol*, 204(Pt 19):3389–99, 2001.

[175] C. H. Turner. Three rules for bone adaptation to mechanical stimuli. *Bone*, 23(5):399–407, 1998.

[176] S.P. Fritton, K.J. McLeod, and C.T. Rubin. Quantifying the strain history of bone: spatial uniformity and self-similarity of low-magnitude strains. *J Biomech*, 33(3):317–325, 2000.

[177] J. Muir, S. Judex, Y. X. Qin, and C. Rubin. Postural instability caused by extended bed rest is alleviated by brief daily exposure to low magnitude mechanical signals. *Gait Posture*, 33(3):429–35, 2011.

[178] P. Pitukcheewanont and D. Safani. Extremely low-level, short-term mechanical stimulation increases cancellous and cortical bone density and muscle mass of children with low bone density. *The Endocrinologist*, 16:128–32, 2006.

[179] L. E. Necking, R. Lundstrom, G. Lundborg, L. E. Thornell, and J. Friden. Skeletal muscle changes after short term vibration. *Scand J Plast Reconstr Surg Hand Surg*, 30(2):99–103, 1996.

[180] M. D. Grounds, H. G. Radley, G. S. Lynch, K. Nagaraju, and A. De Luca. Towards developing standard operating procedures for pre-clinical testing in the mdx mouse model of duchenne muscular dystrophy. *Neurobiol Dis*, 31(1):1–19, 2008.

[181] Y. Leng, Z. Zheng, C. Zhou, C. Zhang, X. Shi, and W. Zhang. A comparative study of bone marrow mesenchymal stem cell functionality in c57bl and mdx mice. *Neurosci Lett*, 523(2):139–44, 2012.

Appendix A

Tabled Literature Review of Vibration Studies in Rodents

Appendix 1. Summary of the skeletal effects attributed to low intensity, high frequency vibration in rodent models published through 2009.

Reference	Population	Age	Protocol	Duration	Acceleration (*g*)	Frequency (Hz)	Outcome
C57BL/6 Mice							
Judex, Donahue, Rubin, 2002 (Judex, Donahue et al. 2002)	C57BL/6, BALB/cBYJ, And C3H/HeJ	16 wk	10 min; 5 d/wk	15 d and 21 d	0.25	45	C57BL/6 mice had sig greater BFR than other strains. Metaphysis: ↑ 69% BFR/TV, ↑ 50% Tb.Th
Luu, Capilla, Rosen, Gilsanze, Pessen, Judex, Rubin 2009 (Luu, Capilla et al. 2009)	males	7 wk	15 min; 5 d/wk	6 wk	0.2	90	Metaphysis: ↑ 10.4% Tb.N, ↑ 23% Conn.D, ↓ 11% Tb.Sp
Garman, Gaudette, Donahue, Rubin, Judex 2007 (Garman, Gaudette et al. 2007)	female	19 wk	10 min; 5 d/wk	3 wk	0.3 0.6	45	0.3g Metaphysis: ↑ 88% BFR/BS, ↓ 23% Conn.D 0.6g Metaphysis: ↑ 66% BFR/BS; ↓ 25% Conn.D 0.6 Cortical bone of Metaphysis: ↑ 13% Co.Th, ↑ 10% Co.Area
Christiansen, Silva 2006 (Christiansen and Silva 2006)		7 mo	15min/d; 7 d/wk	5wk	0.1 0.3 1.0	45	Metaphysis 0.1: Metpahysis 1.0: ↑ 32% BV/TV ↑ 43% BV/TV Veretebrae 0.3: Tb BV/TV Significantly decreased from 0.1 and 1.0 g

BFR/TV, Bone formation rate per tissue volume; Tb.Th, Trabecular thickness; Tb.N, Trabecular number; Conn.D, Connective density; Tb.Sp, Trabecular spacing; BFR/BS, Bone formation rate per bone surface; Co.Th, Cortical Thickness; Co.Area, Cortical area;, BV/TV, Bone volume per tissue volume; ↑ Increased; ↓ Decreased; *g* acceleration measured in units of gravity

Reference	Population	Age	Protocol	Duration	Acceleration (*g*)	Frequency (Hz)	Outcome
BALB Mice							
Xie, Rubin, Judex 2008 (Xie, Rubin et al. 2008)	female	8 wk	15 min; 5 d/wk	6 wk	0.3	45	Metaphysis: ↑ 74% Tb MS/BS, ↑ 8% Tb.BV, ↑ 8% Co.A, ↑ 21% CSMI, ↑ 12.5% Marrow Area
Ozcivici, Garman, Judex 2007 (Ozcivici, Garman et al. 2007)	Hindlimb Unloaded female	4 mo	20 min; 5 d/wk	3 wk	0.6	45	Vibrated limb vs HU limb: Vibration ↓ loss of BV/TV, Tb stiffness, Conn.D, and Tb.N Metaphysis vs AC: ↓ 12% Tb.N, ↓ 22% Tb.Th, ↓6% Conn.D, ↓ 44% Tb stiffness, and ↓ 38%
Xie, Jacobson, Choi, Busa, Donahue, Miller, Rubin, Judex 2006 (Xie, Jacobson et al. 2006)	Female Vibration vs Vibration + Rest Inserted Loading	8 wk	15 min 165 min; 5 d/wk	3 wk	0.3	45	Metaphysis 15 min: ↑ 30% Co BFR
Judex, Zhong, Squire, Ye, et al. 2005 (Judex, Zhong et al. 2005)	female	16 wk	10 min; 5 d/wk	4 d and 21 d	0.3	45	↑ 55% Tb and Co BFR/BS Trabecular Bone: ↑ 32% BFR, ↑18% MS/BS

Tb MS/BS, Trabecular mineralized surface per bone surface; Co.Area, Cortical area; CSMI, Cross-sectional moment of inertia; HU, hindlimb unloaded; Tb, Trabeculae; Conn.D, Connective density; Tb.N, Trabecular number; AC Age-matched controls; Tb.Th, Trabecular thickness; Co BFR, cortical bone formation rate; BFR, Bone formation rate, ↑ Increased; ↓ Decreased; *g* acceleration measured in units of gravity

Reference	Population	Age	Protocol	Duration	Acceleration (*g*)	Frequency (Hz)	Outcome
Rats							
Rubinacci, , et al. 2008 (Rubinacci, Marenzana et al. 2008)	Female OVX Sprague Dawley	3 mo	20 min; 5 d/wk	2 mo	0.6 3.0	30	Diaphysis 3.0g: ↑ 10% ToA, ↑ 8% CoArea, ↑ 5% periosteal perimeter, ↑ 7% endosteal perimeter
Oxlund, Ortoft, Andreassen, Oxlund 2003 (Oxlund, Ortoft et al. 2003)	OVX+WBV	12 mo	30 min	90 d	1.16 3.62 8.15	17 30 45	17Hz: ↑ 81% MAR 30Hz: ↑ 100% MAR 45Hz: ↑ 84% periosteal BFR, inhibition of Endocortical resorption
Rubin, Xu, Judex 2001 (Rubin, Xu et al. 2001)	AC Vib HU HU+Vib	12 wks	30 min; 5 d/wk	28 d	0.25	90	Vib vs AC: ↑ 97% BFR/BV, ↑ 76% MS/BS HU + Vib vs HU: ↑ ~33% BFR/BV, ↑ 40% MS/BS
Flieger et al. 1998 (Flieger, Karachalios et al. 1998)	Sham Sham + Vib OVX OVX + Vib	12 wks	30 min; 5 d/wk	12 wk	2.0	50	Vib preserved bone mass in OVX mice
Yang, Jia, Ding, Wang, Qian, Shang 2009 (Yang, Jia et al. 2009)	HU Vib HU+Vib	4 wks	15 min; 7 d/wk	28 d	0.1-1.0	10-60	HU+Vib vs HU: ↑ 10 % femur BMD, ↑ 7% Tibia BMD Elastic Modulus: ↑ 28% and 43% in Vib and HU+ VIb compared to respective control. Stiffness: ↑23% HU+Vib compared to HU.
Judex, et al. 2007 (Judex, Lei et al. 2007)	OVX OVX + 45Hz OVX +90Hz	6-8 mo	10 min; 5 d/wk	28 d	0.15	45 90	Metaphysis 90Hz: ↑ 159% Tb BFR/BS, ↑ 40% Co BFR/BS (vs 45Hz) Epiphysis 90Hz: ↑ 22% Tb BV, ↑ 11% Tb.Th, ↓ 35% Tb.ConnD

ToA, Total Area; CoArea, Cortical area; MAR, mineral apposition rate; BFR, Bone formation rate; AC Age-matched controls; BFR/BV, Bone formation rate per bone volume; MS/BS, Mineralized surface per bone surface; HU, hindlimb unloaded; OVX, ovariectomized; VIB, vibrated; BFR/BS, Bone formation rate per bone surface; Tb BV, Trabecular bone volume; Tb.Th, Trabecular thickness; Conn.D, Connective density; ↑ Increased; ↓ Decreased; *g* acceleration measured in units of gravity

REFERENCES

Christiansen, B. A. and M. J. Silva (2006). "The effect of varying magnitudes of whole-body vibration on several skeletal sites in mice." Ann Biomed Eng 34(7): 1149-1156.

Flieger, J., T. Karachalios, et al. (1998). "Mechanical stimulation in the form of vibration prevents postmenopausal bone loss in ovariectomized rats." Calcif Tissue Int 63(6): 510-514.

Garman, R., G. Gaudette, et al. (2007). "Low-level accelerations applied in the absence of weight bearing can enhance trabecular bone formation." J Orthop Res 25(6): 732-740.

Judex, S., L. R. Donahue, et al. (2002). "Genetic predisposition to low bone mass is paralleled by an enhanced sensitivity to signals anabolic to the skeleton." Faseb J 16(10): 1280-1282.

Judex, S., X. Lei, et al. (2007). "Low-magnitude mechanical signals that stimulate bone formation in the ovariectomized rat are dependent on the applied frequency but not on the strain magnitude." J Biomech 40(6): 1333-1339.

Judex, S., N. Zhong, et al. (2005). "Mechanical modulation of molecular signals which regulate anabolic and catabolic activity in bone tissue." J Cell Biochem 94(5): 982-994.

Luu, Y. K., E. Capilla, et al. (2009). "Mechanical stimulation of mesenchymal stem cell proliferation and differentiation promotes osteogenesis while preventing dietary-induced obesity." J Bone Miner Res 24(1): 50-61.

Oxlund, B. S., G. Ortoft, et al. (2003). "Low-intensity, high-frequency vibration appears to prevent the decrease in strength of the femur and tibia associated with ovariectomy of adult rats." Bone 32(1): 69-77.

Ozcivici, E., R. Garman, et al. (2007). "High-frequency oscillatory motions enhance the simulated mechanical properties of non-weight bearing trabecular bone." J Biomech 40(15): 3404-3411.

Rubin, C., G. Xu, et al. (2001). "The anabolic activity of bone tissue, suppressed by disuse, is normalized by brief exposure to extremely low-magnitude mechanical stimuli." Faseb J 15(12): 2225-2229.

Rubinacci, A., M. Marenzana, et al. (2008). "Ovariectomy sensitizes rat cortical bone to whole-body vibration." Calcif Tissue Int 82(4): 316-326.

Xie, L., J. M. Jacobson, et al. (2006). "Low-level mechanical vibrations can influence bone resorption and bone formation in the growing skeleton." Bone 39(5): 1059-1066.

Xie, L., C. Rubin, et al. (2008). "Enhancement of the adolescent murine musculoskeletal system using low-level mechanical vibrations." J Appl Physiol 104(4): 1056-1062.

Yang, P., B. Jia, et al. (2009). "Whole-body vibration effects on bone before and after hind-limb unloading in rats." Aviat Space Environ Med 80(2): 88-93.

Appendix B

Authorization of Use for Copyrighted Materials

Chapter 2
Figure 2.3
Date: Mon, 6 Dec 2010 16:08:11 +0000 (GMT)
From: Author Services <support@elsevier.com>
To: golne003@umn.edu
Subject: Your article [NMD_2360] - Copyright Form Completed

Article title: Bone is functionally impaired in dystrophic mice but less so than skeletal muscle
Reference: NMD2360
Journal title: Neuromuscular Disorders
Corresponding author: Ms. Susan A. Novotny First author: Ms. Susan A. Novotny

Dear Ms. Novotny,
Please find attached a copy of the "Journal Publishing Agreement" which you completed online on 6-DEC-2010.
If you have any questions, please do not hesitate to contact us. To help us assist you, please quote our reference NMD2360 in all correspondence.
We are committed to publishing your article as quickly as possible.
Yours sincerely,
Elsevier Author Support
http://support.elsevier.com

POSTING AND COPYRIGHT POLICIES
As an author you retain significant rights for use of your own work, including the right to:
- Post a pre-print version of the article on various websites (with some exceptions)
- Make copies (print or electronic) of the article for your own personal use, including classroom teaching
- Use the article in a printed compilation of your own works. For more information on our full copyright and repository compliance policies, as well as obtaining permissions, please consult http://www.elsevier.com/authorsrights.

PERSONAL USE

Use by an author in the author's classroom teaching (including distribution of copies, paper or electronic), distribution of copies to research colleagues for their personal use, use in a subsequent compilation of the author's works, inclusion in a thesis or dissertation, preparation of other derivative works such as extending the article to book-length form, or otherwise using or re-using portions or excerpts in other works (with full acknowledgment of the original publication of the article).

Figure 2.4

Title: Emerging Therapies for the Prevention or Treatment of Postmenopausal Osteoporosis

Author: Masahiko Sato et al.

Publication: Journal of Medicinal Chemistry

Publisher: American Chemical Society

Date: Jan 1, 1999

PERMISSION/LICENSE IS GRANTED FOR YOUR ORDER AT NO CHARGE

This type of permission/license, instead of the standard Terms & Conditions, is sent to you because no fee is being charged for your order. Please note the following:

- Permission is granted for your request in both print and electronic formats, and translations.
- If figures and/or tables were requested, they may be adapted or used in part.
- Please print this page for your records and send a copy of it to your publisher/graduate school.
- Appropriate credit for the requested material should be given as follows: "Reprinted (adapted) with permission from (COMPLETE REFERENCE CITATION). Copyright (YEAR) American Chemical Society." Insert appropriate information in place of the capitalized words.
- One-time permission is granted only for the use specified in your request. No additional uses are granted (such as derivative works or other editions). For any other uses, please submit a new request.

Figure 2.8

ELSEVIER LICENSE
TERMS AND CONDITIONS

Feb 15, 2013

This is a License Agreement between Susan A Novotny ("You") and Elsevier ("Elsevier") provided by Copyright Clearance Center ("CCC"). The license consists of your order details, the terms and conditions provided by Elsevier, and the payment terms and conditions.

All payments must be made in full to CCC. For payment instructions, please see information listed at the bottom of this form.

Supplier	Elsevier Limited The Boulevard,Langford Lane Kidlington,Oxford,OX5 1GB,UK
Registered Company Number	1982084
Customer name	Susan A Novotny
License number	3086670186938
License date	Feb 12, 2013
Licensed content publisher	Elsevier
Licensed content publication	Bone
Licensed content title	Osteocyte lacunar size–lamellar thickness relationships in human secondary osteons
Licensed content author	A Ardizzoni
Licensed content date	February 2001
Licensed content volume number	28
Licensed content issue number	2
Number of pages	5
Start Page	215
End Page	219
Type of Use	reuse in a thesis/dissertation
Portion	figures/tables/illustrations

Number of figures/tables/illustrations	1
Format	both print and electronic
Are you the author of this Elsevier article?	No
Will you be translating?	No
Order reference number	
Title of your thesis/dissertation	2. Bone's functional and geometric properties in dystrophin-deficient mice and the efficacy of low intensity vibration training to improve musculoskeletal function
Expected completion date	Mar 2013
Estimated size (number of pages)	150
Elsevier VAT number	GB 494 6272 12
Permissions price	0.00 USD
VAT/Local Sales Tax	0.0 USD / 0.0 GBP
Total	0.00 USD

Figure 2.9

SPRINGER LICENSE
TERMS AND CONDITIONS

Feb 15, 2013

This is a License Agreement between Susan A Novotny ("You") and Springer ("Springer") provided by Copyright Clearance Center ("CCC"). The license consists of your order details, the terms and conditions provided by Springer, and the payment terms and conditions.

All payments must be made in full to CCC. For payment instructions, please see information listed at the bottom of this form.

License Number	3086600873485
License date	Feb 12, 2013
Licensed content publisher	Springer
Licensed content publication	Calcified Tissue International
Licensed content title	Skeletal strain and the functional significance of bone architecture
Licensed content author	Clinton T. Rubin
Licensed content date	Jan 1, 1984
Volume number	36
Issue number	1
Type of Use	Thesis/Dissertation
Portion	Figures
Author of this Springer article	No
Order reference number	
Title of your thesis / dissertation	2. Bone's functional and geometric properties in dystrophin-deficient mice and the efficacy of low intensity vibration training to improve musculoskeletal function
Expected completion date	Mar 2013
Estimated size(pages)	150
Total	0.00 USD

Figure 2.10

ELSEVIER LICENSE
TERMS AND CONDITIONS

Feb 15, 2013

This is a License Agreement between Susan A Novotny ("You") and Elsevier ("Elsevier") provided by Copyright Clearance Center ("CCC"). The license consists of your order details, the terms and conditions provided by Elsevier, and the payment terms and conditions.

All payments must be made in full to CCC. For payment instructions, please see information listed at the bottom of this form.

Supplier	Elsevier Limited The Boulevard,Langford Lane Kidlington,Oxford,OX5 1GB,UK
Registered Company Number	1982084
Customer name	Susan A Novotny
License number	3086600668434
License date	Feb 12, 2013
Licensed content publisher	Elsevier
Licensed content publication	Bone
Licensed content title	Characteristics of in vitro osteoblastic cell loading models
Licensed content author	N. Basso,J.N.M. Heersche
Licensed content date	February 2002
Licensed content volume number	30
Licensed content issue number	2
Number of pages	5
Start Page	347
End Page	351
Type of Use	reuse in a thesis/dissertation
Portion	figures/tables/illustrations
Number of	1

figures/tables/illustrations	
Format	both print and electronic
Are you the author of this Elsevier article?	No
Will you be translating?	No
Order reference number	
Title of your thesis/dissertation	2. Bone's functional and geometric properties in dystrophin-deficient mice and the efficacy of low intensity vibration training to improve musculoskeletal function
Expected completion date	Mar 2013
Estimated size (number of pages)	150
Elsevier VAT number	GB 494 6272 12
Permissions price	0.00 USD
VAT/Local Sales Tax	0.0 USD / 0.0 GBP
Total	0.00 USD

Figure 2.11 Panel A

JOHN WILEY AND SONS LICENSE
TERMS AND CONDITIONS

Feb 15, 2013

This is a License Agreement between Susan A Novotny ("You") and John Wiley and Sons ("John Wiley and Sons") provided by Copyright Clearance Center ("CCC"). The license consists of your order details, the terms and conditions provided by John Wiley and Sons, and the payment terms and conditions.

All payments must be made in full to CCC. For payment instructions, please see information listed at the bottom of this form.

License Number	3086611136443
License date	Feb 12, 2013
Licensed content publisher	John Wiley and Sons
Licensed content publication	Journal of Bone and Mineral Research
Licensed content title	The Effect of Mechanical Loading on the Size and Shape of Bone in Pre-, Peri-, and Postpubertal Girls: A Study in Tennis Players
Licensed copyright line	Copyright © 2002 ASBMR
Licensed content author	S. L. Bass,L. Saxon,R. M. Daly,C. H. Turner,A. G. Robling,E. Seeman,S. Stuckey
Licensed content date	Dec 1, 2002
Start page	2274
End page	2280
Type of use	Dissertation/Thesis
Requestor type	University/Academic
Format	Print and electronic
Portion	Figure/table
Number of figures/tables	1
Original Wiley figure/table number(s)	Figure 2
Will you be translating?	No
Total	0.00 USD

Figure 2.11 Panel B

SPRINGER ORDER DETAILS

Feb 15, 2013

Order Number	500734581
Order date	Feb 12, 2013
Licensed content publisher	Springer
Licensed content publication	Journal of Bone and Mineral Metabolism
Licensed content title	Bone quality: the material and structural basis of bone strength
Licensed content author	Ego Seeman
Licensed content date	Jan 1, 2008
Volume number	26
Issue number	1
Type of Use	Thesis/Dissertation
Portion	Figures
Author of this Springer article	No
Order reference number	
Title of your thesis / dissertation	2. Bone's functional and geometric properties in dystrophin-deficient mice and the efficacy of low intensity vibration training to improve musculoskeletal function
Expected completion date	Mar 2013
Estimated size(pages)	150
Total	Not Available

Figure 2.13

JOHN WILEY AND SONS LICENSE
TERMS AND CONDITIONS

Feb 15, 2013

This is a License Agreement between Susan A Novotny ("You") and John Wiley and Sons ("John Wiley and Sons") provided by Copyright Clearance Center ("CCC"). The license consists of your order details, the terms and conditions provided by John Wiley and Sons, and the payment terms and conditions.

All payments must be made in full to CCC. For payment instructions, please see information listed at the bottom of this form.

License Number	3086620968401
License date	Feb 12, 2013
Licensed content publisher	John Wiley and Sons
Licensed content publication	Journal of Bone and Mineral Research
Licensed content title	Improved Bone Structure and Strength After Long-Term Mechanical Loading Is Greatest if Loading Is Separated Into Short Bouts
Licensed copyright line	Copyright © 2002 ASBMR
Licensed content author	Alexander G. Robling,Felicia M. Hinant,David B. Burr,Charles H. Turner
Licensed content date	Aug 1, 2002
Start page	1545
End page	1554
Type of use	Dissertation/Thesis
Requestor type	University/Academic
Format	Print and electronic
Portion	Figure/table
Number of figures/tables	1
Original Wiley figure/table number(s)	Figure 1 and Figure 2
Will you be translating?	No
Total	0.00 USD

Figure 2.14 and 2.15
From: Deborah Gray D.Gray@boneandjoint.org.uk
Sent: Thu 2/14/2013 4:06 AM
RE: Permission to use Figure in Dissertation (BJJ Feedback Form)

Dear Susan Novotny

Thank you for your inquiry.

Please find our permission statement below:

Uhthoff HK, Jaworski ZFG. Bone loss in response to long-term immobilisation. *J Bone Joint Surg [Br]* 1978;60-B:420-429. (Figures 2, 5, 6)

Thank you for your permission request. We are pleased to grant permission for you to reproduce figures 2, 5 and 6 from the aforementioned article, *provided full and correct acknowledgement of source is given*. On this occasion the permission is granted *free of charge* as the material is to be used in your thesis and therefore falls under the category of academic purposes, and is not for widespread or commercial publication or distribution.

If you have any further questions, please do not hesitate to contact me.

Kind regards,

Deborah

==========
Deborah Gray (Miss)
Production Management Assistant
The British Editorial Society of Bone and Joint Surgery
22 Buckingham Street, London, WC2N 6ET
t: 020 7782 0010 e: d.gray@boneandjoint.org.uk
www.bjj.boneandjoint.org.uk
==========

Our title has changed to *The Bone & Joint Journal*, formerly known as *JBJS (Br)*

Figure 2.16

JOHN WILEY AND SONS LICENSE
TERMS AND CONDITIONS

Feb 15, 2013

This is a License Agreement between Susan A Novotny ("You") and John Wiley and Sons ("John Wiley and Sons") provided by Copyright Clearance Center ("CCC"). The license consists of your order details, the terms and conditions provided by John Wiley and Sons, and the payment terms and conditions.

All payments must be made in full to CCC. For payment instructions, please see information listed at the bottom of this form.

License Number	3086671237653
License date	Feb 12, 2013
Licensed content publisher	John Wiley and Sons
Licensed content publication	Wiley Interdisciplinary Reviews: Systems Biology and Medicine
Licensed content title	Systems biology of skeletal muscle: fiber type as an organizing principle
Licensed copyright line	Copyright © 2012 Wiley Periodicals, Inc.
Licensed content author	Sarah M. Greising,Heather M. Gransee,Carlos B. Mantilla,Gary C. Sieck
Licensed content date	Jul 18, 2012
Start page	457
End page	473
Type of use	Dissertation/Thesis
Requestor type	University/Academic
Format	Print and electronic
Portion	Figure/table
Number of figures/tables	1
Original Wiley figure/table number(s)	Figure 2
Will you be translating?	No
Total	0.00 USD

Figure 2.17
Copyright Permission Policy

These guidelines apply to the reuse of articles, figures, charts and photos in the *Journal of Biological Chemistry*, *Molecular & Cellular Proteomics* and the *Journal of Lipid Research*.

For other parties using material for noncommercial use: Other parties are welcome to copy, distribute, transmit and adapt the work — at no cost and without permission — for noncommercial use as long as they attribute the work to the original source using the citation above.

Examples of noncommercial use include:

> Reproducing a figure for educational purposes, such as schoolwork or lecture presentations, with attribution. Appending a reprinted article to a Ph.D. dissertation, with attribution.

Figure 2.18

ELSEVIER LICENSE
TERMS AND CONDITIONS

Feb 15, 2013

This is a License Agreement between Susan A Novotny ("You") and Elsevier ("Elsevier") provided by Copyright Clearance Center ("CCC"). The license consists of your order details, the terms and conditions provided by Elsevier, and the payment terms and conditions.

All payments must be made in full to CCC. For payment instructions, please see information listed at the bottom of this form.

Supplier	Elsevier Limited The Boulevard,Langford Lane Kidlington,Oxford,OX5 1GB,UK
Registered Company Number	1982084
Customer name	Susan A Novotny
License number	3086630555381
License date	Feb 12, 2013
Licensed content publisher	Elsevier
Licensed content publication	Neuromuscular Disorders
Licensed content title	Low bone mineral density and decreased bone turnover in Duchenne muscular dystrophy
Licensed content author	Ann-Charlott Söderpalm,Per Magnusson,Anne-Christine Åhlander,Jón Karlsson,Anna-Karin Kroksmark,Már Tulinius,Diana Swolin-Eide
Licensed content date	December 2007
Licensed content volume number	17
Licensed content issue number	11–12
Number of pages	10
Start Page	919
End Page	928
Type of Use	reuse in a thesis/dissertation

Portion	figures/tables/illustrations
Number of figures/tables/illustrations	1
Format	both print and electronic
Are you the author of this Elsevier article?	No
Will you be translating?	No
Order reference number	
Title of your thesis/dissertation	2. Bone's functional and geometric properties in dystrophin-deficient mice and the efficacy of low intensity vibration training to improve musculoskeletal function
Expected completion date	Mar 2013
Estimated size (number of pages)	150
Elsevier VAT number	GB 494 6272 12
Permissions price	0.00 USD
VAT/Local Sales Tax	0.0 USD / 0.0 GBP
Total	0.00 USD

Figure 2.19

NATURE PUBLISHING GROUP LICENSE
TERMS AND CONDITIONS

Feb 15, 2013

This is a License Agreement between Susan A Novotny ("You") and Nature Publishing Group ("Nature Publishing Group") provided by Copyright Clearance Center ("CCC"). The license consists of your order details, the terms and conditions provided by Nature Publishing Group, and the payment terms and conditions.

All payments must be made in full to CCC. For payment instructions, please see information listed at the bottom of this form.

License Number	3086631023050
License date	Feb 12, 2013
Licensed content publisher	Nature Publishing Group
Licensed content publication	Nature Reviews Rheumatology
Licensed content title	Mechanical signals as anabolic agents in bone
Licensed content author	Engin Ozcivici, Yen Kim Luu, Ben Adler, Yi-Xian Qin, Janet Rubin et al.
Licensed content date	Jan 1, 2010
Volume number	6
Issue number	1
Type of Use	reuse in a thesis/dissertation
Requestor type	academic/educational
Format	print and electronic
Portion	figures/tables/illustrations
Number of figures/tables/illustrations	1
High-res required	no
Figures	Figure 2
Author of this NPG article	no
Your reference number	
Title of your thesis / dissertation	2. Bone's functional and geometric properties in dystrophin-deficient mice and the efficacy of low intensity vibration training to improve

	musculoskeletal function
Expected completion date	Mar 2013
Estimated size (number of pages)	150
Total	0.00 USD

Chapter 3
Date: Mon, 6 Dec 2010 16:08:11 +0000 (GMT)
From: Author Services <support@elsevier.com>
To: golne003@umn.edu
Subject: Your article [NMD_2360] - Copyright Form Completed

Article title: Bone is functionally impaired in dystrophic mice but less so than skeletal muscle
Reference: NMD2360
Journal title: Neuromuscular Disorders
Corresponding author: Ms. Susan A. Novotny First author: Ms. Susan A. Novotny

Dear Ms. Novotny,

Please find attached a copy of the "Journal Publishing Agreement" which you completed online on 6-DEC-2010.

If you have any questions, please do not hesitate to contact us. To help us assist you, please quote our reference NMD2360 in all correspondence.

We are committed to publishing your article as quickly as possible.

Yours sincerely,
Elsevier Author Support
http://support.elsevier.com

POSTING AND COPYRIGHT POLICIES
As an author you retain significant rights for use of your own work, including the right to:
- Post a pre-print version of the article on various websites (with some exceptions)
- Make copies (print or electronic) of the article for your own personal use, including classroom teaching
- Use the article in a printed compilation of your own works. For more information on our full copyright and repository compliance policies, as well as obtaining permissions, please consult http://www.elsevier.com/authorsrights.

PERSONAL USE

Use by an author in the author's classroom teaching (including distribution of copies, paper or electronic), distribution of copies to research colleagues for their personal use, use in a subsequent compilation of the author's works, inclusion in a thesis or dissertation, preparation of other derivative works such as extending the article to book-length form, or otherwise using or re-using portions or excerpts in other works (with full acknowledgment of the original publication of the article).

Chapter 4

Editorial Policies and Practices

Copyright: Authors submitting manuscripts to Journal of Musculoskeletal Neuronal Interaction retain the copyright of the article if it is published.

http://www.ismni.org/jmni/